AD-A071 793 COLORADO STATE UNIV FORT COLLINS COLL OF FORESTRY AN--ETC F/G 2/6

TERRAIN FEATURE CANOPY MODELING.(U)

APR 79 D S KIMES, J A SMITH, K J RANSON DACW39-77-C-0073

UNCLASSIFIED ARO-13444.2-GS NL

1 OF 3

AD

A071793

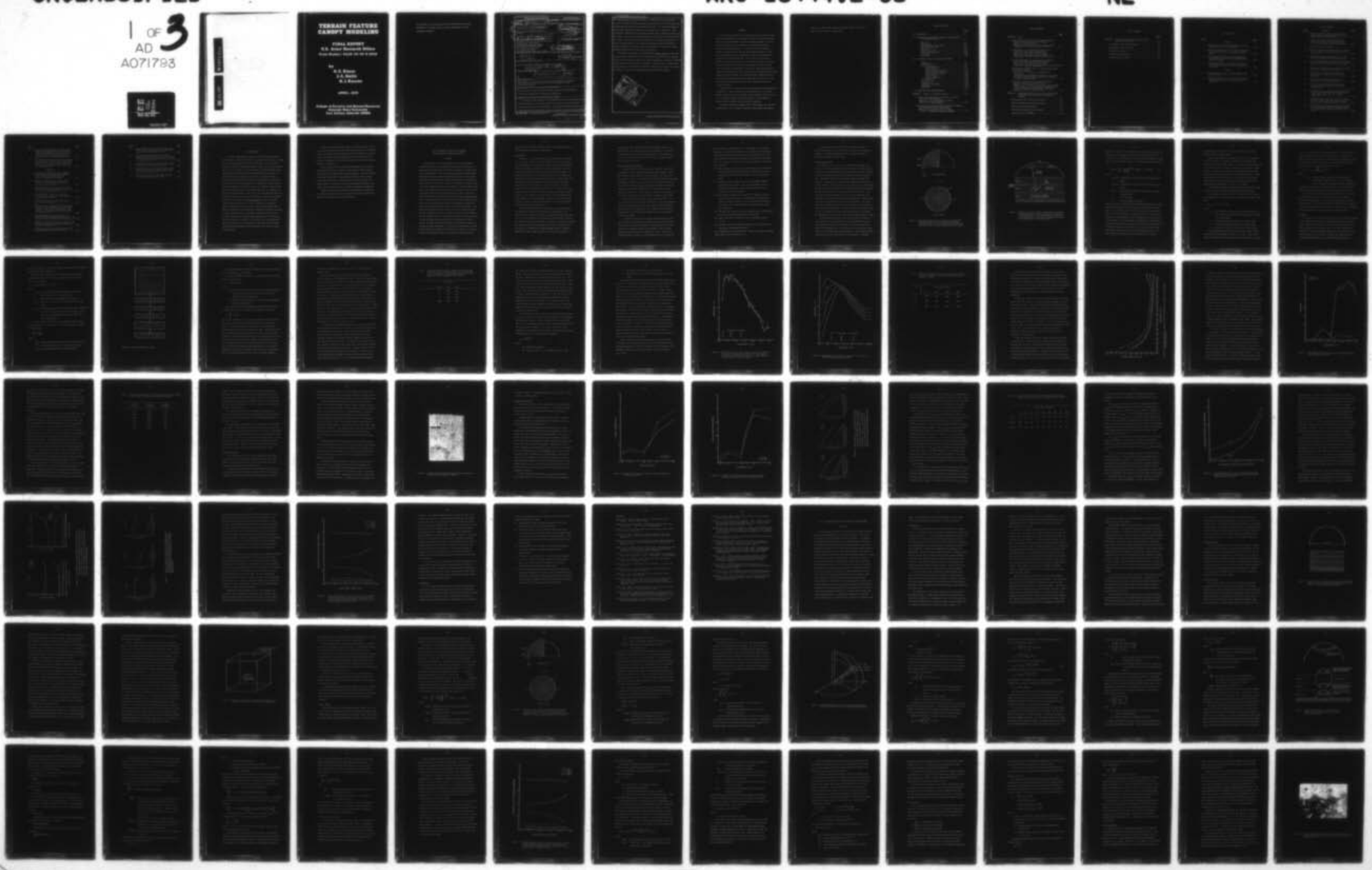

1 OF 3

AD
A071793

1·0 2·8 2·5 3·2 3·6 2·2 4·0 2·0 1·1 1·8 1·25 1·4 1·6

NATIONAL BUREAU OF STANDARDS
MICROCOPY RESOLUTION TEST CHART

TERRAIN FEATURE CANOPY MODELING

FINAL REPORT

U.S. Army Research Office

Grant Number: DAAG 29-78-G-0045

by

D. S. Kimes

J. A. Smith

K. J. Ranson

APRIL, 1979

College of Forestry and Natural Resources
Colorado State University
Fort Collins, Colorado 80523

THE FINDINGS IN THIS REPORT ARE NOT TO BE CONSTRUED AS AN OFFICIAL DEPARTMENT OF THE ARMY POSITION, UNLESS SO DESIGNATED BY OTHER AUTHORIZED DOCUMENTS.

SECURITY CLASSIFICATION OF THIS PAGE (When Data Entered)

REPORT DOCUMENTATION PAGE

READ INSTRUCTIONS BEFORE COMPLETING FORM

1. REPORT NUMBER: (18) ARO (19) 13444.2-GS
2. GOVT ACCESSION NO.
3. RECIPIENT'S CATALOG NUMBER

4. TITLE (and Subtitle): (6) Terrain Feature Canopy Modeling
5. TYPE OF REPORT & PERIOD COVERED: (9) Final Report
6. PERFORMING ORG. REPORT NUMBER

7. AUTHOR(s): (10) D.S. Kimes, J.A. Smith ~~and~~ K.J. Ranson
8. CONTRACT OR GRANT NUMBER(s): DAAG29-76-G-0105; (15) DAAG29-78-C-0045

9. PERFORMING ORGANIZATION NAME AND ADDRESS:
College of Forestry and Natural Resources
Colorado State University
Fort Collins, Colorado 80523

10. PROGRAM ELEMENT, PROJECT, TASK AREA & WORK UNIT NUMBERS

11. CONTROLLING OFFICE NAME AND ADDRESS:
U.S. Army Research Office
Post Office Box 12211
Research Triangle Park, N.C. 27709

(11) 30

12. REPORT DATE: April ~~30,~~ 1979
13. NUMBER OF PAGES: 186

14. MONITORING AGENCY NAME & ADDRESS (if different from Controlling Office): (12) 192p.

15. SECURITY CLASS. (of this report): Unclassified

15a. DECLASSIFICATION/DOWNGRADING SCHEDULE: NA

16. DISTRIBUTION STATEMENT (of this Report)

Approved for public release; distribution unlimited

(15) DACW39-77-C-0073,

17. DISTRIBUTION STATEMENT (of the abstract entered in Block 20, if different from Report)

DAAG29-78-G-0045

NA

18. SUPPLEMENTARY NOTES

The findings of this report are not to be construed as an official Department of the Army position, unless so designated by other authorized documents

19. KEY WORDS (Continue on reverse side if necessary and identify by block number)

Remote sensing, thermal terrain modeling, vegetation canopy geometry, reflectance, background electromagnetic signatures.

20. ABSTRACT (Continue on reverse side if necessary and identify by block number)

A thermal canopy signature model (TCSM) was developed to approximate the thermal behavior of a vegetation canopy by a mathematical abstraction of three horizontal layers of vegetation. Canopy geometry within each layer is quantitatively described by the foliage and branch orientation distributions.

DD FORM 1 JAN 73 1473 EDITION OF 1 NOV 65 IS OBSOLETE

Unclassified

SECURITY CLASSIFICATION OF THIS PAGE (When Data Entered)

408135

CONT

20. Canopy geometry, solar irradiance, air temperature, horizontal wind velocity, relative humidity, and ground temperature are used to calculate the energy budgets of average leaves within each layer. The resulting system of conservation equations is solved for the average layer temperature. This information, together with the angular distributions of radiating elements, is then used to calculate the thermal exitance as a function of view angle above the canopy. Optical diffraction techniques were developed and employed to measure canopy geometry. Solar radiation absorption with the vegetation terrain elements is calculated using a modification of a Monte Carlo model (SRVC) developed for the reflective energy regime.

The models were applied to a lodgepole pine (Pinus contorta) canopy and the results for a diurnal cycle are validated with radiometric measurements. Simulated versus measured radiometric average temperatures of Layer 2 correspond approximately within two degrees centigrade. Simulated results suggest that canopy geometry can significantly influence the effective radiant temperature recorded by a sensor above the canopy as a function of view angle.

FOREWARD

The three-year research effort described in this report and other publications (Appendix A) were funded by the U.S. Army Research Office under Grant Numbers DAAG29-76-G-0105 and DAAG29-78-G-0045. Dr. Steve Mock, and, earlier, Dr. Finn Bronner of the Terrestrial Sciences Branch were Technical Monitors. In later stages of the project, a related cooperative effort with the Environmental Laboratory of the U.S. Army Engineers Waterways Experiment Station was initiated under Contract Number DACW-39-77-C-0073. Dr. Ed Link was the Technical Monitor. Joint field experiments with WES were executed at a variety of test sites and close interaction with regard to thermal terrain model development was maintained. This project also benefited from a related research effort entitled, "Evaluation of Illumination and Terrain Geometry on Spectral Response in Mountain Terrain" funded by the U.S. Forest Service under Cooperative Agreement Number 16-741-CA. Mr. Bob Dana of the Rocky Mountain Forest and Range Experiment Station was Technical Monitor.

In addition to the authors, primary participating project personnel included Dr. J. Berry, presently at Yale University, Mr. F. Heimes, presently with the U.S.G.S. Division of Water Resources in Denver, and Ms. J. Kirchner, Graduate Research Assistant in the Department of Forest and Wood Sciences at Colorado State University.

Dr. Kimes received the degree, Doctor of Philosophy, for the work reported here. He is presently employed by NASA Goddard Spaceflight

Center. Mr. Rick Heimes received the degree, Master of Science, in part, for work related to this project.

TABLE OF CONTENTS

TABLE OF CONTENTS

TABLE OF CONTENTS

LIST OF TABLES

LIST OF FIGURES

Figure		Page

1.0 INTRODUCTION

This report summarizes the results of a three-year project sponsored by the U.S. Army Research Office and directed by Dr. James A. Smith, Principal Investigator, Colorado State University. Dr. D. S. Kimes received the Doctor of Philosophy degree, in part, for the work reported here. Mr. K. J. Ranson, Research Associate, Colorado State University, performed many of the analyses and coordinated the field effort. The major objective of the project was initially to apply the optical reflectance modeling procedures (the SRVC model) developed previously by the authors to a forest canopy scene. Subsequently, project objectives were expanded to include development of a thermal canopy exitance model. This latter objective was made possible with the assistance of personnel, principally Dr. E. Link, of the U.S. Army Engineers Waterways Experiment Station. An extensive data base was obtained in cooperation with WES for a lodgepole pine (Pinus contorta) canopy at Leadville, Colorado which was used both for model development and validation. Before the thermal and optical terrain feature canopy models could be applied, techniques for describing and measuring the geometric structure of forest canopies had to be developed. Rapid optical diffraction analysis techniques for analyzing ground photographs of the modeling trees were found to be suitable. The details of the models developed and their applications are described in the following chapters which contain separate introductions and conclusions. The report is organized as follows:

Chapter 2 describes the application of a modified version of the solar radiation vegetation canopy (SRVC) model coupled with a numerical approach to estimate solar absorption within the lodgepole pine canopy system. The Fortran program ABSORPT performs this analysis and is presented in Appendix B along with the results of some of the analyses mentioned in Chapter 2.

Chapter 3 describes the TCSM which incorporates the information and mathematics derived in Chapter 3 along with the thermal radiant, convectional, and transpirational energy exchanges. The model predicts the average canopy element temperature for three horizontal canopy layers, and the effective radiant temperature above and within the canopy system. The results of some of the analyses mentioned in this chapter and the Fortran code of the TCSM are presented in Appendix C.

Chapter 4 presents the summary and recommendations. Appendix A is a reprint of the abstracts of six papers or reports prepared under partial or full support of the present project.

2.0 MATHEMATICAL SIMULATION OF ABSORBED SOLAR RADIATION IN VEGETATION CANOPIES

Abstract

The absorption of total and spectral solar radiation within vegetation canopies as a function of solar zenith angle needs to be quantitatively described for agricultural, ecological, forestry, and military applications. The solar radiation vegetation canopy (SRVC) absorption model was developed to physically account for the optical properties, and geometric and spatial characteristics of canopy elements, and direct and diffuse components of irradiance. Multiple and directional radiation scattering are included. The model predicts the proportion of spectral solar absorption in three horizontal layers and the apparent directional reflectance above the canopy. Field data were collected from a cluster of four lodgepole pine (*Pinus contorta*) trees. Vertical spectral reflectance above the canopy, spectral transmittance to the ground layer, geometric measurements of canopy elements, and optical properties of canopy elements were measured. The model was then applied to the canopy, and the reflectance and transmittance simulated results for a theoretical clear day were compared with the measured results. The simulated results showed that relatively large differentials occurred in spectral absorption by canopy layers, especially in the photosynthetic active radiation region as a function of solar zenith angle. In addition, the proportion of total global irradiance absorbed by individual layers varied as a function of solar zenith angle. However, the proportion of both total and

spectral global irradiance absorbed by the entire canopy system was relatively constant with solar zenith angle.

Introduction

The manner in which a vegetation canopy absorbs solar radiation has an important effect on the thermal properties of the canopy and the photosynthetic efficiency of the canopy. Thus, an understanding of these principles is important in remote sensing with respect to military, agricultural, forestry, and ecological applications. For example, in recent years the thermal region of the electromagnetic spectrum has received keen interest in the remote sensing field. This region may add valuable additional information to make inferences concerning the characteristics of vegetation canopies. However, before the thermal emission characteristics of a canopy can be understood, the manner in which the canopy absorbs solar radiation must be studied. In the field of agriculture there is strong evidence that solar radiation distribution within a canopy as a function of canopy structure strongly affects the productivity of the canopy (Vidovic, 1973; Rhodes, 1971; and Donald, 1961).

Physically based mathematical models serve as convenient tools in studying the complex radiation-vegetation interactions. The objective of the study was to develop a mathematical physically based model to study the manner in which spectral and total solar radiation as a function of solar zenith angle are absorbed in vegetation canopies. The following describes the absorption model and the application of the model to a lodgepole pine (*Pinus contorta*) canopy at Leadville, Colorado for which a unique data base was collected during 1977. A complete study site description is given by Ranson, Kirchner, and Smith (1978). The specific canopy modeled consisted of a cluster of 4 lodgepole pine trees with the mean statistics: 6.0 m height, 30 yr. age, 13.2 cm diameter breast height, and a surrounding stand of 102 m^2/hectare basal area.

Solar Radiation Canopy Models

Several deterministic models have been developed to study the interactions of solar radiation within vegetation canopies. Allen and Richardson (1968), Alderfer and Gates (1971), and Suits (1972) have adapted a system of simultaneous differential equations, developed by Kubelka and Munk (1931), in various ways to vegetation canopies. Suits (1972) developed a model which includes geometric effects and predicts non-Lambertian characteristics of vegetation canopies. Chance and LeMaster (1978) have derived a light absorption model for vegetative plant canopies from the Suits reflectance model (1972).

Another approach developed by Oliver and Smith (1974) is the solar radiation vegetation canopy (SRVC) model. This model simulates the solar radiation flow through the canopy by utilizing physical laws and Monte Carlo techniques. This stochastic model originally predicted the diurnal apparent directional spectral reflectance of a vegetation canopy.

It is believed that the ray tracing technique utilized in the SRVC approach is advantageous as applied to solar radiation interactions within vegetation canopies for several reasons. The total effect of all possible events can be simulated if one knows the probability for each step in a sequence of events. Thus, as new knowledge becomes available on the probabilities for each step, the

SRVC framework can readily accept it. For example, if a researcher describes a non-Lambertian reflection or transmission distribution as a function of the source direction and leaf orientation, this information could be incorporated relatively easily within the SRVC framework. This framework has other advantages when applied to vegetation canopy modeling:

(1) Such a general framework can be easily modified to include additional considerations without having to examine their effect on the solution to differential equations as in the deterministic models.

(2) The model can be modified to accept any reasonable number of components within a scene. Thus, one could model a scene as complex as time permits to obtain reasonable geometric and spectral data of the components.

(3) Any relevant parameter, such as number of components, type of component, their reflectance, transmittance, and absorptance angle distributions, surface area, and spatial dispersion, may be varied in any desirable fashion, and the model can accept this information.

(4) The model can be modified to any reasonable number of discretized inclination and azimuthal angles for simulation.

(5) Diffuse skylight is treated as a set of independent source vectors.

(6) The model accounts for multiple reflection and transmission in both upward and downward directions.

The disadvantage of the proposed model is mainly one of the relatively large computer time involved per run.

For these reasons, the SRVC model was modified to produce a version of the model to study the solar absorption within vegetation canopies. A complete description of the original SRVC model is presented by Oliver and Smith (1974).

SRVC Absorption Model

An abbreviated description of the SRVC absorption model is as follows. The SRVC absorption model assumes that a vegetation canopy is composed of non-homogeneous layers of Lambertian elements of known geometric arrangement, statistical composition, and optical properties. The global radiation is composed of direct and diffuse sky radiation. The direct solar radiation is treated as a point source, and the diffuse radiation is divided into source sectors. These source sectors are created by dividing the hemisphere into inclination bands and then further dividing each band into sectors (Figure 1). This spherical coordinate framework serves as an accounting method for radiation transfer above and within the canopy system. The flux from each sector is simulated as a source vector (Figure 2). The interaction of each initial source vector from the sky with the canopy is then calculated independently. The model utilizes probabilities which govern the distribution of gaps within the vegetation to determine the transition of source vectors from point to point within the canopy.

The formulation developed by Idso and deWit (1970), which is a function of the canopy's geometry, has been incorporated to predict the probability of gap in the direction of the nine hemispherical bands for each canopy layer. In this particular study, three canopy layers of equal height were defined (Figure 2). The positive binomial distribution is used to describe these probabilities. Azimuthal

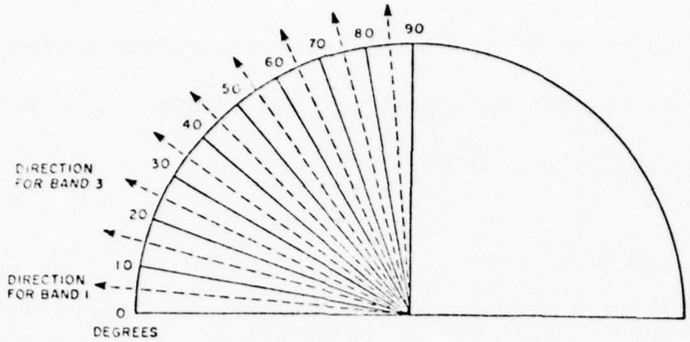

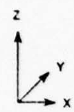

Horizontal view

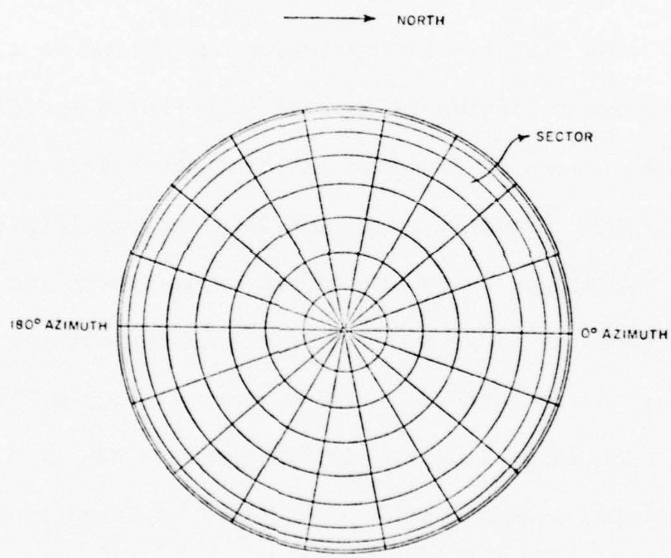

Vertical view

Figure 1. Horizontal and vertical views of the 9 hemispherical inclination bands which are divided into 18 equal azimuthal sectors. If one rotates the horizontal view about the Z axis the bands would occur in three-space.

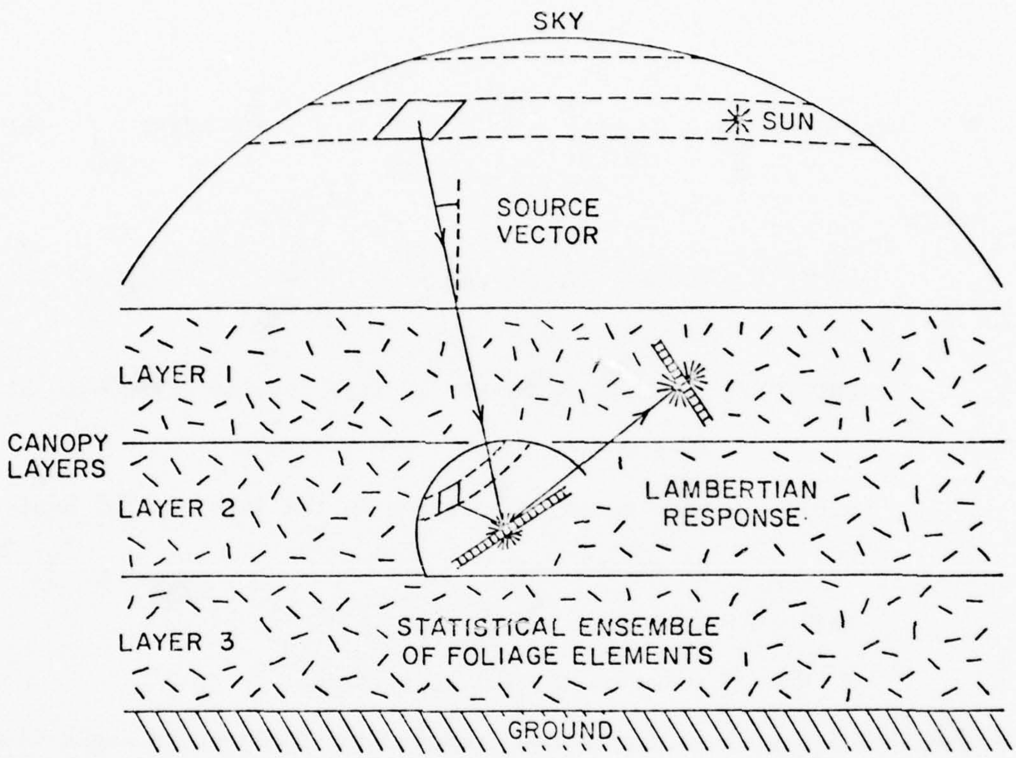

Figure 2. Schematic of a plant canopy approximated by stratified vegetation layers containing a statistical ensemble of Lambertian surfaces. Two interactions are shown with the corresponding source vectors representing reflection and transmission in a Lambertian manner.

symmetry is assumed. The probability of gap is equal to the ratio of the projection of canopy elements in any particular layer to the projection of the underlying soil surface for each hemispherical band. For a hemispherical band direction Θ (inclination angle) the equation is:

$$PGAP(\Theta) = \left[1 - \frac{S \cdot g(\Theta)}{\sin(\Theta)}\right]^{\frac{LAI}{S}} ; \; PHIT(\Theta) = 1 - PGAP(\Theta) \qquad (1)$$

where:

PGAP(Θ) = probability of gap in direction of hemispherical band Θ

PHIT(Θ) = probability of hit in direction of hemispherical band Θ

g(Θ) = mean canopy projection in the direction of hemispherical band Θ

LAI = leaf area index

S = index of spatial dispersion.

The function g(Θ) is determined from element inclination angle distributions which describe the orientation of the elements in a canopy layer. The derivation and computational procedure is presented by deWit (1965). The parameter S ranges from 0 to 1 and is an index of denseness or spatial dispersion of the components in a canopy layer. As S approaches 1, the more regular the dispersion of components and the less frequent a gap is encountered. The leaf area index (LAI) of a canopy layer is equal to the ratio of the total one-sided element area within a layer to the area of the underlying soil area. For a more in-depth discussion of the above theory and the required measurements see Kimes, Smith, and Berry (1978); Smith and Berry (1976); and Idso and deWit (1970).

When a canopy element or a ground element is hit, a proportion of the flux vector is reflected, transmitted, and absorbed into a number of flux vectors which simulate a Lambertian response (Figure 2). The direction of these vectors is determined by the element's orientation. The proportion of reflected and transmitted flux is determined by the spectral characteristics of the canopy elements. These resulting flux vectors are further processed in a similar fashion until all vectors are essentially zero, indicating absorption by canopy elements and ground, or escape from the canopy.

The SRVC model predicts the apparent directional spectral reflectance of a canopy in the nine hemispherical inclination bands.

The SRVC model was modified in the following manner to predict solar absorption. For each source vector-element interaction we know that:

$$P_{E_\lambda} = (\alpha_\lambda + \rho_\lambda + \tau_\lambda) \cdot P_{E_\lambda}$$

where:

P_{E_λ} = the proportion of spectral solar irradiance (E_λ) of a wavelength band represented by a source vector incident on a canopy element

α_λ = spectral absorption coefficient of canopy element

ρ_λ = spectral reflection coefficient of canopy element

τ_λ = spectral transmission coefficient of canopy element.

The reflectance and transmission values of the canopy elements for each discrete wavelength are input to the model. These coefficients are different for different types of canopy elements, and thus

α_λ, ρ_λ, τ_λ are dependent on the material type hit. The proportion of solar irradiance in a discrete wavelength that is absorbed by each canopy layer at a particular solar zenith angle is obtained by summing the absorbed proportion of all the source vectors incident on the canopy elements occurring within a particular layer.

$$\alpha_{\lambda,i,z} = \sum_{\text{all interactions}} \alpha_\lambda \cdot P_{E_\lambda}$$

where:

$\alpha_{\lambda,i,z}$ = the proportion of spectral solar irradiance at wavelength λ within layer i, i = 1, 2, 3, 4 where layer 4 designates the ground at solar zenith angle z.

The SRVC absorption model conserves energy, i.e., the sum of canopy reflectance and absorptance equals the incoming solar irradiance.

To estimate the absorbed total solar irradiance, it is necessary to numerically integrate the spectral absorption at a number of discrete wavelength bands over the entire electromagnetic spectrum. Because computer time required is directly proportional to the number of wavelengths simulated and the number of canopy elements, a simplified numerical integration scheme was devised as explained later.

Approach

To estimate the total and spectral global solar irradiance absorbed by the lodgepole pine canopy, the following information is required: canopy element area index for each canopy layer; normalized spectral solar irradiance curves ranging from 0° - 85° solar zenith angles; proportion of spectral irradiance absorbed by each canopy layer; and the mean canopy element spectral reflectance and transmittance for each discretized wavelength. The entire numerical approach is summarized in Figure 3. First the numerical approach will be presented followed by the data acquisition.

Using the above information and interpolation and integration techniques, the absorbed total solar radiation within each canopy layer is estimated as:

$$I_{i,z} = E_z \cdot \int (f_{\lambda,z} \cdot \alpha_{\lambda,i,z}) d\lambda$$

where:

$I_{i,z}$ = approximated integral of absorbed total solar flux within layer i at solar zenith angle z

E_z = total global solar irradiance at zenith angle z

$f_{\lambda,z}$ = normalized spectral solar irradiance curve at zenith angle z

$\alpha_{\lambda,i,z}$ = simulated proportion of spectral global solar irradiance absorbed by canopy layer i for a mean canopy element reflectance corresponding to wavelength band λ and solar zenith angle z.

The mean absorbed total solar flux absorbed per unit of canopy element surface area within layer i at solar zenith angle z can then be calculated as:

$$\frac{\Phi_{i,z}}{M^2} = \frac{I_{i,z}}{LAI_i}$$

where:

$\frac{\Phi_{i,z}}{M^2}$ = average absorbed total solar flux absorbed in layer i at solar zenith angle z per unit area of element

LAI_i = the total element surface area within layer i.

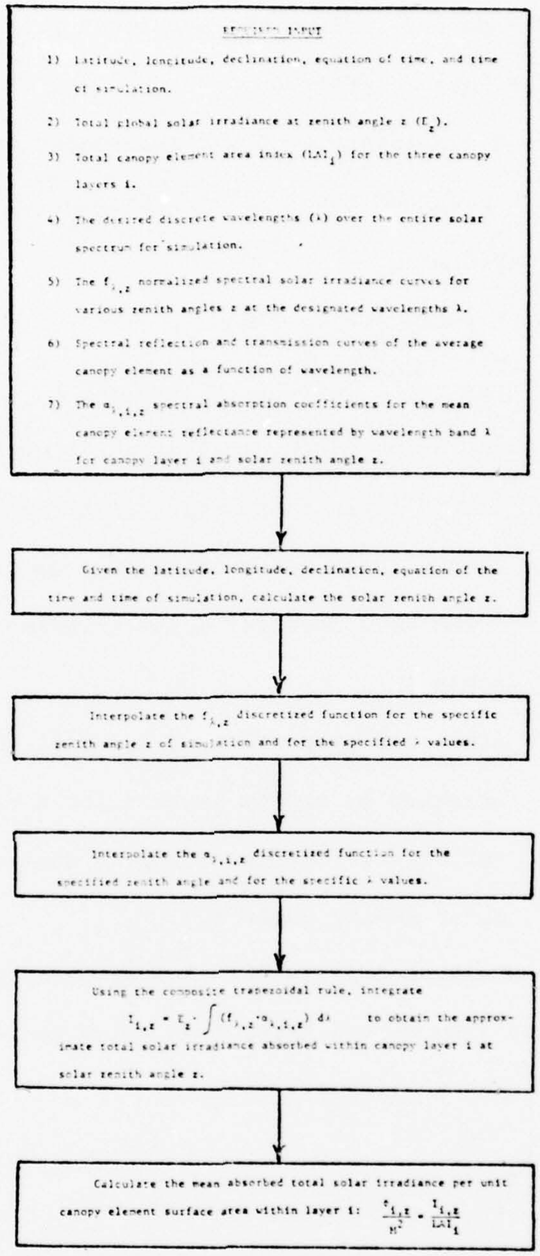

Figure 3. Numerical integration summary.

The spectral global irradiance absorbed by the canopy is estimated by the simulated $\alpha_{\lambda,i,z}$ coefficients.

The total absorption coefficient of a single isolated mean canopy element is estimated by:

$$A_z = \int (f_{\lambda,z} \cdot a_\lambda) d\lambda$$

where:

A_z = the total absorption coefficient of a single isolated mean canopy element under spectral irradiance conditions defined by solar zenith angle z

a_λ = spectral absorptance curve as a function of wavelength of the mean canopy element.

The method of numerical integration and normalization utilized throughout this study is as follows. The problem is to evaluate

$$I = \int_a^b f(x)dx$$

when f(x) is known only at a finite number of points. First, f(x) is approximated by a polynomial p(x) and then p(x) is integrated to obtain I. P(x) is described by using Newton's forward-difference interpolating polynomial (Conte and deBoor, 1965). The data utilized had non-uniform discretization intervals and a few relatively large intervals. In addition, the field data were not necessarily smooth by nature. Under these conditions, a higher order polynomial fit will not necessarily yield a more accurate approximation to the integral. Thus, for the sake of simplicity and computing time, a first degree polynomial was decided to be adequate for the purpose of integration. Thus, the composite trapezoidal rule (Conte and deBoor, 1965) was employed to approximate the integral of the above curves over any desirable [a,b].

The necessary parameters to determine the total and global absorbed radiation were determined as follows. The total canopy element area index (LAI) can be defined as the total surface area of the canopy elements (e.g., leaves, stems, and reproductive structures) divided by the projected ground area. The LAI was estimated by combining the canopy element area index for branches (BAI) and needles (NAI) for each canopy layer. The procedure involved measuring all branch diameters for all four modeling trees near the bole of the tree. Regression equations for lodgepole pine developed by Gary (1976) which relate branch diameter to the total branch and needle surface area for the top, middle, and base of the crown were utilized to derive LAI, BAI, and NAI for the total tree. The proportions of NAI and BAI for each canopy layer of equal height were derived from Gary (1976) and are presented in Table 1. The final estimated LAI for Layers 1, 2, and 3 were 2.4, 4.5, and 1.6, respectively, for a total canopy LAI of 8.5.

The distribution of global and diffuse solar energy as a function of wavelength was measured on a clear day at the study site using the U.S. Forest Service Circular Variable Filter Spectrometer (CVFS). The CVFS uses two continuously varying interference filters for spectral separation in the visible and near infrared regions with a half bandwidth of about 15-22 nm. The system has a 50 mm camera lens and an acrylic diffuser for input optics and a silicon diode operating in the photo voltaic mode as a detector. A digital readout is available (letter dated 14 December 1978 from Robert W. Dana, Physicist, Resources Evaluation Techniques Program, Rocky Mountain Forest and Range Experiment Station, U.S. Forest and Range Experiment Station,

Table 1. Proportion of BAI and NAI of respective totals for the three canopy layers of equal height. Data were derived from measurements on a single lodgepole pine tree (13.2 m height, 13 cm DBH) conducted by Gary (1976).

	Proportion	
Layer	NAI	BAI
1	0.28	0.23
2	0.53	0.49
3	0.19	0.28
total	1.00	1.00

U.S. Forest Service, 240 W. Prospect Street, Fort Collins, Colorado 80521). Thirty-one discrete spectral measurements for both diffuse and direct radiation were recorded within the range of .44 - 1.0 μm at 0850, 1025, and 1152 (Standard Time) during August 6, 1976. All measurements were taken within 13 minutes of the above times. These times correspond to solar zenith angles of 22°, 30°, and 47°, respectively. The proportion of total solar irradiance represented in the UV range (<.44 μm) and two IR ranges (1.0 - 2.0, <2.0 μm) were estimated from tables presented by Kondrat'yev (1965) which typify a theoretical clear and dry atmosphere. The general trends of the field data were compared with those theoretical curves (Kondrat'yev, 1965) by normalizing all solar spectral curves so that the integral of each curve equaled 1.0.

This computation aided in the ease of comparison between shifts in the above spectral curves and in later analysis. The computation involved integrating the relative magnitudes of the points within the .44 - 1.0 μm regions; and from tabular values (Kondrat'yev, 1965), the corresponding proportion of total solar irradiance in the remaining UV and IR regions were obtained. The normalized f_i values within interval (.44, 1.0) were then calculated as:

$$f_i' = \frac{f_i \cdot (1 - p)}{I'}$$

where:

f_i' = normalized f_i values

$f_i = f(x_i)$, $(i = 1, 2, ..., N)$ where $x_i \in (.44 - 1.0)$

I' = approximate integral on interval (.44, 1.0)

p = proportion of total solar energy outside the .44-1.0 μm region.

The measured solar spectrum does not span the entire solar zenith angle range. However, the normalized spectral curves as measured in the field were very similar in regard to spectral trends of the appropriate theoretical spectral curve (Figure 4). Further, because of the relatively small change in atmospheric path length between the three measured curves and the theoretical curve, the trends and absolute normalized magnitudes are similar. In addition, these curves correspond relatively well to the spectral irradiance curves reported by Gates (1966). As a consequence, the 4 theoretical curves as presented by Kondrat'yev (1965) for zenith angles of 0, 70, 80, and 85° (respective atmospheric path lengths of 1.0, 3.0, 6.0, 10.0) were utilized exclusively in this study for consistency (Figure 5). The proportion of solar irradiance in the UV and IR bands for the four theoretical curves are presented in Table 2. These four curves demonstrate that for a clear and dry atmosphere, as zenith angle increases, the path length through the atmosphere and the shift in the direction of longer wavelength increases. The general trends in spectral shifts of these curves were believed adequate.

These 4 normalized spectral solar curves can then be linearly interpolated for any specific zenith angle and for specified discrete wavelength intervals to obtain the desired discretized spectral solar irradiance function ($f_{\lambda,z}$) for zenith angle z and at wavelengths λ_i, i = 1,34.

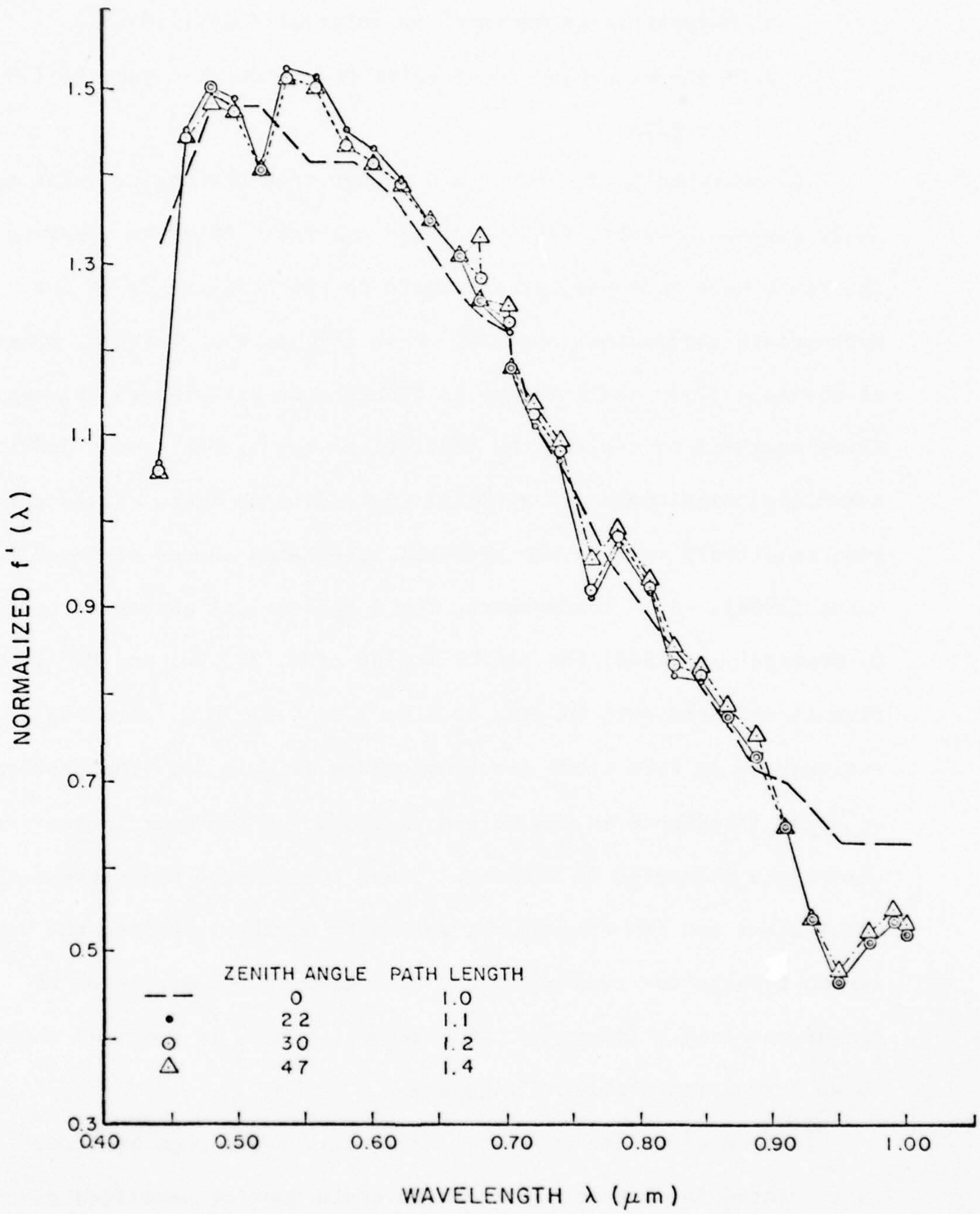

Figure 4. Normalized spectral solar irradiance curves as measured in the field for solar zenith angles of 22°, 30°, and 47°. In addition, the theoretical curve for a zenith angle of 0° from Kondrat'yev (1965) is shown.

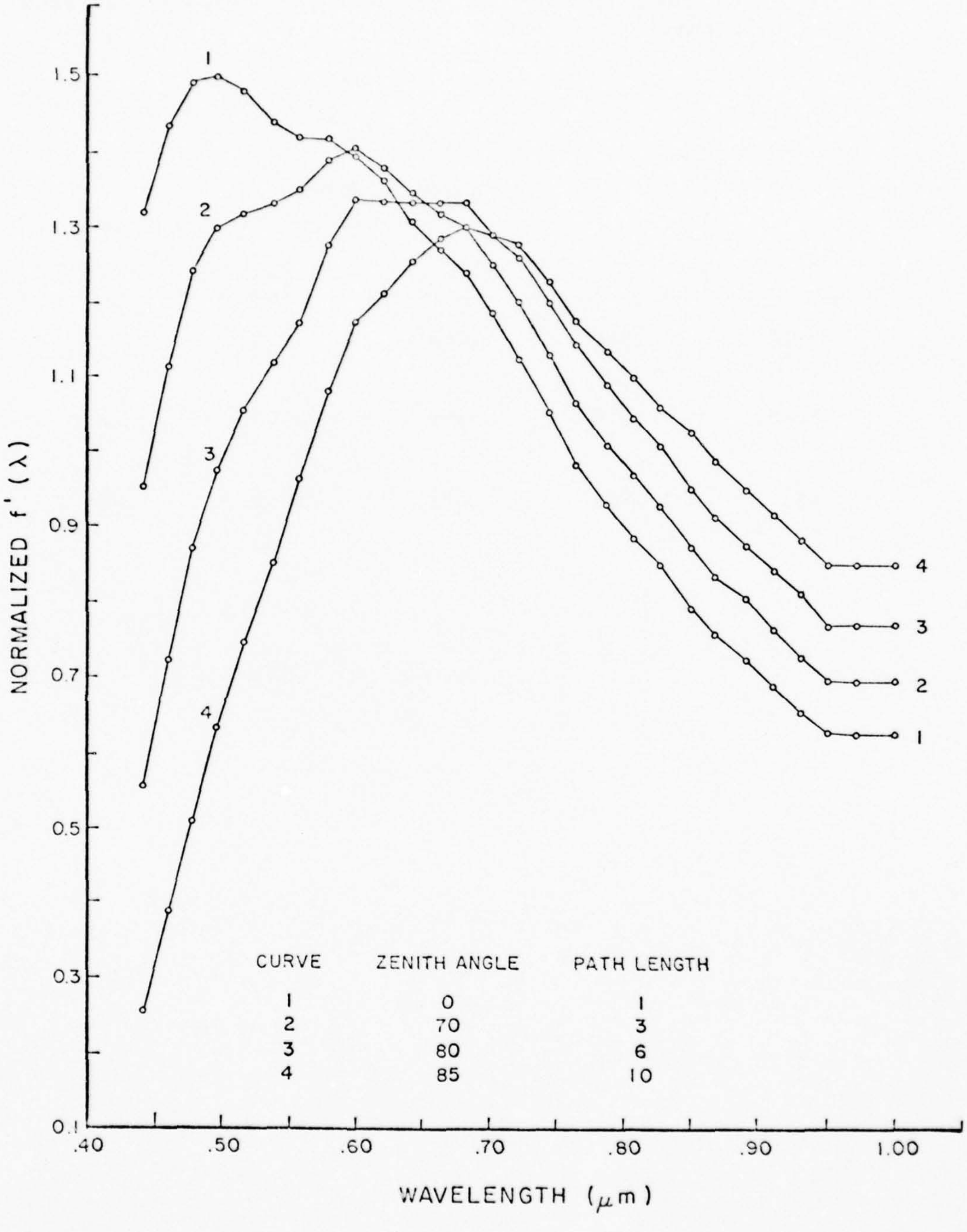

Figure 5. Theoretical solar irradiance curves for a clear and dry atmosphere (from Kondrat'yev, 1965).

Table 2. Theoretical proportion of total solar irradiance in the UV and IR regions as a function of zenith angle (from Kondrat'yev, 1965).

λμm	Solar zenith angle			
	0°	70°	80°	85°
<.44	.089	.048	.021	.007
1.-2.	.239	.269	.305	.343
>2.	.064	.072	.083	.094

The proportion of spectral solar irradiance as a function of solar zenith angle absorbed by each canopy layer is estimated by the SRVC absorption model. To simulate all permutations for each of the 34 discretized wavelengths, 2 canopy components (branches and needles), the entire range of solar zenith angles, and all possible diffuse/direct ratios of solar irradiance would be extremely costly and thus the following approach was employed to reduce the number of required simulations.

The spectral diffuse/direct ratio as derived from the U.S. Forest Service CVFR data collected at Leadville, Colorado, August 6, 1976 is presented in Figure 6. The ratio increased with increasing frequency and increasing solar zenith angle. Wavelengths near the UV region had a ratio of less than 0.15. A sensitivity analysis of the change in absorption coefficients for each layer versus a change in the diffuse/direct ratio for wavelengths of high and low canopy reflectance and zenith angles of 0° and 72° was completed. In the ratio range of 0.0-0.2, the change in the absorption coefficient is less than 0.03 in all cases. Thus, it is believed that for clear sky conditions at Leadville, Colorado, a constant diffuse/direct ratio of 0.06 is adequate for all wavelengths.

Rather than simulate two canopy elements (needles and branches) in each layer, one average element in spectral characteristics was simulated for each layer. The spectral reflectance of the branches and needles and needle transmittance were initially measured using an Isco Model SR Spectral Radiometer. Branches, mosaics of needles, and a barium sulfate reference panel were utilized to obtain reflectances. A metal plate with a thin slit was used to measure needle transmittance.

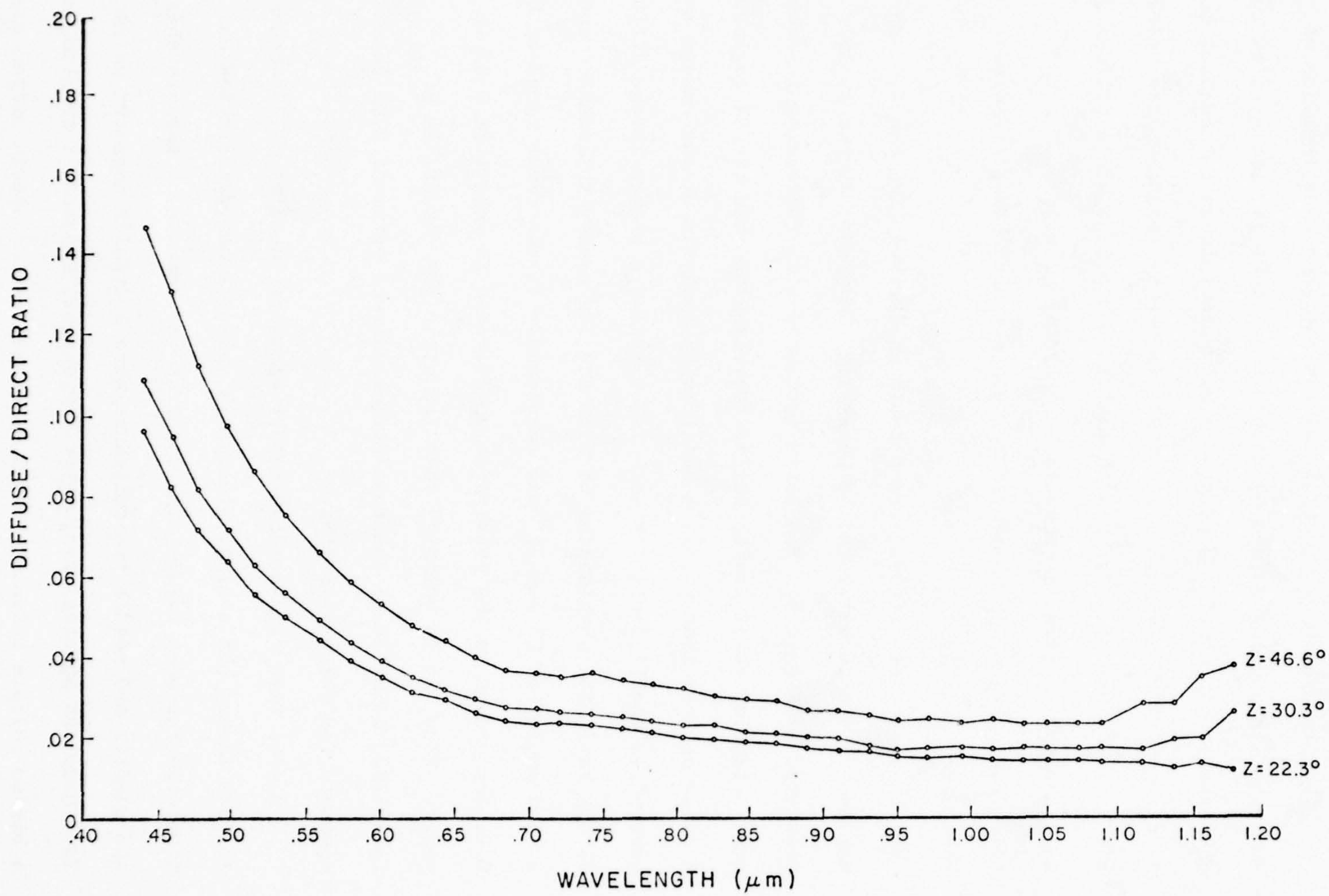

Figure 6. Measured diffuse/direct ratios of solar irradiance as a function of wavelength and zenith angle (Z).

In addition, a Modified Barnes Spectral Master Research Radiometer was utilized to measure the spectral reflectance curve of needles and branches. This radiometer had a 2° field of view (no needle mosaics were required) and produced a continuous curve from 0.25 to 1.20 μm. Using the above two instruments, 14 needle reflectance, 12 needle transmittance, and 11 branch reflectance samples were taken from various portions of a tree. The respective average spectral curves were then weighted according to the proportion of BAI and NAI for each canopy layer as measured by Gary (1976)(Table 1). The resulting spectral reflectance and transmittance curves of the average canopy element for each layer were very similar, thus only one set of mean spectral reflectance and transmittance curves were utilized for all three canopy layers as presented in Figure 7. The mean spectral reflectance curve corresponded closely to spectral reflectance curves of _Pinus resinosa_ needles as presented by Egan (1970). The curves in Figure 7 are used to calculate the spectral absorptance curve of the average canopy element for all three layers which is denoted as a_λ.

It was also essential that canopy absorption be shown insensitive to small changes in the average element transmission. The proportions of absorbed solar irradiance for a wavelength of high canopy reflectance (ρ = .50 for all canopy elements including the ground) for various element transmission coefficients and for zenith angles of 0° and 72° were simulated. The maximum standard deviation of the measured needle transmission for the six discrete wavelengths was 0.02 and corresponded to a near infrared wavelength (Figure 7). In the above sensitivity analysis a ±0.04 (two standard deviations) transmission change produced a maximum absorption coefficient change on

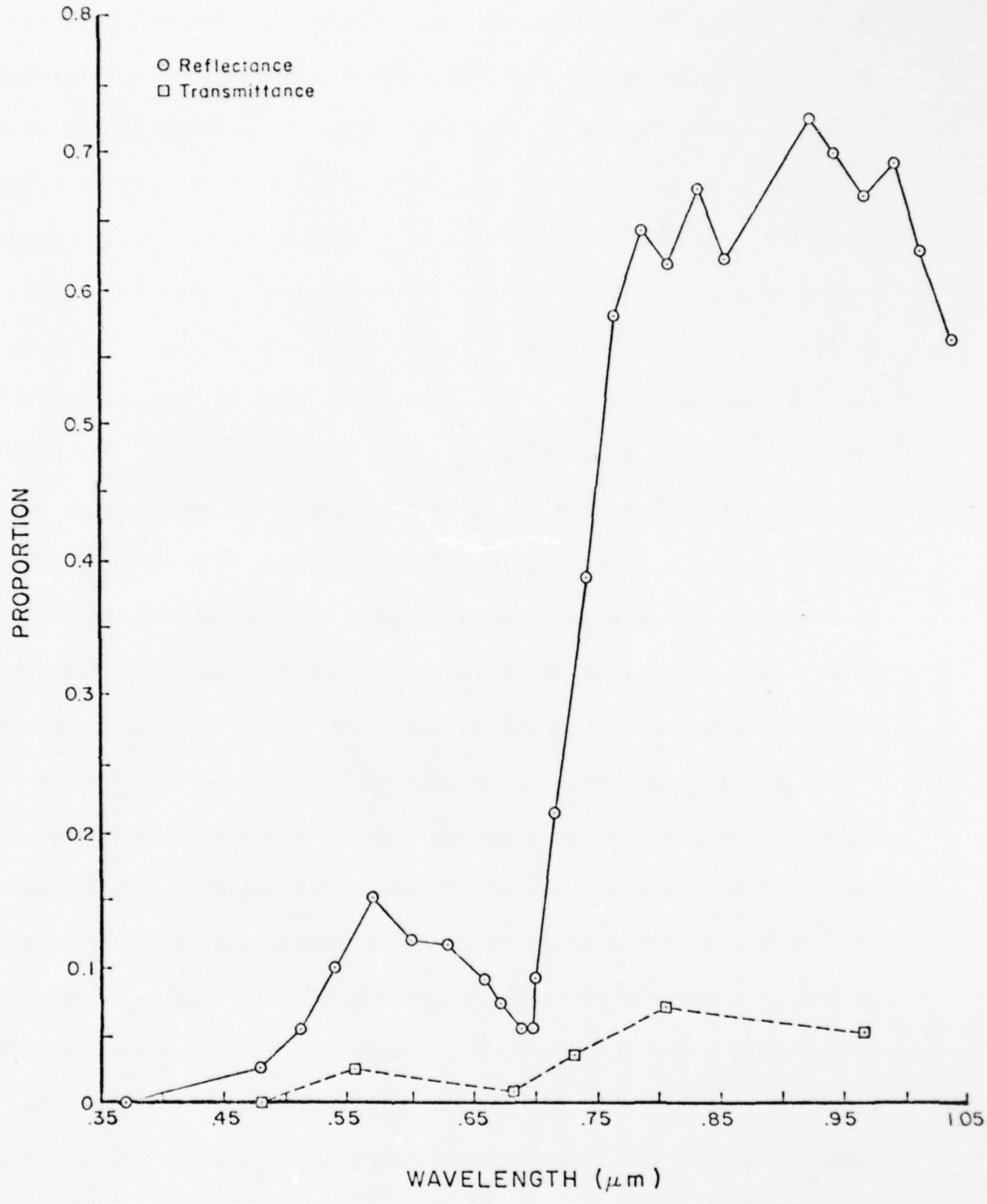

Figure 7. Mean canopy element reflectance and transmittance derived from radiometric field data.

the order of 0.01 for Layer 1 and a 0° solar zenith angle. The standard deviation for the 0.68 μm band was 0.0008. At low reflecting wavelengths any reasonable error in transmission will produce a small change in the absorption coefficients. In addition, it was found that the average canopy reflectance was correlated with the average canopy transmission (R^2 = 0.62 with reflectance being the independent variable).

The above suggests that only a few mean canopy element reflectance (MCR) values need to be simulated with the SRVC absorption model. Six MCR's were simulated ranging from 0.0 to 0.80 reflectance. Each MCR value simulated for all three canopy layers has a corresponding mean canopy element transmission factor and a ground reflectance factor. Thus, the MCR defines the optical properties of the entire canopy system. The above insensitivity and correlation of transmission allows one to make the transmission factors dependent only on MCR rather than wavelength. The background, composed of grasses and litter, was similar to the average canopy element reflectance except in the near IR region where the background was consistently lower in reflectance. As a consequence, at high MCR the corresponding reflectance of the background was scaled down relative to the MCR. The simulated MCR along with the corresponding canopy element transmission and the ground reflectance utilized are presented in Table 3.

Four runs utilizing the SRVC absorption model were made for solar zenith angles of 0°, 47°, 72°, and 87° using the following input parameters. The diffuse/direct ratio utilized for all runs was 0.06. The canopy element inclination angle distributions were derived by the laser diffraction technique as presented by Kimes, Smith and Berry

Table 3. Six mean canopy element reflectances (MCR) with corresponding canopy element transmission and ground reflectance.

Canopy reflectance	Canopy transmission	Ground reflectance
0.00	0.000	0.00
0.16	0.005	0.16
0.32	0.014	0.28
0.48	0.024	0.30
0.64	0.035	0.44
0.80	0.065	0.60

(1979). The S parameter was measured to be 0.1 by measuring the frequency of gap using black and white photographs which were taken looking vertically up through the canopy. A dot grid was applied to the photographs to estimate the probability of gap. The S parameter was then derived from Equation 1. The LAI values for each layer were derived as discussed above.

The resulting runs, which are presented in the Results and Discussion section, can be linearly interpolated for any solar zenith angle and MCR which corresponds to a specific wavelength (Figure 7) to estimate $\alpha_{\lambda,i,z}$.

The total global solar irradiance at zenith angle z was measured using a MARK I-G SOL-A-METER Silicon Cell Pyranometer. This measurement, denoted as E_z, when multiplied by the discretized $f_{\lambda,z}$ determines the magnitude of the spectral curve, whereas $f_{\lambda,z}$ determines the shape of the curve. Some error is introduced due to changing solar spectral effects as a function of solar zenith angle and the sensitivity of the silicon detector. However, this will effect only the magnitude of the spectral curve and not the theoretical spectral trend.

Model Verification

It is very difficult to measure the absorption of solar flux within the layers of the canopy. However, the model can be benchmarked against the measured reflected and transmitted solar flux densities within and above the canopy system.

A unique data base exists for the lodgepole pine stand at Leadville, Colorado (Ranson, Kirchner, and Smith, 1978). The data base consists of optical and thermal spectral measurements for various terrain and temporal features. In this particular study, the Scene Recording Radiometer (SRR) was principally utilized to obtain spectral reflectance and transmittance measurements of the four modeling trees.

The SRR instrument is described by Berry, Heimes, and Smith (1978). The SRR was suspended on support cables attached to two 15 m towers, which allowed spectral reflectance measurements from above the canopy to be obtained (Figure 8). The SRR consists of a six narrow band interference filter wheel interfaced to a Hasselblad EL 500 camera to provide a photographic record of the scene. All filtered spectral data were referenced to a barium sulfate painted panel to provide reflectance values. Filters used were centered at 4800, 6750, 7300, 8000, and 9600 Å. (The standard field of view (FOV) was 22.5°.) Vertical spectral reflectance above the four modeling trees was measured throughout 1977 and compared with the simulated reflectance values.

On September 17, 1977 at 1030 Standard Time the SRR was placed on the ground looking vertically up through the canopy of the modeling trees. A 12.7 mm diameter stop on the SRR optics was utilized with a FOV of 9° which restricted the FOV to the boundaries of the canopy. Two sample points were measured and the mean transmittance to the ground was calculated.

Two experiments were performed to evaluate the spectral reflectance variability of lodgepole pine canopies with changing solar zenith angle. SRR data taken from the tramway system of the four modeling trees were acquired on May 24, 1978, from 0642 - 1526 hours Mountain Daylight Time (MDT). Approximately 10 percent of the scenes was composed of snow understory. In addition, data were acquired for

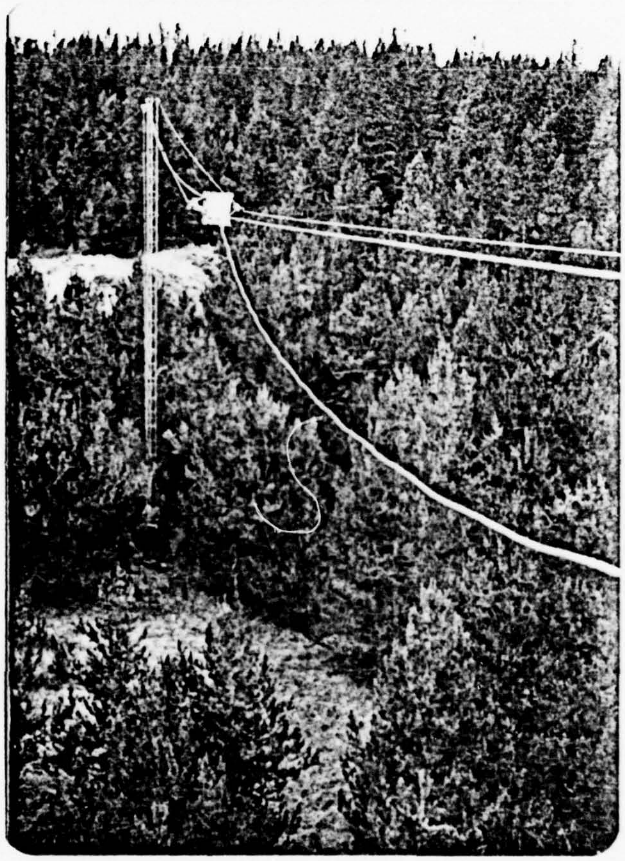

Figure 8. Suspended Scene Recording Radiometer (SRR) instrument on tramway system at Leadville, Colorado.

a different cluster of three lodgepole pine trees on August 4, 1976, from 0657 to 1400 hours MDT.

Results and Discussion

The measured spectral canopy transmittance to the ground versus the simulated values are shown in Figure 9. Considering the small magnitude of the spectral transmittance values, the accuracy of prediction is very good.

A typical comparison between the measured vertical spectral reflectance of the four lodgepole pine trees versus the simulated reflectance is presented in Figure 10.

The simulated total absorption coefficients A_z of a single isolated mean canopy element for solar zenith angles of 0°, 47°, 75°, and 85° were .68, .67, .65, and .60, respectively. Jarvis et al. (1976) states that the optical properties of coniferous needles are poorly known due to difficulties in making spectral measurements with conventional spectrophotometric equipment. However, Gates et al. (1965), assuming zero transmissivity, found a mean value of absorption of 0.88 for needle mosaics of Pinus strobus using a spectral solar irradiance curve of a sunny day. It is important to note that the total A_z is not constant but is a function of the solar irradiance conditions which change as a function of solar zenith angle. Gates (1970) has shown that the total absorption coefficient of leaves of various plants can change as much as 0.13 between sunny and cloudy irradiance conditions.

The SRVC absorption coefficients $\alpha_{\lambda,i,z}$ for the six MCR for solar zenith angles of 0°, 72°, and 89° are presented in Figure 11.

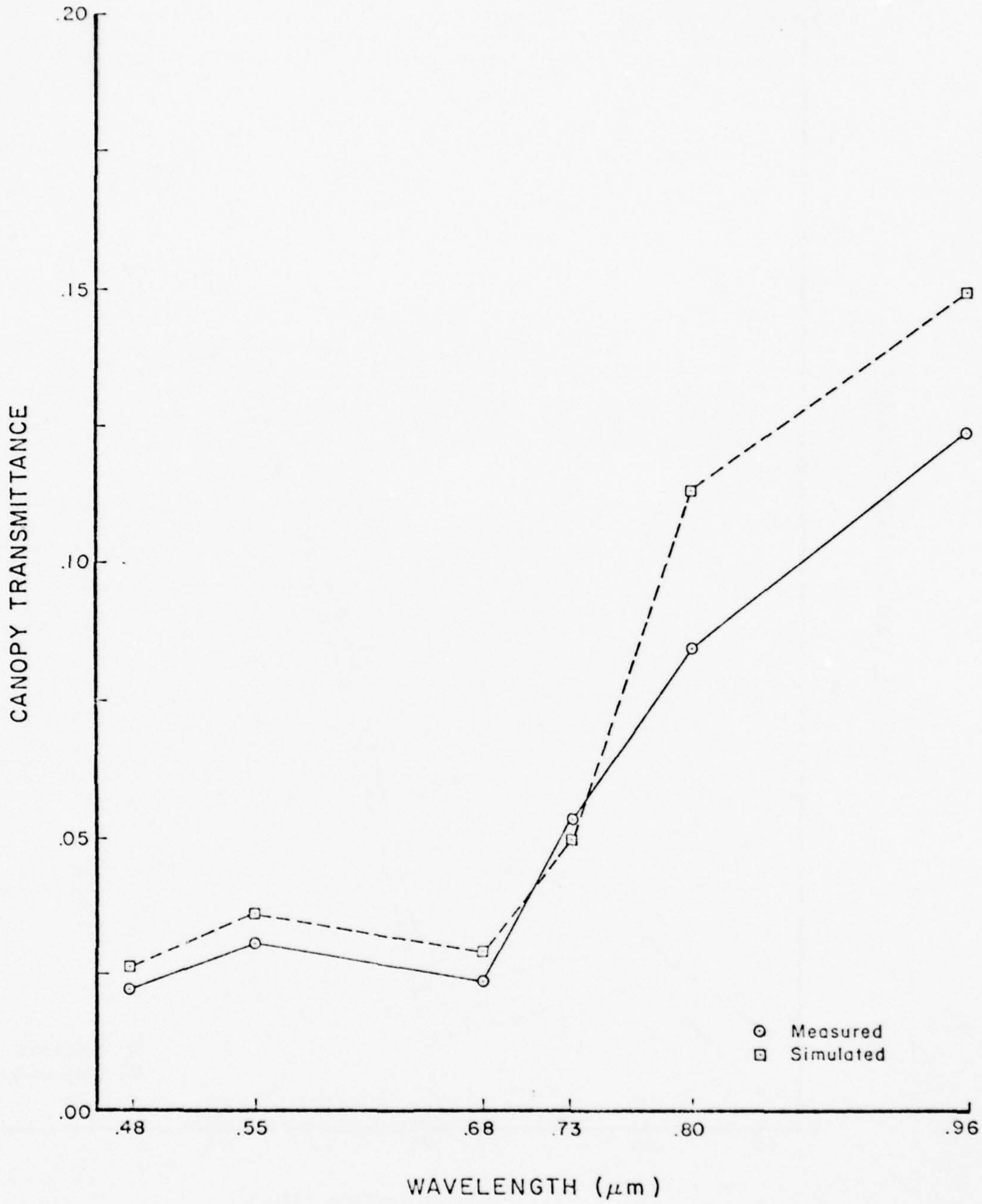

Figure 9. Measured versus simulated spectral canopy transmittance to the ground level.

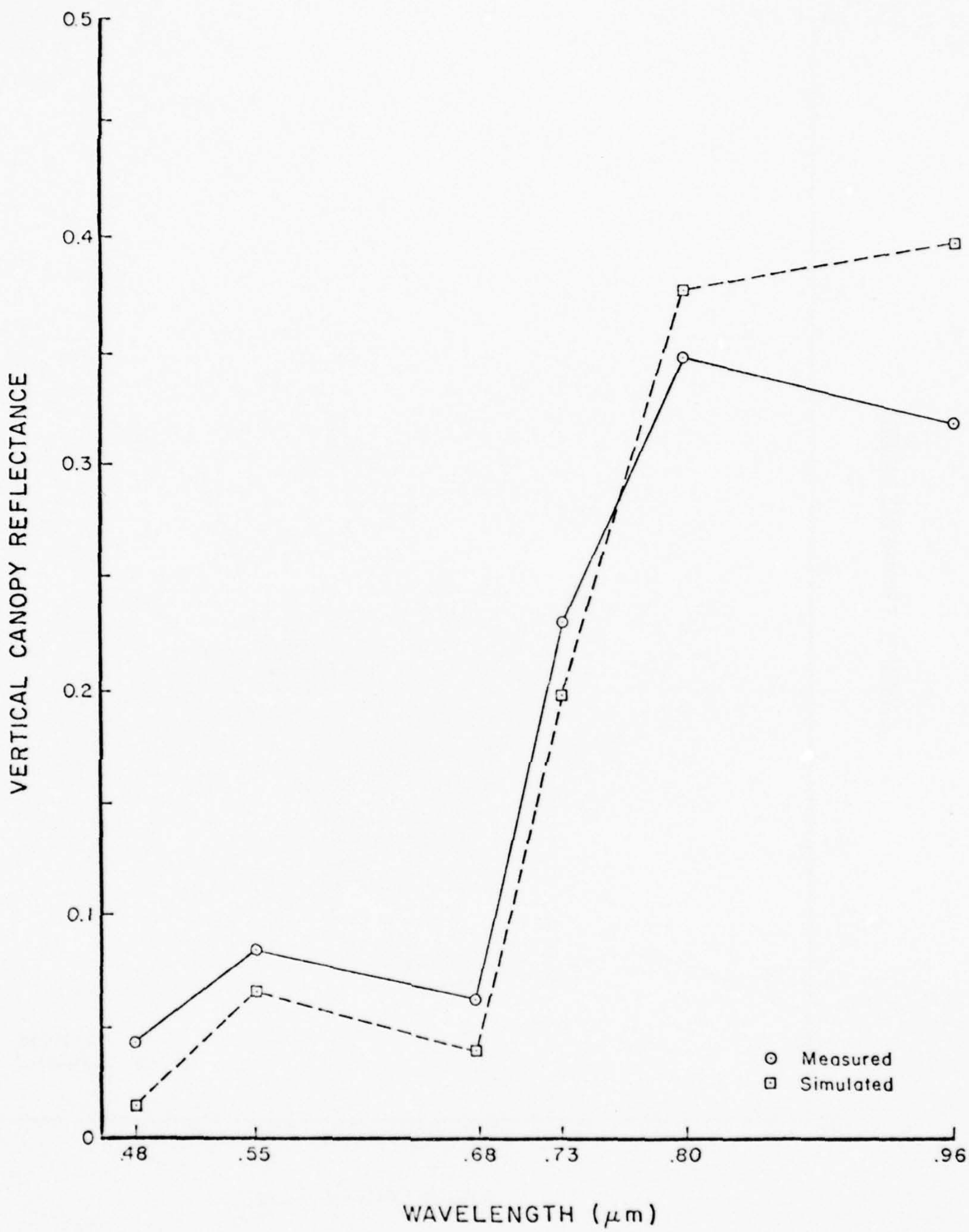

Figure 10. Measured versus simulated vertical spectral canopy reflectance for May 24, 1978, 1200 Standard Time.

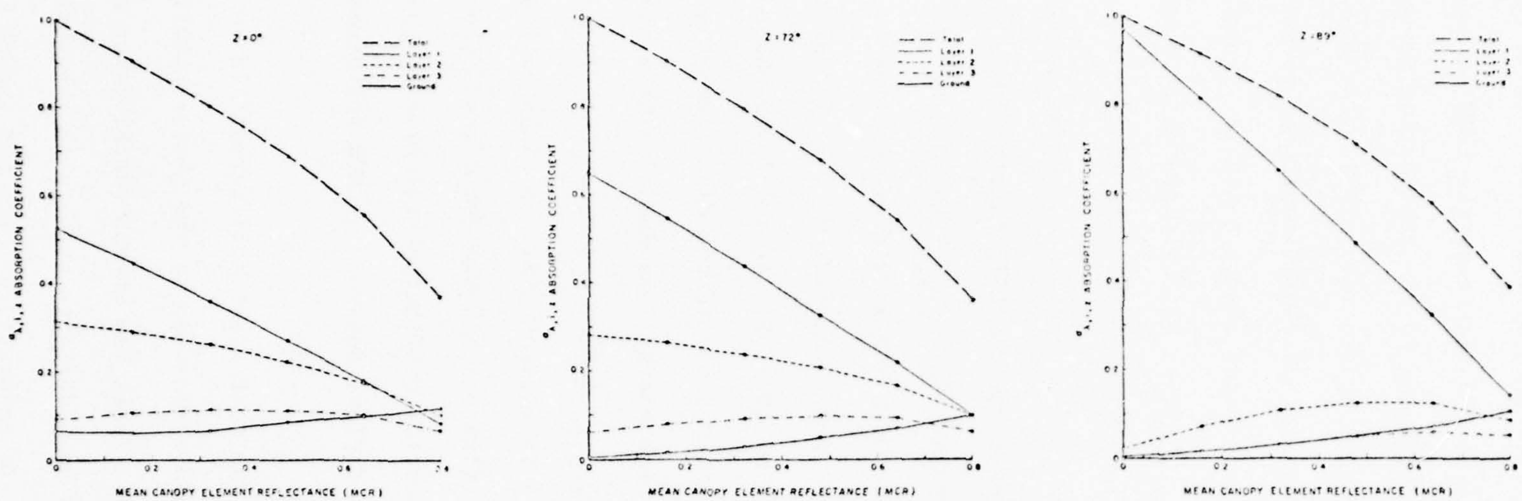

Figure 11. SRVC simulated $\alpha_{\lambda,i,z}$ absorption coefficients for various mean canopy element reflectances and a solar zenith angle of 0°, 72°, and 89°, respectively. The $\alpha_{\lambda,i,z}$ for each canopy layer is presented as well as the total proportion of the spectral irradiance absorbed.

The $\alpha_{\lambda,i,0°}$ and $\alpha_{\lambda,i,47°}$ curves were very similar. It is hypothesized that this similarity is due to the fact that the PGAP at solar zenith angles of 0° and 45°, corresponding to the inclination invervals of 85° and 45°, respectively, in Table 4, are very similar for any given canopy layer. Thus, the transfer of radiation should be somewhat similar. Several interesting trends are apparent in Figure 11.

The trends seen for $\alpha_{\lambda,i,0°}$ can be explained as follows. The differences in the absorption coefficients seen in each canopy layer are due to a complex interaction of radiation, canopy geometry, optical properties of canopy elements, LAI distributions, and spatial arrangement of canopy elements. The $\alpha_{\lambda,1,0°}$ and $\alpha_{\lambda,2,0°}$ decrease as the MCR increases because at high MCR an energy loss due to high element reflection is dominating. However, $\alpha_{\lambda,3,0°}$ is relatively constant and peaks at a MCR of .3 - .5. At the lower MCR relatively little energy is reaching Layer 3 due to the high element absorptance, and at the higher MCR the high energy loss due to high element reflection is dominating. The $\alpha_{\lambda,4,0°}$ (where 4 denotes the ground layer) consistently increases with increasing MCR. At higher MCR a relatively large proportion of flux reaches the ground, and the ground has a relatively high absorption coefficient relative to the canopy elements (Table 3). These factors dominate as MCR increases and thus $\alpha_{\lambda,4,0°}$ increases.

It is important that the most drastic differentials in the $\alpha_{\lambda,i,z}$'s occur at low MCR which would correspond to the photosynthetic active radiation (PAR) absorption. Thus, the uneven distribution of absorbed PAR within the canopy will have definite effects on the photosynthetic efficiency of the canopy. In contrast, at high MCR the $\alpha_{\lambda,i,z}$'s tend

Table 4. Simulated probability of gap (PGAP) through each canopy layer at the nine different inclination view angle intervals.

	Inclination view angle								
	5	15	25	35	45	55	65	75	85
Layer 1	.03	.30	.41	.46	.48	.49	.50	.50	.50
Layer 2	.00	.10	.19	.23	.25	.26	.27	.27	.27
Layer 3	.13	.47	.57	.61	.62	.63	.63	.63	.63

to converge due to the large degree of multiple scattering, and consequently a more even distribution of absorbed spectral flux is assumed.

The $\alpha_{\lambda,1,72^\circ}$ curve increases slightly in magnitude relative to $\alpha_{\lambda,1,0^\circ}$ for all MCR which dictates that the flux reaching Layer 2 should be less, and as a consequence $\alpha_{\lambda,2,72^\circ}$ decreases slightly for all MCR relative to $\alpha_{\lambda,2,0^\circ}$. A similar argument can be made for the slight decrease in $\alpha_{\lambda,3,72^\circ}$ and $\alpha_{\lambda,4,72^\circ}$ which is most noticeable at low MCR. These changes are not large, and can be partially explained by the fact that the simulated PGAP's, which are important in radiation transfer for the solar zenith angles of 0°, 47°, and 72° corresponding to inclination intervals of 85, 45, and 25, respectively, do not change drastically (Table 4).

The $\alpha_{\lambda,i,89^\circ}$ curve shows that Layer 1 absorbs most of the energy except at high MCR. At low MCR (e.g., PAR) Layer 1 essentially absorbs all incident energy due to the very low PGAP (Table 4). The $\alpha_{\lambda,2,89^\circ}$ curve assumes the same general shape as $\alpha_{\lambda,3,z}$ in the previous runs.

Figure 12 presents the simulated proportion of spectral solar irradiance at various MCR values that reaches the ground level at a solar zenith angle of 0° and 89°. As one proceeds from a low MCR to a high MCR, the proportion of spectral solar irradiance reaching the ground increases exponentially due to the increase in element reflectance and multiple scattering. This phenomenon has been observed by many investigators, for example Jarvis _et al_. (1976) and Ross (1976).

Upon inspection, the $\alpha_{\lambda,total,z}$ in Figure 11 change very little as a function of solar zenith angle. Two plots were produced for

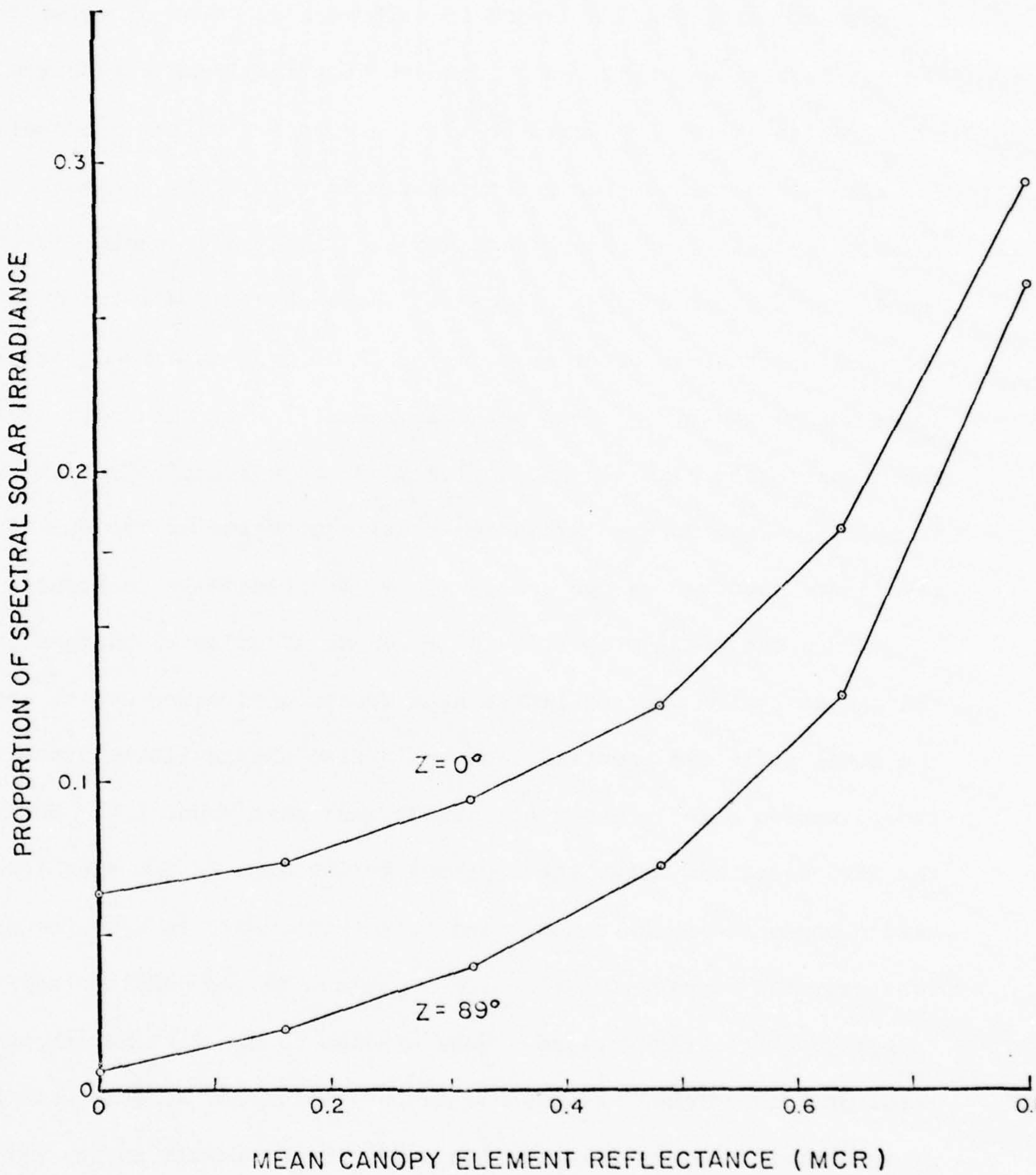

Figure 12. Simulated proportions of solar spectral irradiance for various MCR values that reach the ground level at solar zenith angles of 0° and 89°.

further analysis. Figure 13 shows the SRVC simulated α_i spectral absorption coefficient for a MCR of 0.16 as a function of solar zenith angle. As can be noted, the α_i changes drastically as a function of solar zenith angle; however, the total proportion of the spectral irradiance absorbed by the canopy system is relatively constant. The modeling results from Chance and LeMaster (1978) have shown similar trends for a wheat canopy. Figure 13 shows the SRVC simulated α_i spectral absorption coefficient for a MCR of 0.64 as a function of solar zenith angle. α_i does not change drastically with solar zenith angle due to the high element reflectance and a relatively high degree of multiple scattering. Again the total proportion of the spectral irradiance absorbed by the canopy system is relatively constant.

Since the total proportion of spectral irradiance absorbed by the canopy system changes little as a function of solar zenith angle, the total reflected spectral flux would also change little since the canopy system's reflectance and absorptance must equal 1.0. However, the SRVC model simulates the apparent reflectance in the nine inclination bands above the canopy, and this reflectance is by no means constant with varying solar zenith angle due to the complex radiation-canopy geometry interactions. Many studies do not distinguish between total and directional reflectance factors which may dictate what kind of reflectance versus solar zenith angle trends result in any particular study.

For example, within this study the simulated total spectral flux absorbed by the canopy system is essentially constant with solar zenith angle. However, the simulated vertical spectral reflectance shows definite trends as seen in Figure 14. Sun angle experiments,

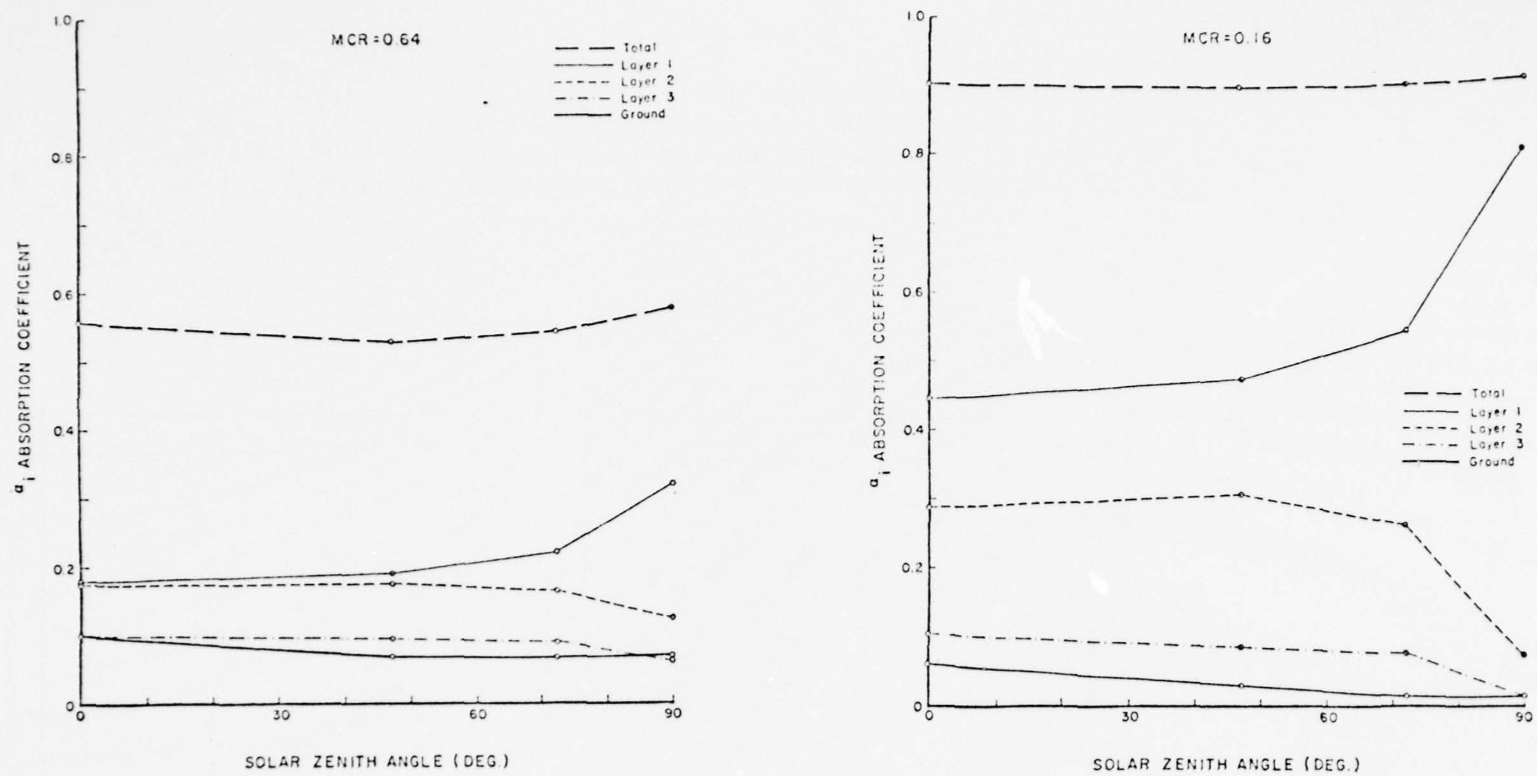

Figure 13. SRVC simulated α_i spectral absorption coefficients for a mean canopy component reflectance (MCR) of 0.64 and 0.16 as a function of solar zenith angle. The α_i for each canopy layer is presented as well as the total proportion of the spectral irradiance absorbed.

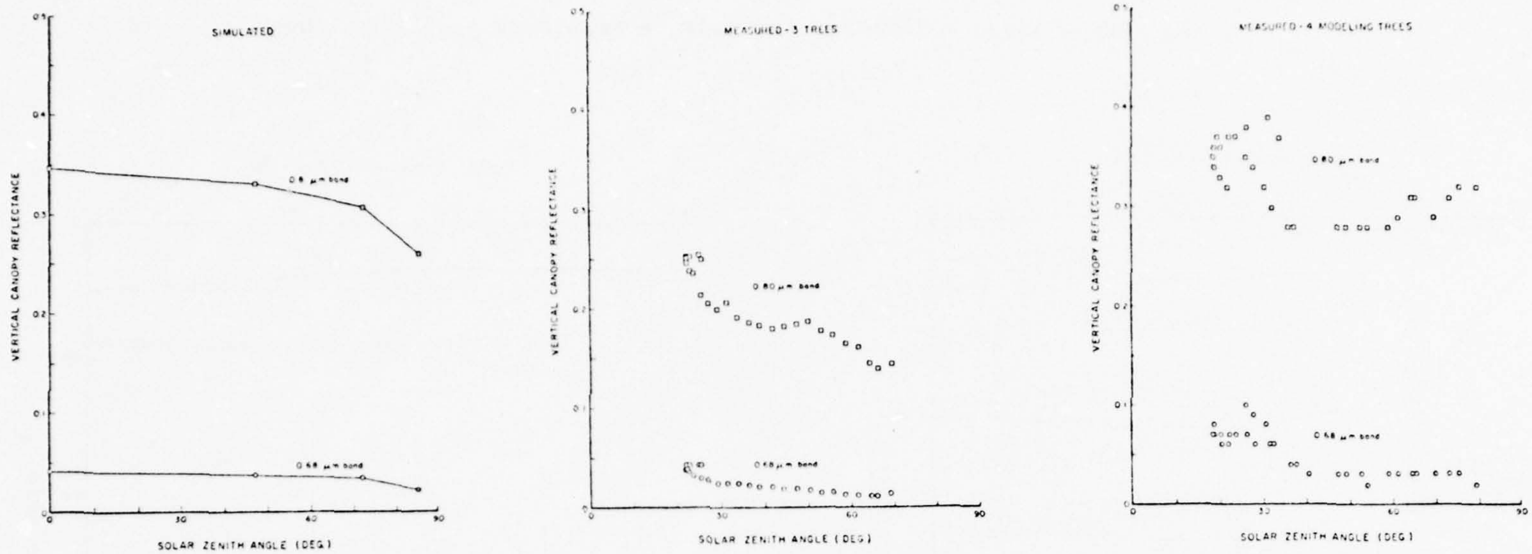

Figure 14. Vertical canopy reflectance as a function of solar zenith angle for the 0.68 and 0.80 μm bands for the simulated data, the measured data of a group of three trees, and the measured data of the four modeling trees.

discussed previously, using the SRR instrument were conducted on the four modeling trees and on a nearby cluster of three trees. The results of vertical reflectance versus solar zenith angle of these two targets for the 0.68 μm band and the 0.80 μm band, corresponding to a MCR of .064 and .538, respectively, are presented in Figure 14. The simulated results of the three trees deviate from the measured results in magnitude, which might be expected since the targets are two distinct points. However, a decreasing reflectance with increasing solar zenith angle is seen in both simulated and measured results. The same general trends exist for the results of the four modeling trees with better correspondence in magnitude to the simulated results (Figure 14).

The simulated proportion of total global solar irradiance absorbed by the lodgepole pine canopy system as a function of solar zenith angle is presented in Figure 15. The total global solar irradiance absorbed by the canopy system is essentially constant with changing solar zenith angle, and therefore, the total reflectance is essentially constant. However, the proportions absorbed by Layers 1 and 2 are clearly dependent on solar zenith angle. As solar zenith angle increases, the PGAP for Layer 1 decreases and thus, the absorption in Layer 1 increases. In contrast, as solar zenith angle increases, the proportion of flux reaching Layer 2 decreases due to the lower PGAP of Layer 1 at higher solar zenith angles.

Bergen (1971, 1974) has shown in a 10 m tall lodgepole pine canopy that the air temperature maximum occurs in the upper crown during the morning period and then descends deeper into the crown as the solar zenith angle decreases for clear sky and low wind speed

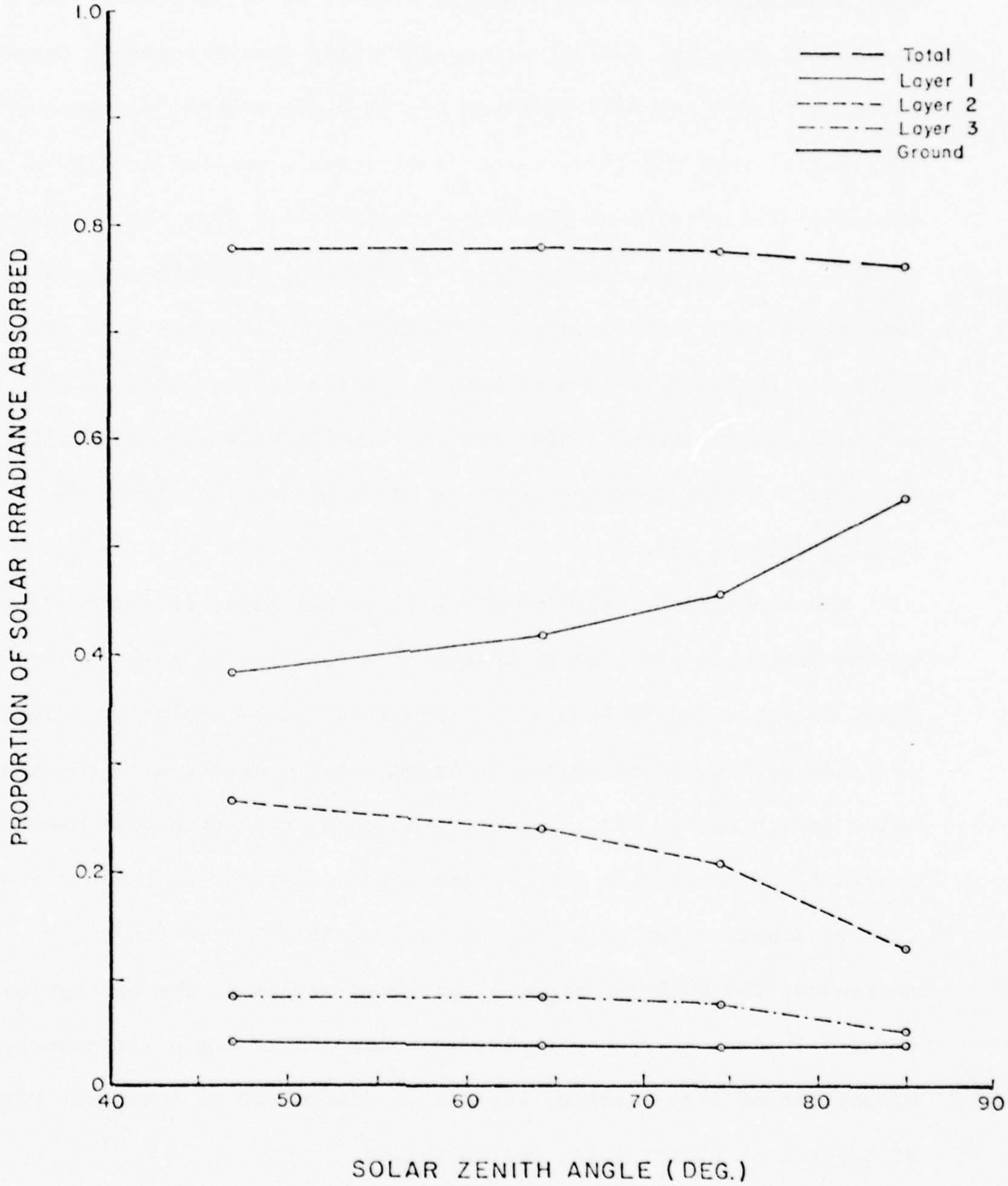

Figure 15. Simulated proportion of global solar irradiance absorbed by the lodgepole pine canopy system (total), Layer 1, Layer 2, Layer 3, and the ground, as a function of solar zenith angle for October 14, 1977.

conditions. The maximum temperatures move from the 9 m level to the 7 m level during the day. This phenomenon suggests that the foliage heated by the solar irradiance is the cause of the shifting maximum air temperature level (Bergen, 1971). Figure 15 demonstrated a shift of levels at which the maximum global solar irradiance is absorbed. At the greatest solar zenith angles, Layer 1 clearly absorbs the largest proportion of global solar irradiance. However, at relatively low solar zenith angles, the proportion of solar global irradiance absorbed by Layers 1 and 2 begins to converge indicating the level of maximum absorbed solar irradiance is shifted down into the canopy. This can be explained by the PGAP as a function of view angle as discussed above. Bergen (1974) states that forest productivity studies require more quantitative data of canopies such as radiation flux absorption.

In future work it is anticipated that the SRVC absorption model will be used to study PAR absorption within canopies of various geometric structures. In addition, the results of this study will be combined with a comprehensive thermal canopy signature model (TCSM) recently developed at Colorado State University to study the thermal behavior of the lodgepole pine canopy.

Conclusions

A solar radiation vegetation canopy absorption model has been developed which has several advantageous features for quantifying solar absorption within vegetation canopies under a variety of environmental and plant conditions. Under a theoretical clear and dry atmosphere and a correspondingly low diffuse/direct solar irradiance ratio, the following measured and simulated results were found for a specific lodgepole pine canopy.

1) The simulated results correspond relatively well with the measured reflectance and transmittance data.

2) Large differentials occur in spectral absorption by canopy layers especially in the photosynthetic active radiation region as a function of solar zenith angle and canopy geometry, which may have significant effects on the photosynthetic efficiency of the canopy.

3) As one proceeds from a low MCR to a high MCR the proportion of spectral irradiance reaching the ground increases exponentially.

4) Although it is believed that the total spectral reflection by the canopy system is relatively constant with solar zenith angle, the vertical spectral reflectance of the canopy decreases with increasing solar zenith angle.

5) Both the total and spectral global irradiance absorption by the entire lodgepole pine canopy system are relatively constant with solar zenith angle. However, the proportion of total and spectral global irradiance absorbed by individual canopy layers varies greatly as a function of solar zenith angle.

References

Alderfer, R.G. and D.M. Gates. 1971. Energy Exchange in Plant Canopies. Ecology, 52(5):855-861.

Allen, W.A. and A.J. Richardson. 1968. Interaction of Light with a Plant Canopy. J. Opt. Soc. Am. 58(8):1023-1028.

Bergen, J.D. 1971. Vertical Profiles of Wind Speed in a Pine Stand. Forest Sci. 17:314-321.

Bergen, J.D. 1974. Vertical Air Temperature Profiles in a Pine Stand: Spatial Variation and Scaling Problems. Forest Sci. 20:64-73.

Berry, J.K. 1976. Extracting Scene Feature Vectors Through Modeling. Ph.D. Dissertation, Colorado State University, Fort Collins, Colorado. 169 p.

Berry, J.K., F.J. Heimes, and J.A. Smith. 1978. A Portable Instrument for Simultaneous Recording of Scene Composition and Spectral Reflectance. Optical Engineering 17(2):143-146.

Chance, J.E. and E.W. LeMaster. 1978. Plant Canopy Light Absorption Model with Application to Wheat. Applied Optics, 17(16):2629-2636.

Conte, S.D. and C. deBoor. 1965. Elementary Numerical Analysis. McGraw-Hill Book Company. 396 p.

deWit, C.T. 1965. Photosynthesis of Leaf Canopies. Agr. Res. Rep. 663:1-57.

Donald, C.M. 1961. Competition for Light in Crops and Pastures. Symp. Soc. Exp. Biol. 15:282-313.

Egan, W.G. 1970. Nonimaging Optical Differentiation of Forest Foliage. For. Sci. 16:79-94.

Gary, H.L. 1976. Crown Structure and Distribution of Biomass in a Lodgepole Pine Stand. USDA For. Serv. Res. Pap. RM-165, Rocky Mountain For. and Range Experiment Station, Fort Collins, Colorado. 20 p.

Gates, D.M. 1966. Spectral Distribution of Solar Radiation at the Earth's Surface. Science, 151(3710):523-529.

Gates, D.M. 1970. Physical and Physiological Properties of Plants. In: Remote Sensing with Special Reference to Agriculture and Forestry. National Academy of Sciences, Washington, D.C. 424 p.

Gates, D.M., H.J. Keegan, J.C. Schleter, and V.R. Weidner. 1965. Spectral Properties of Plants. Applied Optics, 4:11-20.

Idso, S.B. and C.T. deWit. 1970. Light Relations in Plant Canopies. Applied Optics, 9(1):177-184.

Jarvis, P.G., G.B. James and J.J. Landsberg. 1976. Coniferous Forest. In: Vegetation and the Atmosphere, Vol. 2 (J.L. Monteith, ed.) Academic Press, New York, New York. 439 p.

Kondrat'yev, K. Ya. 1965. Actinometry. Translation of "Aktinometriya" Gidometeorologi Cheskoye Izdatel' Stvo, Leningrad, 1965. National Aeronautics and Space Administration, Washington, D.C. Nov. 1965. NASA TT F-9712.

Kubelka, P. and F. Munk. 1931. Ein Beitrag Zur Optik Der Farbanstriche. Z. Tech. Physik, 11:593-601.

Oliver, R.E. and J.A. Smith. 1974. A Stochastic Canopy Model of Diurnal Reflectance. Final Report. U.S. Army Research Office, Durham, North Carolina, DAH C04-74-60001. 105 p.

Ranson, K.J., J.A. Kirchner, and J.A. Smith. 1978. Scene Radiation Dynamics, Vol. II, Data Library. Final Report. Environmental Laboratory, U.S. Army Engineer Waterways Experiment Station. DACW 39-77-C-0073.

Rhodes, I. 1971. The Relationship Between Productivity and Some Components of Canopy Structure in Ryegrass (Lolium spp.) II. Yield, Canopy Structure and Light Interception. J. Agric. Sci., Camb. 77:283-292.

Ross, J. 1976. Radiative Transfer in Plant Communities. In: Vegetation and the Atmosphere, Vol. 1. Principles (J.L. Monteith, ed.) Adacemic Press, London.

Suits, G.H. 1972. The Calculation of the Directional Reflectance of a Vegetation Canopy. Remote Sensing of Environment, 2:117-125.

Vidovic, J. 1973. Effect of the Change of Leaf Angle Arrangement on Productivity of Maize (Zea mays L.) Stands. Bio. Plantarum (Phraha), 16(3):174-183.

3.0 A THERMAL VEGETATION CANOPY MODEL OF SENSOR RESPONSE

Abstract

A thermal canopy signature model (TCSM) was developed to approximate the thermal behavior of a vegetation canopy by a mathematical abstraction of three horizontal layers of vegetation. The geometry of canopy elements within each layer is quantitatively described by the foliage orientation distribution and number density. Given this geometric information for each layer and the driving variables (direct/diffuse solar irradiance, air temperature, horizontal wind velocity, relative humidity, and ground temperature) the energy budgets of average leaves within each layer are determined. The resulting system of conservation equations is solved for the average layer temperature. This information is then used to calculate the response of a thermal infrared sensor at varying view angles above and within the canopy. The model is applied to lodgepole pine (Pinus contorta) canopy and the results are validated with both radiometric and contact temperature measurements. The simulated average layer temperatures closely follow air temperature due to the high leaf area index values of the lodgepole pine canopy and the small dimensions of the needles. Simulated versus measured radiometric average temperatures of Layer 2 correspond approximately within 2°C. Simulated results suggest that canopy element geometry can significantly influence the effective radiant temperature of a sensor above the canopy as a function of view

angle. This phenomenon has important implications on the optimum view angle for making inferences about the target of interest.

Introduction

Radiant energy interacts with a vegetation canopy in a complex manner. A vegetation canopy can generally be defined as a stand of one or many plant species. The interactions of radiation and other energy exchanges with the individual canopy elements (leaves, stems, and reproductive structures) include solar radiant absorption, reflection, and transmission; thermal radiant emission, absorption, and reflection; convection; transpiration; conduction; photosynthesis; and respiration. The interactions between the ensemble of canopy elements, the sky, ground, and air determines the resulting thermal behavior, solar radiation regime, and thermal radiation regime of the canopy structure. Ross (1976) discusses the factors which determine the resulting radiation regimes in plant canopies. Monteith (1973) and Gates (1968) discuss the thermal behavior of vegetation elements.

An understanding of the underlying principles involved in the above radiation and energy regimes is important to remote sensing applications. Such basic knowledge is needed to improve the accuracy of remote sensing techniques for determining species identification, vegetation stress, vegetation biomass and the nature of the underlying soil and/or rock.

One method used to study these interactions is by mathematical modeling techniques. Canopy modeling enables the experimentalist to conveniently organize, in a mathematical sense, all the complex interactions which take place in a vegetation canopy, and thus enables one to integrate information and interpret the data collected. In addition, models can serve as a guide to experimentation. As in any scientific research, knowledge of the underlying basic principles of a phenomenon needs to be understood before a surge of practical applications can be realized.

Several solar radiation canopy models which incorporate canopy geometry exist. Some of the more recent developments have been made by Oliver and Smith (1974), Suits (1972), Idso and deWit (1970), and Allen and Richardson (1968). It is known that the spectral signature of most vegetation canopies varies with both direction of sensor view and solar zenith angle. This variation is primarily due to differences in canopy geometry which influence the transfer of radiation within a vegetation canopy. The canopy geometry can be described by such physical characteristics as the distribution of plants on the ground, leaf area index and its distribution as a function of height, leaf angle frequency distribution and leaf azimuth angle frequency distributions. These canopy characteristics, in regard to radiation transfer, are discussed by Oliver and Smith (1974), Idso and deWit (1970), and deWit (1965).

The thermal infrared region (3-20 μm) of the electromagnetic spectrum in recent years has received keen interest. This radiation region may add valuable additional information to make inferences concerning the characteristics of vegetation canopies. Many thermal models exist for different non-vegetated targets of interest. Several models exist for planar solid objects. For example, Watson (1971) developed a thermal model for predicting the diurnal surface temperature variation of the ground, and the University of Michigan (1969) developed a model for the prediction of time-dependent temperatures and radiance of planar targets and backgrounds. However, few thermal models exist for plant canopies.

Gates (1968) presents an energy budget for a single plant leaf isolated in space. In addition, Kimes, Ranson, Kirchner, and Smith (1978), and Wiebelt and Henderson (1977) have developed thermal models of an individual leaf. Other investigators model the thermal dynamics of vegetation canopies assuming a simplistic single homogeneous layer abstraction. For example, vegetation is treated as a single homogeneous layer with an associated transmission factor for solar radiation in the University of Michigan model (1969). Heilman et al. (1976) used actual thermal scanning data to measure crop effective radiant temperatures and used an evapotranspiration (ET) equation to estimate crop ET. However, they assume they are viewing only the top layer of the crop with the scanner and ignore the canopy geometry. The literature review failed to reveal any thermal canopy models which physically account for the canopy geometry and the thermal dynamics within the canopy.

It is known that vegetation canopies are non-Lambertian at optical wavelengths, primarily due to canopy geometry. Similarly, in the thermal region, it is believed that while individual canopy elements are isotropic radiators, the response from the canopy may also be non-Lambertian because canopy geometry causes spatial variations in many energy flow processes.

With the number of thermal sensor systems currently operating in present satellites (e.g., Heat Capacity Mapping Mission) and proposed for future satellites (e.g., Thematic Mapper on Landsat D), thermal models will become increasingly important in interpreting the resulting data. Vegetation is often the target of interest, especially in agriculture and forestry applications. However, in many cases the substrate (e.g., soil, rock) underlying the vegetation is of interest. Thermal modeling of vegetation canopies could play an important role in interpreting thermal data (Watson, Rowan, and Offield, 1971) and in design studies for discriminating between vegetation types or background materials under a variety of environmental conditions.

Model Description

The primary objectives of this study were to produce a thermal canopy model which simulates, in a physically based manner, (1) the geometric arrangement of primary canopy elements, (2) the decreased direct/diffuse solar radiation absorption due to the scattering of neighboring canopy components, (3) the increased thermal absorption of leaves due to the thermal emissions of neighboring canopy components, (4) the true average temperature of scene elements within three horizontal, infinite canopy layers, and (5) the response of a thermal sensor at varying view angles above the canopy and at horizontal looking positions within the canopy.

Canopy Abstraction

The vegetation canopy is abstracted as three, statistically independent, horizontal, infinite layers (Figure 1). The canopy elements (e.g., leaves, branches, and other plant organs) within each layer are described as a statistical ensemble which is used to define the canopy geometry. Mid-elements that represent canopy elements which occur at the horizontal plane occupying the middle of each layer are defined. An energy budget equation is formulated for the

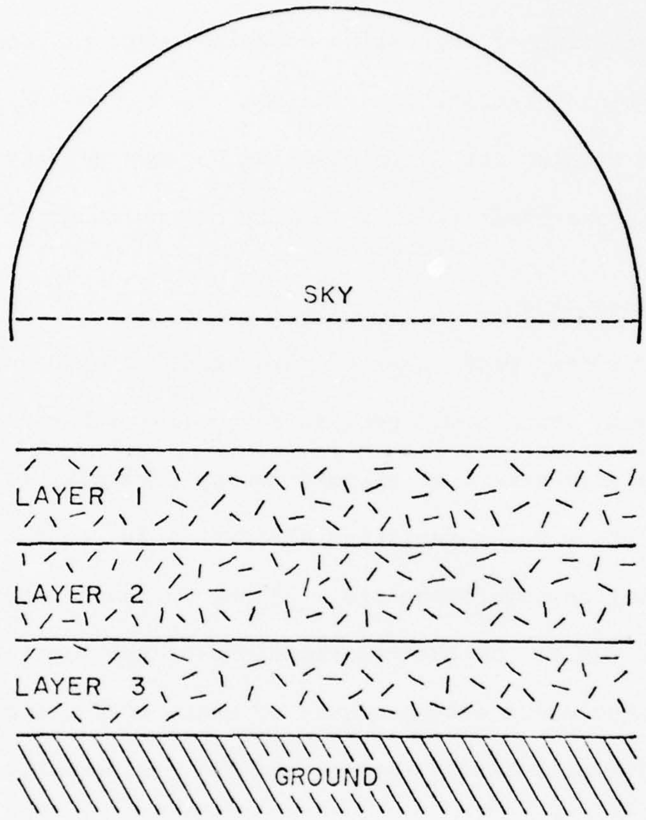

Figure 1. Abstraction of the thermal canopy signature model (TCSM) showing the sky, ground, and three canopy layers which contain a statistical ensemble of elements.

mid-elements of each layer. These equations account for the energy inflow and outflow processes of the elements. The energy transfers are calculated on a power per unit area of element ($w \cdot m^{-2}$) basis. The roots of the resulting system of equations are the average surface temperature of the mid-elements in the three layers. It is assumed that these values represent the average temperature of the elements in each respective layer. These values can then be utilized to calculate the response of a thermal sensor at varying view angles.

The flow of energy within a canopy is time dependent. However, the TCSM assumes a steady-state condition in which elements of the canopy are neither gaining nor losing a net amount of energy. In addition, the energy loss due to photosynthesis and energy gain by respiration is assumed negligible and has been ignored. Heat exchange by conduction is also considered negligible, and all surfaces of finite elements within a layer are considered to be the same temperature. These approximations are good for elements of relatively small dimensions (Gates, 1975). The above steady-state and conduction assumptions may not be adequate when dealing with canopies which exhibit a large fraction of the total element surface areas as relatively large branches and trunks. To approximate time dependent events, one can consider a series of incremental changes in steady-state energy flow as discussed later.

Several other assumptions are made. First, the spectral effects in the thermal region are assumed insignificant. Kondrat'yev (1965) states that natural surfaces can be treated in the first approximation as gray body radiators and emitters. Data from Leeman _et al_. (1971)

show that the thermal spectral emissivity of plants are essentially constant with wavelength.

Secondly, the reflection of thermal flux within the canopy is ignored. Ross (1976) states that the transfer theory for the thermal radiation in a vegetation canopy differs from shortwave theory in that the scattering of thermal radiation may be neglected but the emission of thermal radiation from plant elements must be acknowledged. It is believed that within natural vegetation canopies, reflected thermal radiation is a negligible contribution to the total energy budget. Blaxter (1967) reported the emissivity of "green grass" as 0.99. Idso, Baker and Blad (1969) reported the emissivity of 34 plants ranging approximately from 0.94 to 1.00, with 30 of the plants above 0.96. The effect of ignoring thermal reflectance on the final temperature of a single leaf was explored using the following analogy (Figure 2). The walls of the box are considered to be leaves which have an emissivity of .95. The energy budget is used to calculate the leaf temperature of the theoretical box in which thermal reflections are complete both for the exterior and interior of the box, simulating a theoretical enclosed canopy. Two calculations, one ignoring and one accounting for thermal reflectance, are made of the single leaf temperature which is completely enclosed in the box composed of other leaves. It is believed the difference between these two calculations will simulate the worst possible case for ignoring thermal reflectance. Within a normal canopy a single leaf is rarely completely surrounded by neighboring leaves and thus some of the reflected thermal radiation escapes out the sides of the system. However, this is not the case in the "black needle box." The energy budget with the specific

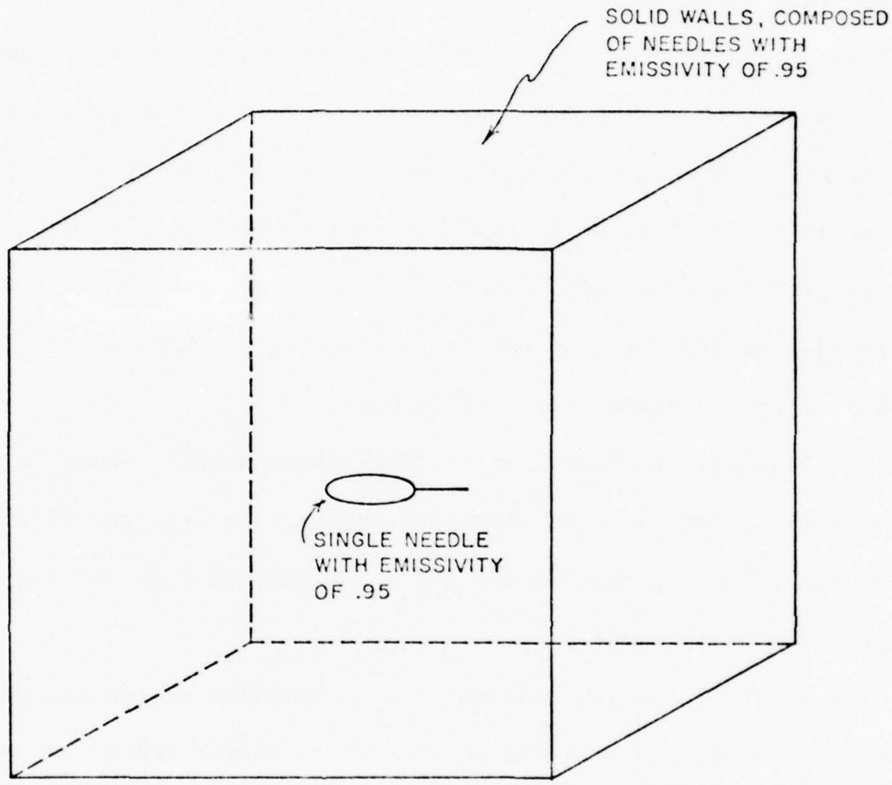

Figure 2. Analogy of a black box consisting of solid needles and a single needle within the interior of the black box.

coefficients used to calculate the above leaf temperature is presented in detail by Kimes, Ranson, Kirchner, and Smith (1978).

Several permutations of environmental conditions were simulated for this simple example. The constants were: wind velocity 1 cm/sec, leaf dimension 1.0 cm, internal leaf resistance to water vapor diffusion .66 min/cm, leaf emissivity 0.95. Simulations were run with permutations of air temperature (0, 15, 35°C), relative humidity (10, 50, 100%), accounting for and ignoring transpiration, and no solar irradiance and 336 w/m^2 absorbed solar irradiance by the leaf. The results showed that the maximum difference between the two calculations for all permutations was 1.59°C ±0.01.

Finally, the individual canopy elements are assumed to emit thermal radiation in an isotropic manner. Kondrat'yev (1965) and Hudson (1969) state that the radiation emitted from natural surfaces is essentially isotropic.

In the following discussion a description of the canopy geometry will be presented followed by the energy budget equations for each layer which account for the thermal radiation transfers, solar radiation absorption, thermal exitance, transpiration and convection exchanges.

Canopy Geometry

Important parameters in describing radiation transfer in complex structures are the gap frequency and the extinction of radiation within the structure. Monteith (1965), Warren Wilson (1965), deWit (1965), and other authors have developed various formulas for these parameters.

Nilson (1971) presented a good review of these formulations for theoretical models of canopy geometry which have been utilized.

The geometry of the thermal canopy model is abstracted in the following manner. Since the model is numerical as opposed to analytical in nature, the hemispheres above and below a particular layer are discretized into 9 hemispherical inclination bands 0-90 degrees (Figure 3). Each of the 9 bands is further discretized into 18 azimuthal sectors (Figure 3). Within each sector the radiation transfers between the three canopy layers, ground and sky are calculated.

The formulation developed by Idso and deWit (1970) has been incorporated to predict the probability of gap in the direction of the nine hemispherical bands for each of the three canopy layers. The positive binomial distribution is used to describe these probabilities and azimuthal symmetry is assumed. The probability of gap in a particular band direction is equal to the ratio of the projection of elements in a layer to the projection of the underlying soil surfaces. For a hemispherical band direction j the equation is:

$$PGAP_{jm} = \left[1 - \frac{S_m \cdot G_{jm}}{\sin(\Theta_j)}\right]^{\frac{LAI_m}{S_m}} \; ; \; PHIT_{jm} = 1 - PGAP_{jm}$$

where:

$PGAP_{jm}$ = probability of gap for layer m in direction of hemispherical band j

$PHIT_{jm}$ = probability of hit for layer m in direction of hemispherical band j

G_{jm} = mean canopy projection of elements in layer m in the direction of hemispherical band j

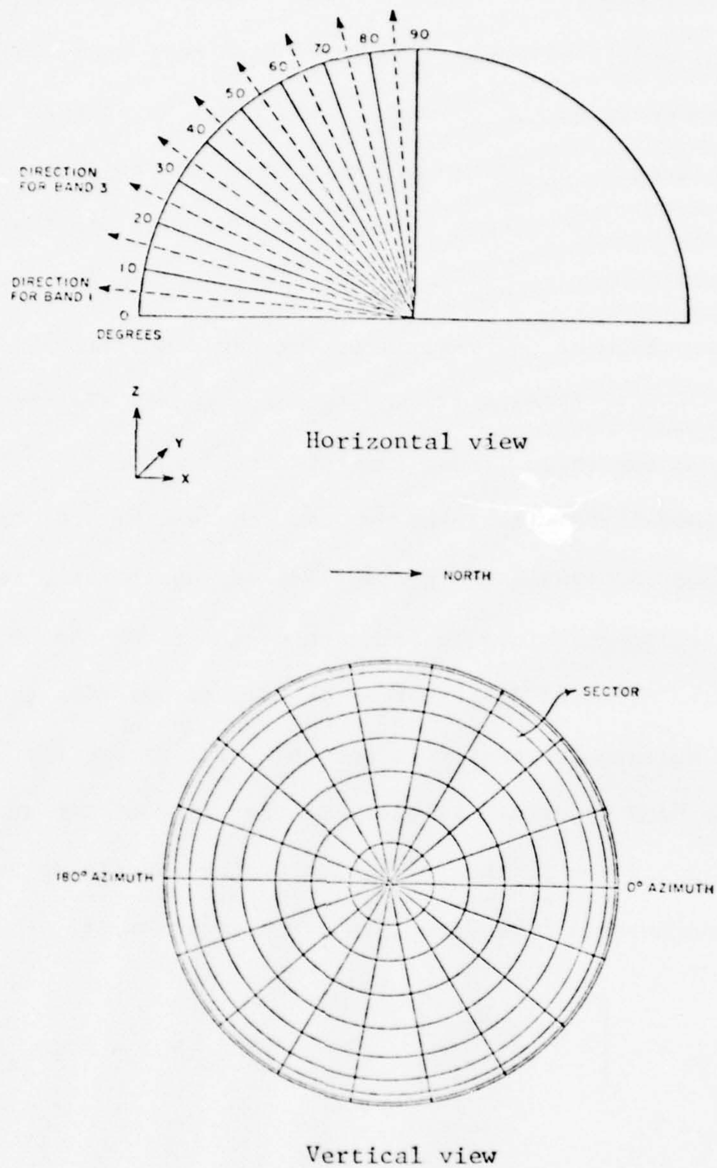

Figure 3. Horizontal and vertical views of the 9 hemispherical inclination bands which are divided into 18 equal azimuthal sectors. If one rotates the horizontal view about the Z axis the bands would occur in three-space.

LAI_m = element area index for layer m

S_m = index of spatial dispersion of elements in layer m

$\sin(\Theta_j)$ = sine function of the inclination angle Θ of hemispherical band j.

The function G_{jm} is determined from inclination angle frequency distributions of the elements in a layer. The derivation and computational procedure is presented by deWit (1965). The parameter S_m ranges from 0 to 1 and is an index of denseness or spatial dispersion of the elements in a canopy. As S approaches 1.0, the more regular the dispersion of elements is and the less frequently a gap is encountered. The leaf area index of a canopy layer is equal to the ratio of the total one-sided element area within a layer to the area of the underlying soil area. For a more in-depth discussion of the above theory and the required measurements see Idso and deWit (1970), and Oliver and Smith (1974).

The resulting $PGAP_{jm}$ and $PHIT_{jm}$ are important parameters in describing the radiation transfers with each hemispherical sector. In addition, the probabilities of gap and hit of half of each layer are required, and these parameters are calculated as:

$$PGAP'_{jm} = (PGAP_{jm})^{\frac{1}{2}}$$

$$PHIT'_{jm} = 1 - PGAP'_{jm}$$

where:

$PGAP'_{jm}$ = probability of gap for one half of layer m in the direction of hemispherical band j

$PHIT'_{jm}$ = probability of hit for one half of layer m in the direction of hemispherical band j.

Thermal Radiation Transfers

The following describes the manner in which thermal radiation transfers are calculated within the model. Each layer emits and receives thermal radiation in the hemispheres occurring above and below a particular layer. The transfer of thermal radiation within each hemispherical sector between the three canopy layers, the sky, and ground is calculated as follows. As seen in Figure 4, for small angles (Θ, ϕ) the two sides of a sector can be described as $r \cos\Theta \, d\phi$ and $r \, d\Theta$, and the area of the sector is described as approximately $r^2 \cos\Theta \, d\Theta \, d\phi$. One can then define the solid angle of a sector as:

$$d\Omega = \frac{r^2 \cos\Theta \, d\Theta \, d\phi}{r^2}$$

$$= \cos\Theta \, d\Theta \, d\phi$$

where:

Ω = steradians of a sector.

And it follows that

$$\Omega = \int_{\phi_1}^{\phi_2} \int_{\Theta_1}^{\Theta_2} \cos\Theta \, d\Theta \, d\phi$$

where:

ϕ_1, ϕ_2 = define the azimuthal limits of sector i in hemispherical band j

Θ_1, Θ_2 = define the inclination limits of sector i in hemispherical band j.

To calculate the thermal irradiance on a mid-leaf from a particular layer in any given sector we proceed as follows. Assuming that canopy elements in a particular layer emit thermal radiation in an isotropic manner, the radiance from the material is

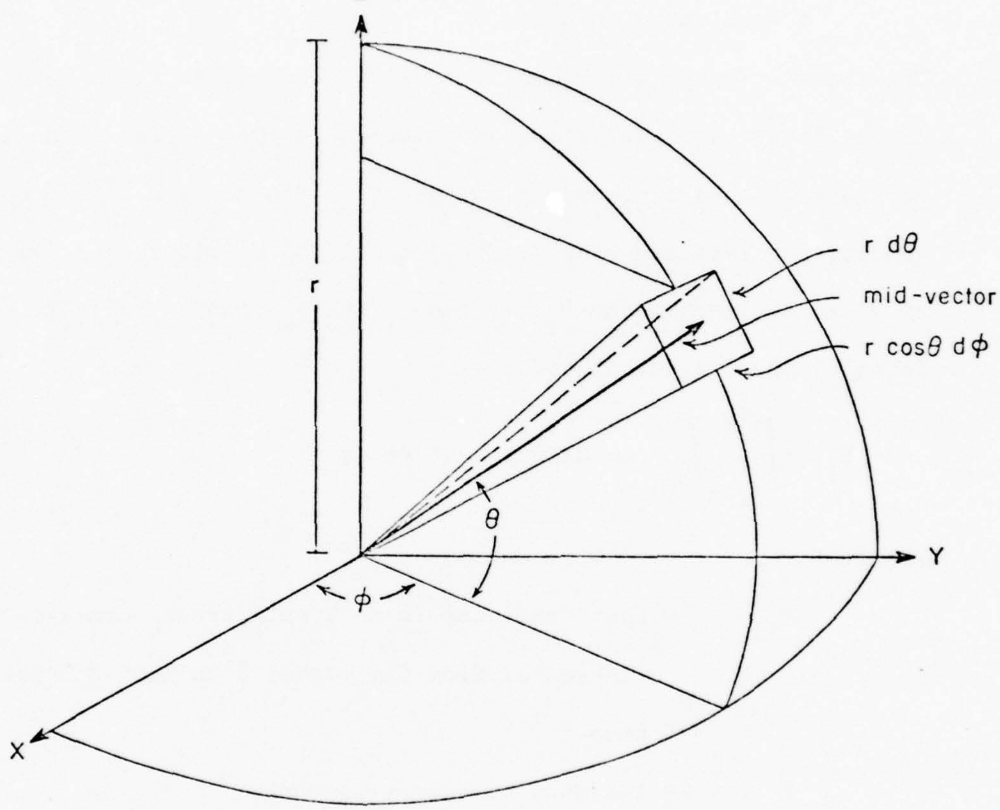

Figure 4. Three-dimensional view of the solid angle represented by a particular sector with its corresponding mid-vector.

$$L = \frac{M}{\pi} \tag{1}$$

where:

L = radiance ($w \cdot m^{-2} \cdot sr^{-1}$)

M = exitance ($w \cdot m^{-2}$).

The above radiance L is equal for all viewing directions; however, a canopy layer has special characteristics in that it is not solid but has gaps which are dependent on the direction of view. As a consequence, the irradiance on a panel normal to the mid-vector (Figure 4) of a sector, defined by Θ_1, Θ_2 and ϕ_1 and ϕ_2 from an infinite horizontal layer, is calculated by

$$E_{ij} = \int_{\phi_1}^{\phi_2} \int_{\Theta_1}^{\Theta_2} L \cdot PHIT(\Theta) \cos\Theta \, d\Theta \, d\phi$$

where:

E_{ij} = the irradiance ($w \cdot m^{-2}$) on a panel normal to the mid-vector from the sector i in hemispherical band j

L = radiance of canopy elements

$PHIT(\Theta)$ = probability of hit for viewing angle Θ.

The above assumes that elements within a layer have a homogeneous surface temperature and emissivity. The equations and theory of flux transfer from extended sources through solid angles to receiving elements are presented by the National Bureau of Standards (1978).

Assuming that $PHIT(\Theta)$ is constant within sector ij, then

$$E_{ij} = L \cdot PHIT_j \int_{\phi_1}^{\phi_2} \int_{\Theta_1}^{\Theta_2} \cos\Theta \, d\Theta \, d\phi.$$

Because the 18 sectors within band j have equal solid angles, the above equation can be reduced to:

$$E_{ij} = \frac{L\ PHIT_j}{18} \int_0^{2\pi} \int_{\Theta_1}^{\Theta_2} \cos\Theta \ d\Theta \ d\phi$$

$$E_{ij} = \frac{L \cdot PHIT_j \cdot \pi}{9} \int_{\Theta_1}^{\Theta_2} \cos\Theta \ d\Theta.$$

This expression can be further evaluated as:

$$E_{ij} = L \cdot PHIT_j \cdot \pi \frac{(\sin\Theta_2 - \sin\Theta_1)}{9} \qquad (2)$$

Combining equations (1) and (2) for a particular sector

$$E_{ij} = M \cdot PHIT_j \cdot \frac{(\sin\Theta_2 - \sin\Theta_1)}{9}$$

For simplicity, the quantity $(\sin\Theta_2 - \sin\Theta_1)/9$ will be defined by $SECTOR_j$ where j denotes the hemispherical band interval:

$$E_{ij} = M \cdot PHIT_j \cdot SECTOR_j.$$

The above assumes that the panel which represents a mid-element is normal to the direction of the source and that there exist no obstructions between the emitting canopy layer and the panel. The following calculations correct for the fact that the panel or mid-element is not always oriented normal to the source.

The desired correction factor is the cosine of the angle between the source vector and the normal vector of the panel. The theory is based on the existence of planar elements. The inclination angles of the canopy elements and source, and the azimuthal angles of the leaves and source are discretized as before. The canopy elements are assumed to have azimuthal symmetry. The direction cosines of all source sectors are calculated as:

$$\overline{V}_S = \begin{bmatrix} XS_{ij} \\ YS_{ij} \\ ZS_{ij} \end{bmatrix} = \begin{bmatrix} \cos(\Theta_{ij})\cdot\cos(\phi_{ij}) \\ \cos(\Theta_{ij})\cdot\sin(\phi_{ij}) \\ \sin(\Theta_{ij}) \end{bmatrix}$$

where:

$\overline{V}_S$ = vector of direction cosines for source sector i in hemispherical band j

Θ_{ij} and ϕ_{ij} = the inclination and azimuth angle, respectively, of the mid-vector in sector i and hemispherical band j.

The direction cosines for the normal vector of all planar element inclination angle intervals are calculated as follows. The azimuth angle is fixed to zero degrees since the canopy is assumed azimuthally symmetric, both in geometric and thermal radiant energy modes. Thus, regardless of the azimuthal orientation of an element, the thermal radiant contributions to the element are constant for any specific element inclination angle.

$$\overline{V}_L = \begin{bmatrix} XL_j \\ YL_j \\ ZL_j \end{bmatrix} = \begin{bmatrix} -\sin(\Theta_j) \\ 0.0 \\ \cos(\Theta_j) \end{bmatrix}$$

where:

$\overline{V}_L$ = vector of direction cosines for the normal of a planar element with inclination j

Θ_j = element inclination of hemispherical band j.

Now one can calculate the absolute value of the dot products for all source-element angle permutations. These values are equal to the correction factors desired.

$$COS_{ijk} = |\bar{V}_S \cdot \bar{V}_L|$$

where:

COS_{ijk} = the correction factors desired for permutations of source sector i in hemispherical band j and element inclination k.

In addition, one must apply the absorption coefficient for thermal radiation. As a result, the equation becomes

$$\frac{\Phi_{ijk}}{m^2} = M \cdot PHIT_j \cdot SECTOR_j \cdot ABSORB \cdot COS_{ijk}$$

where:

$\frac{\Phi_{ijk}}{m^2}$ = the thermal flux density ($w \cdot m^{-2}$) absorbed by a mid-element inclined at inclination angle k from source sector i in hemispherical band j

ABSORB = thermal absorption coefficient.

The above assumes that there exist a single layer and a removed single element receiving flux from that layer. However, the contribution of absorbed thermal flux density from all hemispherical sectors, both upward and downward directions for each canopy layer, the sky, and ground, to each layer's mid-elements must be calculated (Figure 5).

The calculations should account for the fact that within each sector the flux which originates from any given layer is obstructed by other leaves before the flux reaches any specified mid-element in another layer. In addition, a relatively large number of permutations must be calculated since each layer is simultaneously emitting thermal flux to other layers and absorbing emitted flux from the surrounding leaves, other layers, the sky, and the ground. For each permutation

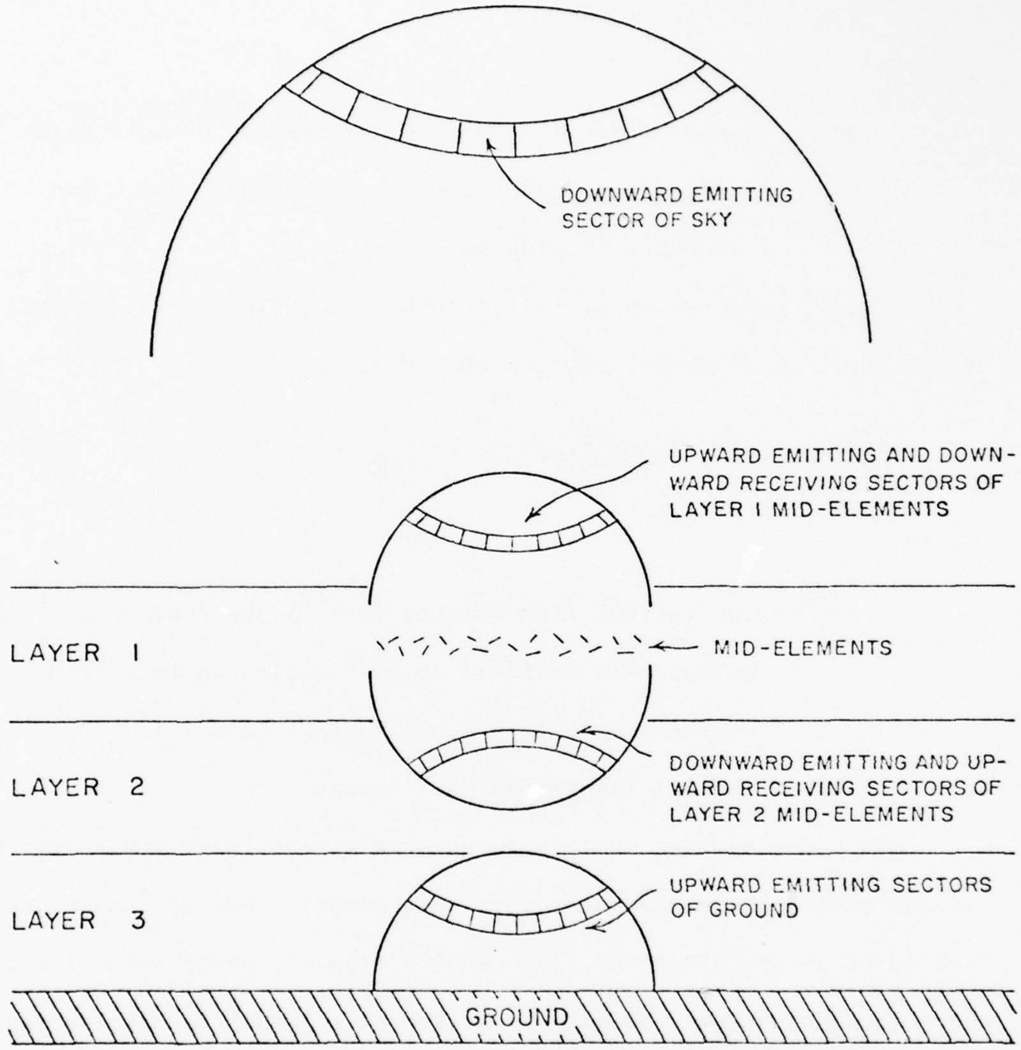

Figure 5. Hemispherical sectors are shown for the sky, Layer 1, and the ground. Note only sectors in one band are shown.

a contribution coefficient which replaces $PHIT_j$ is calculated. For example, the mid-elements in Layer 1 will receive thermal flux from the sky, Layer 1, Layer 2, Layer 3, and the ground. For all sectors defined within a specific hemispherical band j, the contributing coefficients are calculated as follows.

The proportion of sky thermal flux within a sector in band j reaching the mid-elements in Layer 1 is

$$PGAP'_{j1}.$$

The contributing coefficient from Layer 1 to the Layer 1 mid-elements is

$$2\cdot(PHIT'_{j1})$$

The coefficient of 2 represents the two half-layers of Layer 1.

The contributing coefficient from Layer 2 to the Layer 1 mid-elements can be derived in the following manner. The probability of gap to Layer 2 is $PGAP'_{j1}$. Once Layer 2 is reached, the projected surface area of interest is $PHIT_{j2}$. Thus, the contributing coefficient is

$$PGAP'_{j1}\cdot PHIT_{j2}.$$

A similar argument can be made for the contributing coefficient from Layer 3 to the Layer 1 mid-elements:

$$PGAP'_{j1}\cdot PGAP_{j2}\cdot PHIT_{j3}.$$

The contributing coefficient from the ground to Layer 1 mid-elements is

$$PGAP'_{j1}\cdot PGAP_{j2}\cdot PGAP_{j3}.$$

The contributing coefficients for both upward and downward directions of a particular sector and layer should sum to 2.0 representing the two sides of the mid-elements. And, in fact, if one sums the above coefficients, the total is 2.0.

In a similar fashion, the contributing coefficients from all source sectors to Layers 2 and 3 mid-elements are calculated.

The final equation which calculates, within a particular sector, the amount of flux density absorbed by a mid-element at a particular inclination angle from any given source layer is

$$\frac{\Phi_{ijk\iota m}}{m^2} = M_\iota \cdot CONT_{j\iota m} \cdot SECTOR_j \cdot ABSORB_m \cdot COS_{ijk}$$

where:

$\frac{\Phi_{ijk\iota m}}{m^2}$ = within source sector i in hemispherical band j, it is the thermal flux density absorbed by a mid-element in layer m inclined at inclination angle k from source elements in layer ι. Note the index ι represents the sky and ground in addition to the 3 canopy layers.

M_ι = average thermal exitance of elements in layer ι

$CONT_{j\iota m}$ = contributing coefficient for mid-elements in layer m absorbing flux from elements in layer ι for all sectors within hemispherical band j

$ABSORB_m$ = average thermal absorption coefficient for elements in layer m.

Except for the sky thermal exitance, M_ι can be further expressed in terms of the Stefan-Boltzmann Law:

$$M_\iota = \sigma \cdot \epsilon_\iota \cdot T_\iota^4$$

where:

σ = Stefan-Boltzmann constant

ε_ι = average emissivity of elements in layer ι

T_ι = true average surface temperature (°K) of the mid-elements in layer ι (unknown).

Note that the average surface temperatures of the three canopy mid-elements are not known and these values must be derived mathematically. In addition, the ground temperature is known (input) and the sky exitance is calculated by an empirical equation as a function of air temperature (input). Thus, the final equation becomes

$$\frac{\Phi_{ijk\iota m}}{m^2} = \sigma \cdot \varepsilon_\iota \cdot T_\iota^4 \cdot \mathrm{CONT}_{j\iota m} \cdot \mathrm{SECTOR}_j \cdot \mathrm{ABSORB}_m \cdot \mathrm{COS}_{ijk} .$$

The total flux density emitted by elements in layer ι and absorbed by a particular mid-element in layer m at inclination k can be described by

$$\frac{\Phi_{k\iota m}}{m^2} = \sigma \cdot \varepsilon_\iota \cdot T_\iota^4 \cdot \mathrm{ABSORB}_m \cdot \left[\sum_{j=1}^{9} \mathrm{CONT}_{j\iota m} \cdot \mathrm{SECTOR}_j \cdot [\sum_{i=1}^{18} \mathrm{COS}_{ijk}] \right] .$$

The total flux density absorbed by a mid-element in layer m at inclination angle k is computed by summing all sources:

$$\frac{\Phi_{km}}{m^2} = \sum_{\iota=1}^{5} \frac{\Phi_{k\iota m}}{m^2}$$

where ι = 1, 2, 3, 4, 5 represents the sky, Layer 1, Layer 2, Layer 3, and the ground, respectively.

Nine equations for each layer are constructed. Each equation represents the absorbed flux density for each mid-element inclination. For each layer the appropriate equation is weighted by the frequency of occurrence of the elements within the corresponding inclination class. The nine equations are then summed to represent the average absorbed thermal flux density within the three canopy layers. In addition, the flux density absorbed (w/m^2) is on a per unit area basis. Thus, the m^2 term above must represent both the top and bottom surfaces of the leaf. As a consequence, the factor of ½ is introduced:

$$\frac{\Phi_m}{m^2} = \tfrac{1}{2} \sum_{k=1}^{9} \frac{\Phi_{km}}{m^2} \cdot FREQD_{km}$$

where:

$\frac{\Phi_m}{m^2}$ = the average absorbed thermal flux density by the mid-elements in layer m

$FREQD_{km}$ = the probability of occurrence of inclination k for elements in layer m.

The resulting three equations for each layer represent the average absorbed thermal flux density. To complete the energy budget for each layer we must include: absorbed solar radiation, convection, transpiration, and thermal radiant emission.

Solar Radiation Absorption

Several models have been developed to study the interactions of solar radiation within vegetation canopies. Allen and Richardson (1968), Alderfer and Gates (1971), and Suits (1972) have adapted a system of simultaneous differential equations developed by Kubelka and Munk (1931) in various ways to vegetation canopies. Suits (1972) developed a model which includes geometric effects and predicts non-Lambertian characteristics of vegetation canopies.

Another approach, developed by Oliver and Smith (1974), is the Solar Radiation Vegetation Canopy (SRVC) model. The model is stochastic in nature and predicts the diurnal apparent directional spectral reflectance of a vegetation canopy. The same geometry descriptors as described above are utilized within the SRVC model.

To calculate the average absorbed solar radiation within each canopy layer, it is important to include the complex scattering of light as a function of canopy geometry. For the purpose of calculating the absorbed solar radiation, it is believed that the mathematical framework of the SRVC model is the most physically based and the most easily adapted to calculate the absorbed solar radiation of the above models. A complete description of the SRVC model is presented by Oliver and Smith (1974).

The SRVC model has been modified to estimate spectral absorption within vegetation canopies and has been specifically applied to a cluster of four modeling lodgepole pine trees (Kimes and Smith, 1979). The results show that the total global irradiance absorbed by the lodgepole pine canopy system is relatively constant with solar zenith angle. However, the proportion of total global irradiance absorbed by individual canopy layers varies as a function of solar zenith angle (Figure 6). The mean total solar flux absorbed per unit canopy element surface area for any given layer and solar zenith angle can be readily calculated from the information in Figure 8 as presented by Kimes and Smith (1979).

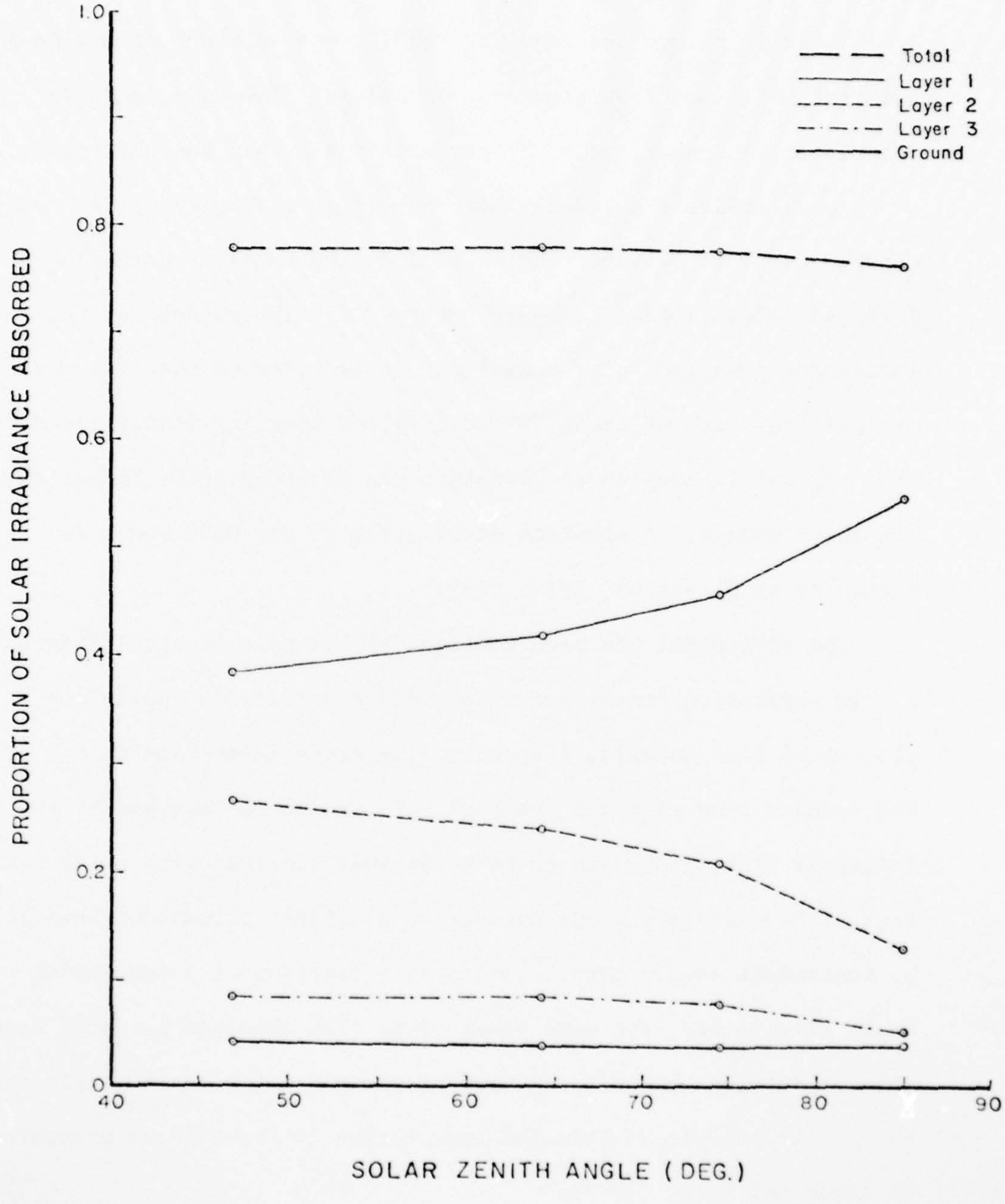

Figure 6. Simulated proportion of global solar irradiance absorbed by the lodgepole pine canopy system (total), Layer 1, Layer 2, Layer 3, and the ground, as a function of solar zenith angle for October 14, 1977.

Other Energy Transfers

Other energy transfers to and from the mid-elements include: thermal exitance, transpiration, and convection.

The thermal exitance of all mid-elements is calculated by the Steffan Boltzmann Law:

$$M_\iota = \sigma \cdot \varepsilon_\iota \cdot T_\iota^4$$

where:

M_ι = mean exitance of mid-elements in layer ι

σ = Steffan Boltzmann constant

ε_ι = emissivity of mid-elements in layer ι (input)

T_ι = mean surface temperature of mid-elements in layer ι (°K).

The ground thermal exitance is calculated in a similar fashion.

Gates (1968) presented the equation used for transpiration, and Lee and Gates (1964) discussed the formulation in detail. The driving force is the difference between the water vapor density within the leaf and in the free atmosphere beyond the boundary layer. The water vapor density within the leaf is assumed to be at saturation at the leaf temperature. Controlling variables on transpiration include the resistance to diffusion offered by the diffusion pathway, such as the stomata and the boundary layer. The equation for any particular mid-leaf is

$$TRANS_\iota = H(T_\iota)\left(\frac{s\rho l(T_\iota) - RH \cdot s\rho a(T_a)}{R_\iota + R_a}\right) \cdot (697.8)$$

where:

$TRANS_\iota$ = transpirational loss from leaf in layer ι ($w \cdot m^{-2}$)

$H(T_\iota)$ = latent heat of vaporization of water at the leaf temperature T_ι ($cal \cdot gm^{-1}$)

$s\rho l(T_l)$ = water vapor density inside the leaf at saturation at the leaf temperature T_l ($gm \cdot cm^{-3}$)

RH = relative humidity of air (input)

$s\rho a(T_a)$ = water vapor density at saturation of the free air beyond the boundary layer of the leaf at the air temperature T_a ($gm \cdot cm^{-3}$)

R_l = internal leaf resistance to water vapor diffusion in $min \cdot cm^{-1}$ (input)

R_a = resistance of the boundary layer to water vapor diffusion ($min \cdot cm^{-1}$).

$H(T_l)$, $s\rho l(T_l)$, and $s\rho a(T_a)$ were calculated using physically based formulas. Values of R_a for lodgepole pine needles were estimated from a mass transfer determination of Landsberg and Ludlow (1969) who used Sitka spruce shoots. The formula is

$$R_a = (0.04 + 1.27\ (\mu^{-0.5}))/60$$

where:

μ = wind speed in $cm \cdot sec^{-1}$ (input).

The constant R_l value used for the lodgepole pines in this study was 0.66 min/cm. Gates (1966) and Miller and Gates (1967) reported R_l values of 0.72, 0.33, and 0.50 min/cm for Picea mariana, Pinus resinosa, and Pinus strobus, respectively. Jarvis et al. (1976) and Tenhunen and Gates (1975) presented recent investigations of the stomatal opening and closing as influenced by environmental factors and concluded that the complex control of the stomata has not yet been described adequately.

Since the mid-elements represent both leaves and branches when dealing with woody plants, one can assume that branches do not transpire and the transpiration equation can be weighted according to the branch area index and the leaf area index.

The following convection equation was utilized. Tibbals et al. (1964) conducted quantitative measurements on silver castings of blue spruce and white fir branches in a controlled radiation and windtunnel chamber. The authors report convective coefficients for free convection in both species. However, Gates (1968) notes that rarely in nature is there any air movement less than 8.8 cm·sec^{-1} (0.2 m.p.h.). As a consequence, an equation describing forced convection can be used to approximate all convectional exchanges. Tibbals et al. (1964) found that both longitudinal and horizontal wind flows gave equal coefficients for spruce.

For $\mu>30.0$ $\qquad h_c = (0.95\mu^{0.97})\cdot(.698)$

For $\mu<30.0$ $\qquad h_c = (20.4 + 0.2\mu^{0.97})\cdot(.698)$

where:

μ = wind velocity in cm·sec^{-1} (input)

h_c = convectional coefficient in $w\cdot m^{-2}\cdot{}^\circ C^{-1}$.

The convectional exchange of a mid-element is calculated as

$$Q_{FC} = h_c\cdot(T_s - T_a)$$

where:

Q_{FC} = power per unit area of mid-element loss or gain ($w\cdot m^{-2}$)

h_c = convection coefficient in $w\cdot m^{-2}\cdot{}^\circ C^{-1}$

T_s = surface temperature of mid-element in °C

T_a = air temperature of the free air beyond the boundary layer in °C (input).

Wind speed is highly variable from point to point within the canopy (Bergen, 1974). As a consequence, the mean measured wind speed values were utilized for all three canopy layers.

The sky thermal exitance was calculated by an empirical equation dependent only on air temperature near the ground surface, and clear sky conditions were assumed. Hudson (1969) presented several references which estimate sky thermal exitance.

It is important to note that a multitude of convectional, transpirational, sky thermal exitance, and solar absorption formulations exist that may be more suitable for specific modeling objectives. For this reason the model has been structured so that different formulations of the above can be easily incorporated within the model.

Model Solution

The total energy budget equations for each canopy layer can now be formed. The result is a system of three nonlinear equations and three unknowns being the surface temperature of the mid-elements in each layer which represent the respective average temperature of each layer.

$$\vec{F} = \begin{bmatrix} \text{Layer 1 energy budget equation} \\ \text{Layer 2 energy budget equation} \\ \text{Layer 3 energy budget equation} \end{bmatrix} = \tilde{0}$$

To solve this system of equations the model calls the ZSYSTM algorithm which exists in the International Mathematical and Statistical Library (1977). ZSYSTM is a numerical routine which uses Brown's method (1969, 1971) for solving N simultaneous nonlinear equations in N unknowns. The method is at least quadratic convergent and requires only $N^2/2 + 3N/2$ function evaluations per iterative step as compared with $N^2 + N$ evaluations for Newton's method.

The roots of the system predict the average temperature of the layers and are used to calculate the following thermal predictions.

Thermal Predictions

The model predicts the thermal radiance, effective radiant temperature (ERT), and equivalent exitance in the 9 viewing inclination bands at 10° intervals above the canopy. The contribution of each layer and the ground to the nine sensing positions are calculated as follows. The thermal radiance in the band directions j are

$$
\begin{aligned}
L_j = \pi^{-1}\cdot[&PHIT_{j1}\cdot\varepsilon_1\cdot\sigma\cdot X_1^4 \\
&+ PGAP_{j1}\cdot PHIT_{j2}\cdot\varepsilon_2\cdot\sigma\cdot X_2^4 \\
&+ PGAP_{j1}\cdot PGAP_{j2}\cdot PHIT_{j3}\cdot\varepsilon_3\cdot\sigma\cdot X_3^4 \\
&+ PGAP_{j1}\cdot PGAP_{j2}\cdot PGAP_{j3}\cdot\varepsilon_4\cdot\sigma\cdot X_4^4]
\end{aligned}
$$

where:

each row represents the thermal radiance contribution to the sensor by Layer 1, Layer 2, Layer 3, and Layer 4 (ground), respectively.

L_j = thermal radiance of the sensor at viewing angle j ($w\cdot m^{-2}\cdot sr^{-1}$)

X_m = average surface temperature of elements in layer m (°K): m = 1, 2, 3, 4.

The thermal radiance (L_j) can be converted to the equivalent exitance (M_j) by

$$M_j = L_j\cdot\pi$$

and the effective radiant temperature (ERT_j °K) in band direction j can be calculated as

$$ERT_j = \left[\frac{M_j}{\sigma}\right]^{1/4}$$

where σ is the Stefan-Boltzmann constant.

The model also predicts the response of a thermal sensor looking horizontally from the ground into any of the three layers. When looking horizontally at a canopy the probability of gap is 0.0 according to the assumptions in the model. Thus, for a relatively narrow field of view the ERT of any given layer, when looking horizontally, is calculated simply by using the Stefan-Boltzmann equation with the appropriate emissivity factor and average layer temperature.

In addition, for each simulation, the average predicted temperature of each layer, ground thermal exitance, sky thermal exitance, absorbed solar flux density of each layer, thermal exitance of each layer, absorbed thermal flux density of each layer, convectional exchange, transpirational exchange, the geometric coefficients (including CONT, COS, SECTOR, LAI, S, FREQD) and all input parameters are displayed.

Field Measurements

A unique thermal and environmental data base for a lodgepole pine canopy at Leadville, Colorado was collected during 1977. Four clustered, lodgepole pine trees were chosen for intensive study as shown in Figure 7. These modeling trees had the following mean statistics: 6.0 m height, 30 year age, 13.2 cm DBH, and a surrounding stand of 102 m^2/hectare basal area. The S parameter, foliage area indices, and foliage angle frequency distributions of the modeling canopy were measured as reported by Kimes, Smith, and Berry (1979), and Kimes and Smith (1979).

Personnel from the Army Corps of Engineers Waterways Experiment Station, Environmental Laboratory (WES/EL) at Vicksburg, Mississippi developed a system for automated collecting, processing and displaying environmental baseline data as described by West and Floyd (1976). The system was utilized to monitor environmental conditions at the study site for the months of July, September, and October, 1977. All sensor measurements were recorded once every hour continuously for the duration of the study. The measurements taken included air temperature, global solar irradiance, wind speed, wind direction, rainfall, soil temperature, and vegetation surface temperature. The specific make and calibration procedures of the above instrumentation are described by West and Floyd (1976).

Figure 7 is an oblique photograph of the study area showing the sensor positions. At station M1 in the meadow opening, air temperature, wind speed, wind direction, global solar irradiance, and precipitation were measured. Air temperature was measured at a height of 1 m. All of the above measurements were also taken at station M2 within the tree area. In addition, the air temperature within the center of the four modeling trees (M3) was recorded.

The surface temperature of the base of needles at three branch tips of the modeling trees were measured by contact thermisters; one thermister was located 1 m above the ground in Layer 3, the second thermister was located 2 m above the ground in Layer 2, and the final thermister was located in the top of the modeling trees.

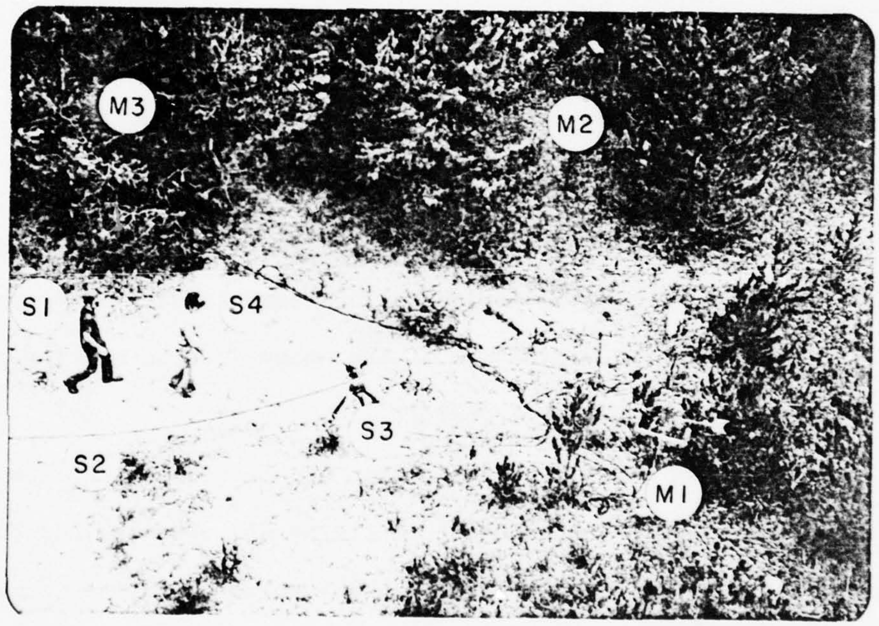

Figure 7. Oblique photograph of modeling trees, the meteorological measurement stations (M1, M2, M3) and the 4 stake positions (S1, S2, S3, S4).

AD-A071 793 COLORADO STATE UNIV FORT COLLINS COLL OF FORESTRY AN--ETC F/G 2/6
TERRAIN FEATURE CANOPY MODELING.(U)
APR 79 D S KIMES, J A SMITH, K J RANSON DACW39-77-C-0073
UNCLASSIFIED ARO-13444.2-GS NL

2 OF 3
AD
A071793

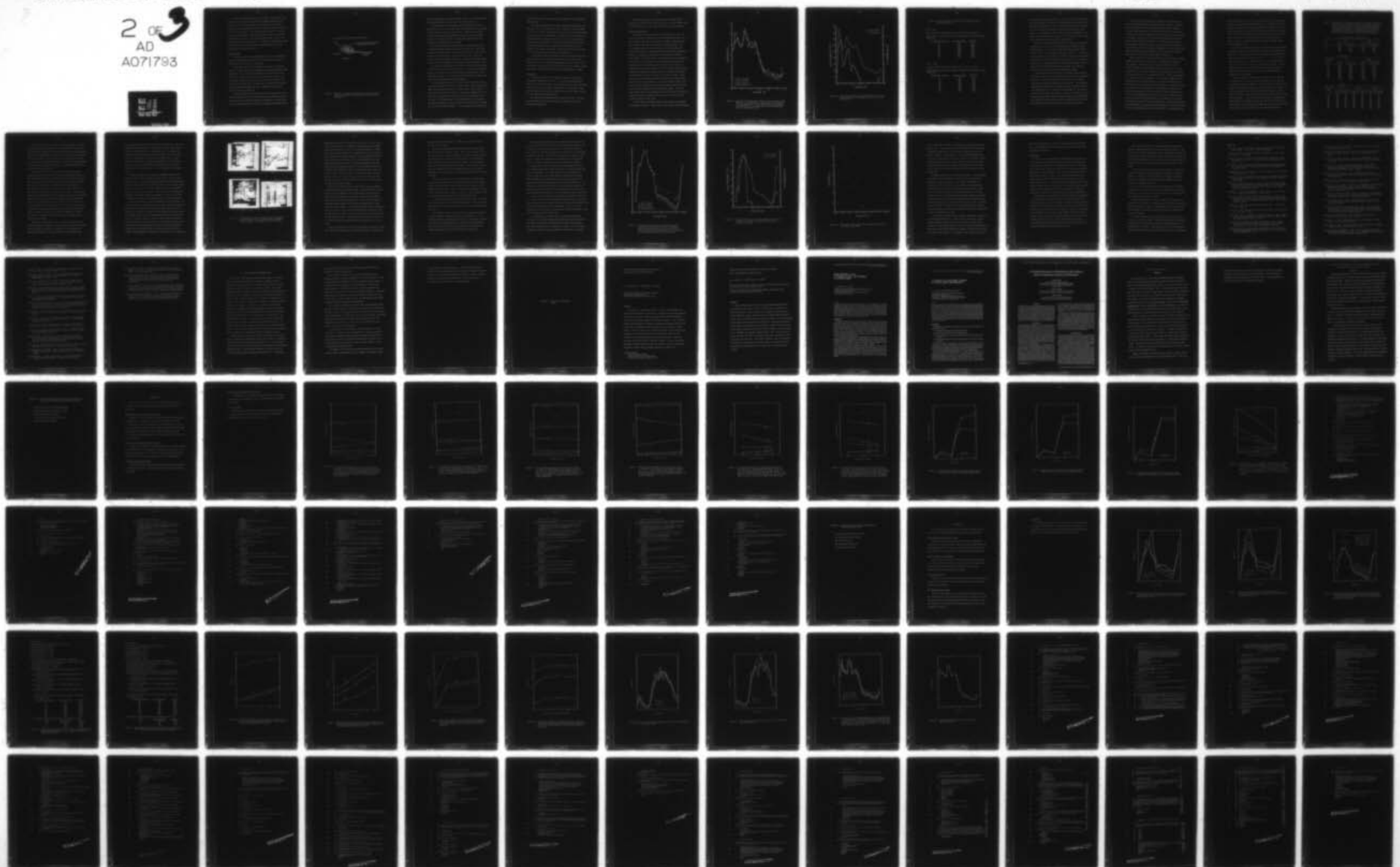

2 OF 3

AD
A071793

NATIONAL BUREAU OF STANDARDS
MICROCOPY RESOLUTION TEST CHART

Several other supporting data were recorded. During July 15-16, 1977, the Wahl Digital Heat Spy -DSH- 14 Thermal Radiometer with a band pass of 4.8 to 20.0 μm and a 3.5° field of view was used to measure the average horizontal effective radiant temperature (ERT) of Layer 2 of the canopy at four stake positions (Figure 7). Simultaneously, black and white Polaroid photographs derived from the AGA-Thermovision were taken. The system operates in the 2.0 to 5.6 μm region and scans a particular scene. In addition, during August 14-15, the Wahl Heat Spy was used to measure needle temperature at five branch tips in the modeling trees.

Data Reduction

An initial analysis of the Wahl Heat Spy and contact thermister data was completed to decide which data form was most suitable for testing the TCSM's accuracy of prediction.

The Heat Spy and contact thermister were taken of the needle-branch tip complex which has a relatively large concentration of mass (Figure 8). Due to the small diameters of the needles it was not feasible to securely fasten the contact thermisters to them. As a consequence, the thermisters were placed between the bases of the needles at the branch tips. The bases of the needles at the branch tips were very concentrated and thus, completely surrounded the contact thermisters (Figure 8).

The Heat Spy ERT's were correlated with the temperatures of the contact thermisters on many different natural and man-made surfaces during the month of July at Vicksburg, Mississippi by WES/EL personnel. The results showed that the two instruments corresponded within

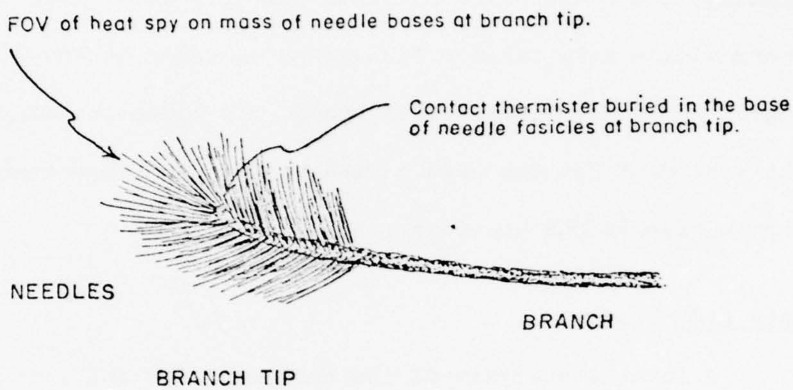

Figure 8. Diagram of a branch tip showing the target of the Wahl Heat Spy Radiometer and the placement of the contact thermister.

1°C under homogeneous solar heating loads. Thus, it was believed that the two measurements correlated well for the same target.

Two branch tips on the modeling trees had contact thermisters placed at the base of the needles next to the branch tip and were also simultaneously measured with the Heat Spy. In general, the contact thermisters recorded higher temperature values, of 2°C or greater, relative to the Heat Spy ERT's. One possible explanation of this deviation in measurements is as follows.

The contact thermisters were buried in a relatively large mass of compressed needles which occurs near the branch tip. Under this situation, relatively little convectional or transpirational exchange of these compressed portions of the needles can occur, which may account for the discrepancy seen above. In addition, some conduction from the warmer branches may be operating as will be discussed later.

In contrast, the field of view of the Heat Spy was on the branch tip (Figure 8) which was exposed to the air. It is believed that this portion of the branch tip undergoes limited convectional and transpirational exchange. As a result, the Heat Spy ERT's were lower than those of the corresponding contact thermisters.

In this modeling study the criteria used for validation is the accuracy of prediction of the mean canopy element surface temperatures and/or the mean horizontal ERT of a canopy layer. Gary (1976) has shown that the needle area index for a particular lodgepole pine tree accounts for approximately 87% of the total element surface area of the tree. The large majority of the needles extend into free space and undergo relatively high convectional and transpirational exchange due to the small needle diameters. As a consequence, the majority of the canopy's surface area should closely approximate air temperature (Gates, 1975).

The above measurements (the contact thermister temperatures and Heat Spy ERT's) of the branch tip do not reflect the surface temperatures of the needles extending into free space, and bias the measured canopy temperature to be too high. Therefore, these measurements are generally above air temperature and do not reflect the mean canopy element surface temperatures. Initial comparisons between the simulated mean element surface temperatures for the three layers for October 14-15 and the three contact thermister measurements in Layers 1, 2, and 3 show a very poor accuracy of prediction.

It is believed that the horizontal ERT's as measured by the Wahl Heat Spy from the four stake positions during July 15-16 were the least biased of all validating measurements, since the field of view incorporated a cross section of canopy element types. However, during the August 14-15 date only the ERT of five branch tips were taken.

Simulations

The thermal behavior of the modeling canopy was simulated for two complete diurnal cycles. For the July 15-16, 1977 simulation, the mean of the Heat Spy ERT's, as measured from the 4 stake positions, was used to test the accuracy of prediction. Two simulations using the air temperatures within the canopy (M3) and in the meadow opening (M1) were performed during this date.

One simulation was performed for October 14-15, 1977. The Heat Spy measurements of branch tip needles were utilized to test the accuracy of prediction.

Sensitivity analyses were performed on the following model parameters: average canopy element emissivity, average canopy element internal resistance to water vapor diffusion, and canopy geometry.

Results and Discussion

The simulated horizontal ERT's for the three layers for July 15-16, using the air temperature probe in the middle of Layer 2 of the modeling canopy (M3), are presented in Figure 9 along with the mean horizontal Heat Spy ERT's from the 4 stake positions. The corresponding measured solar irradiance and air temperature are presented in Figure 10. Wind speed was 0.0 m/s for all measurement periods. The minimum recorded wind speed possible was 10 cm/s. Gates (1968) stated that rarely is wind speed in natural environments below 8 cm/s. As a consequence, for periods when wind speed was recorded to be 0.0, a minimum value of 10 cm/s was utilized. It should be noted that the simulated data were derived from the meteorological data which were recorded at hourly intervals and the Heat Spy measurements were not necessarily synchronous in time. Consequently, one must compare the general trends of the simulated data with the Heat Spy measurements. In fact, the erratic nature of the solar irradiance (Figure 10) suggests that between hourly intervals, the true solar irradiance function could vary widely. This fact could explain some of the deviations during the day shown in Figure 9. During the night the simulated values deviated from the measured temperature by less than 1.5°C.

Selected output for 0930 and 0330 (Standard Time) simulations is presented in Table 1. During the day the average layer temperature

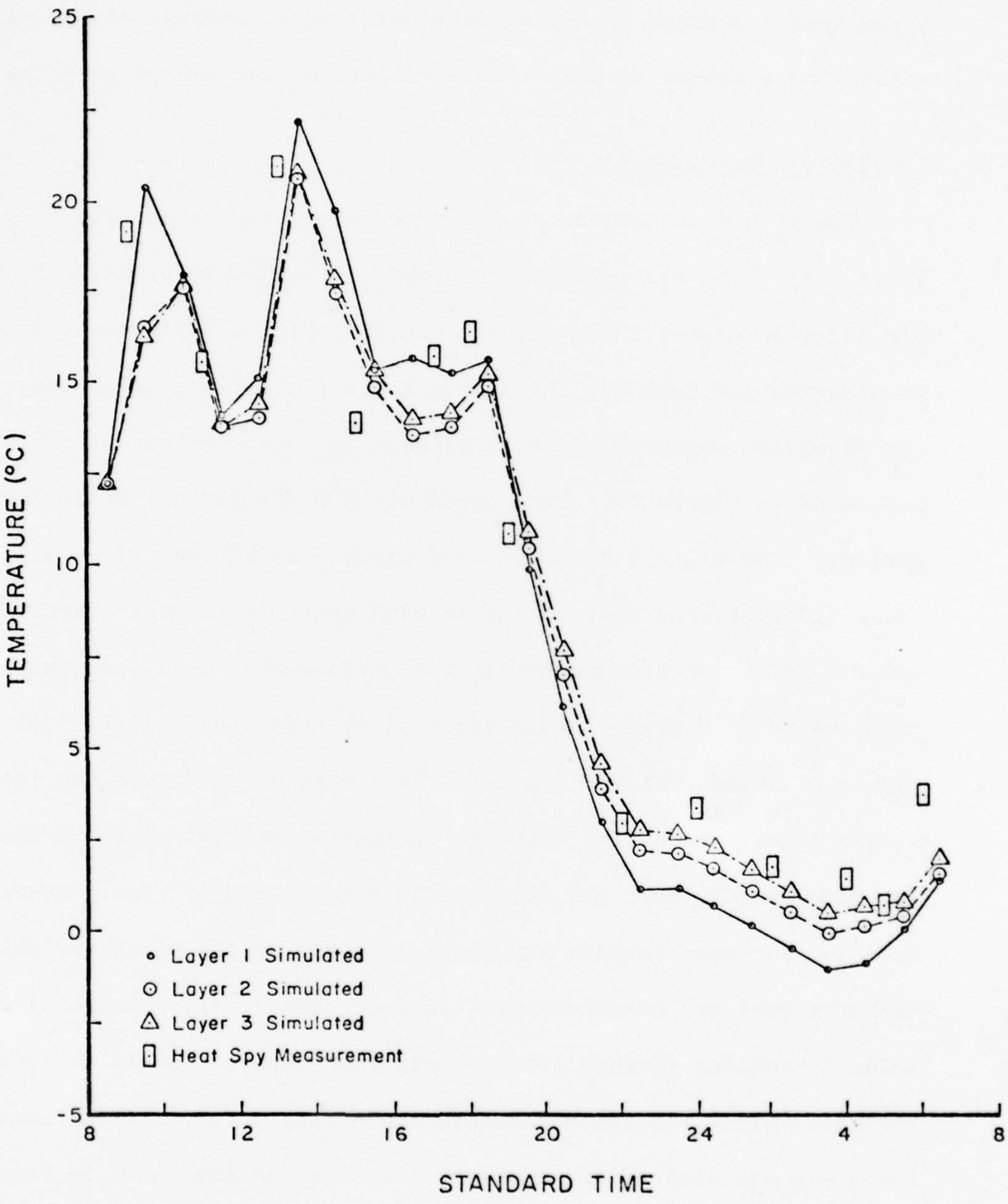

Figure 9. Simulated versus measured lodgepole pine canopy horizontal ERT's for July 15-16, 1977. Measured ERT's are the mean of 4 horizontal ERT's of the middle layer as measured by the Wahl Heat Spy. Air temperature was recorded within center of canopy (M3 site).

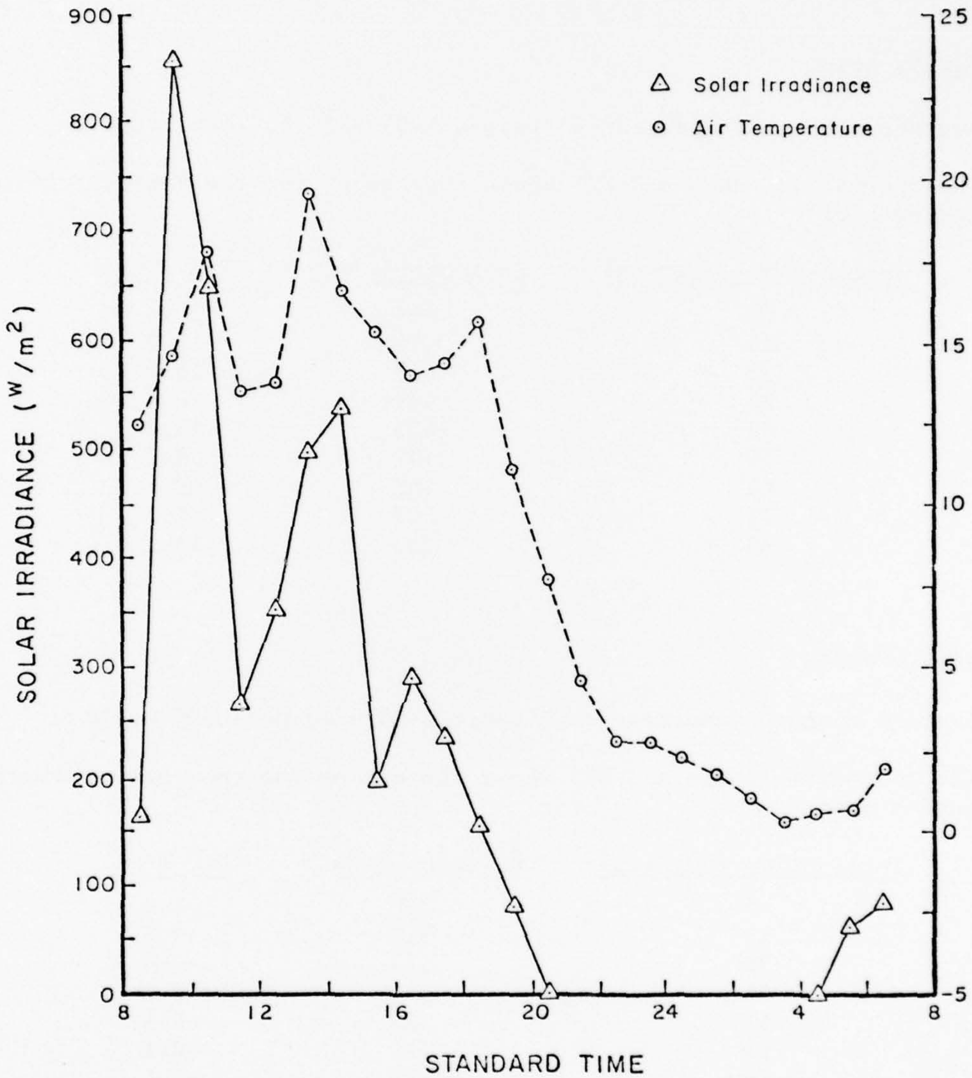

Figure 10. Measured global solar irradiance (highest value of M1 and M2 sites) and air temperature (M3 site) for July 15-16, 1977.

Table 1. Selected output for 0930 and 0330 (Standard Time) July 15-16, 1977.

Time = 0930

Average element temperatures (Layers 1-3) = 20.4, 16.6, 16.3°C

The thermal exitance and ERT above the canopy for the various viewing angles are:

Inclination (degrees)	Exitance (w/m^2)	ERT (°C)
5	419	20.3
15	413	19.2
25	410	18.6
35	408	18.4
45	408	18.2
55	407	18.1
65	407	18.1
75	407	18.1
85	407	18.1

Time = 0330

Average element temperatures (Layers 1-3) = -1.0, -0.0, 0.5°C

The thermal exitance and ERT above the canopy for the various viewing angles are:

Inclination (degrees)	Exitance (w/m^2)	ERT (°C)
5	310	-1.0
15	311	-0.6
25	313	-0.4
35	314	-0.2
45	314	-0.1
55	314	-0.1
65	315	-0.1
75	315	-0.1
85	315	-0.1

decreases as one proceeds from Layer 1 to Layer 3 due to solar heating and canopy geometry interactions. During the nighttime, however, the layers cool differentially due to the relatively low thermal exitance of a clear sky and the relatively high surface temperature of the ground. As a consequence, Layer 3 has the highest temperature. The three contact thermisters in Layers 1, 2, and 3 support this relationship. These trends are discussed by Geiger (1961).

The ERT of a sensor above the canopy as a function of view angle is dependent on the above layer temperature differentials and the canopy geometry. At the lowest sensor inclination angles, the ERT strongly relfects the temperature of Layer 1 (Table 1). As the sensor view inclination angle increases, the second, third, and ground layer temperatures more strongly influence the sensor ERT. It is believed that particular canopy geometries (leaf angle distribution, leaf area index, and leaf spatial distributions) can have very significant effects on the ERT of the sensor at varying view angles.

Sensitivity analyses were run at two different times (0930 and 0330) during July 15-16 to characterize two extremes of environmental conditions. The fixed parameters for Layers 1, 2, and 3 used in conducting the sensitivity analysis are as follows. The emissivity (including the ground), wind velocity, and leaf resistance to water vapor diffusion were 1.0, 10.0 cm/s, and 0.66 min/cm, respectively, for both 0930 and 0330 time periods. The solar irradiance, air temperature, ground temperature and relative humidity for the 0930 time were 855 w/m^2, 14.6°C, 11.7°C, and 0.20, respectively, and for the 0330 time were 0.0 w/m^2, 0.4°C, 5.0°C, and 0.85, respectively.

The results of the sensitivity analysis of emissivity for the day and night environmental conditions show that within a reasonable emissivity range for natural vegetation (0.96-1.00) the change in average element temperature is on the order of 0.6°C for all layers. A change of the internal resistance to waver vapor diffusion parameter (R_l) within a range of 0.3-1.2 min$\cdot$cm^{-1} has an equally small effect on the average element temperature of the three layers for the day environmental conditions. However, at lower values the parameter is very sensitive for day environmental conditions. For the night conditions, the average element temperature of the three layers changed less than 0.3°C for the R_l range of 0.05-1.2 min$\cdot$cm^{-1}.

In this study the R_l was held constant at 0.66 min$\cdot$cm^{-1}. Running (1978) has found that R_l is variable for lodgepole pine needles in full sunlight. The minimum daily R_l may vary from 0.11 to 0.50 min$\cdot$cm^{-1} depending on the pre-dawn leaf water potential. The daily variation of R_l is largely dependent on the humidity and may vary as much as four times that of the minimum daily R_l. Thus, the assumption of a constant R_l is very erroneous. As the season progresses, the pre-dawn leaf water potential drops as a result of decreasing available soil water, and during the October simulation a constant R_l value of 0.30 min$\cdot$cm^{-1} or above would be a relatively good value for both day and night conditions in light of the fact that the insensitivity of R_l on canopy temperatures was above this value. However, during the July simulation for full sunlight on the needles, an R_l value on the order of 0.15 min$\cdot$cm^{-1} is more appropriate. Using the day environmental conditions, the average element temperature in Layer 1 decreases 3°C for an R_l change from 0.66 to 0.15 min$\cdot$cm^{-1}. This tendency would cause the temperature of Layer 1 to be much closer to air temperature for the July simulation (Figures 9 and 10). R_l of needles tend to be maximal at radiation values less than 10% of full sunlight, and stomata are generally closed in the dark (Hinckley, Lassoie, and Running, 1978). Thus, in the relatively shaded portions of the canopy (Layers 2 and 3) one would expect the average R_l to be high, and Layer 1, which intercepts a large proportion of the solar irradiance, would have a minimal R_l value.

Tan, Black, and Nnyamah (1978) have noted that in well ventilated coniferous canopies, leaf temperatures are relatively similar to air temperature. Figures 9 and 10 indicate the close correspondence between air temperature and the simulated mean canopy element temperatures for Layers 2 and 3. However, Layer 1 significantly deviates from air temperature during times of high solar irradiance. If more appropriate values of R_l for each layer would have been used, as suggested above, the simulated average layer temperatures would approximate air temperature.

Table 2 presents the average element temperature, sensor ERT, and probability of gap for two canopy geometries, and for both day and night environmental conditions. The two geometries used were the normal foliage angle distribution, which was measured and utilized in all other analyses above, and the theoretical erectophile foliage angle distribution. Both distributions are presented by Kimes, Smith, and Berry (1978). It should be noted that although canopy geometry clearly affects the manner in which solar radiation is absorbed by a canopy system, and thus the layer temperature, the solar flux absorbed by each layer was held constant for this sensitivity analysis.

Table 2. Sensitivity analysis for the effect of two canopy geometries (normal and erectophile) versus average element temperature (A) and effective radiant temperature (ERT)(B) above the canopy as a function of view angle for both day and night environmental conditions. In addition, the probability of gap (PGAP) for the nine inclination intervals and each layer are compared between the two canopy geometries (C).

(A) Average Element Temperature (°C)

Layer	Day		Night	
	Normal	Erectophile	Normal	Erectophile
1	20.4	20.8	-1.0	-0.8
2	16.6	16.6	0.0	0.0
3	16.3	16.4	0.5	0.4

(B) ERT (°C)

Inclination angle	Day		Night	
	Normal	Erectophile	Normal	Erectophile
5	20.3	20.8	-1.0	-0.8
15	19.2	20.3	-0.6	-0.7
25	18.6	19.5	-0.4	-0.5
35	18.4	18.7	-0.2	-0.2
45	18.1	18.0	-0.1	0.2
55	18.1	17.4	-0.1	0.6
65	18.1	16.8	-0.1	1.0
75	18.1	16.3	-0.1	1.4
85	18.1	16.0	-0.1	1.6

(C) PGAP

Inclination angle	Layer 1		Layer 2		Layer 3	
	Normal	Erectophile	Normal	Erectophile	Normal	Erectophile
5	.03	.00	.00	.00	.13	.00
15	.30	.11	.10	.02	.47	.23
25	.41	.30	.19	.10	.57	.44
35	.46	.44	.23	.21	.61	.57
45	.48	.54	.25	.31	.62	.66
55	.49	.62	.26	.40	.63	.72
65	.50	.68	.27	.48	.63	.77
75	.50	.72	.27	.54	.63	.80
85	.50	.74	.27	.57	.63	.82

As shown in Table 2-A, the effect of canopy geometry on thermal radiation transfers is minimal and as a consequence the average element temperature changes very little between the two canopy geometries. However, the canopy geometry clearly has an effect on the contribution of thermal radiation from each layer to the sensor above the canopy as a function of view angle (Table 2-B). These trends can be explained by the different probabilities of gap at the various view angles for each layer as seen in Table 2-C.

The simulated results in Figure 9 were derived from the air temperature probe in the center of the four modeling trees (M3), and the correspondence between simulated and measured data was relatively good. However, it was noted that individual air temperature probes were not well correlated. For example, the air temperatures as measured by the air temperature probes at the M1, M2, and M3 sites were compared for the July 14 and 16 diurnal cycles. During the daylight hours the individual probes were highly erratic and uncorrelated, and at night the probe in the meadow opening (M1) was consistently lower than the probes within the canopy (M2, M3) by as much as 2°C. As a consequence, the simulated results for July 15-16, using the air temperature in the meadow opening (M1), were relatively poor, especially at night, in accuracy of prediction as compared to Figure 9. The above 2°C temperature differential at night can explain these relatively poor results.

Bergen (1971, 1974) showed that air temperature differentials within lodgepole pine canopies can be as much as 4-5°C in the vertical profile for clear, sunny days. In addition, six simultaneous air temperature measurements at various horizontal points within the canopy showed air temperature differences as large as 2°C. Thus, air temperature measurements at a single point (1 m above the ground) as utilized within this study will introduce error. In addition, on cloudless nights, ground cooling by net radiation loss often occurs, and an air temperature inversion near the ground occurs. Geiger (1961) has shown that even minimal wind speed of 10 to 100 cm/s can disrupt temperature stratification during the night in which 2°C differentials can commonly occur. These fluctuations can introduce error.

In addition, Bergen (1971) presented windspeed variation for a typical clear day and at a typical station within a 10 m tall lodgepole pine stand. Average differentials between simultaneous profiles were about 10% below the live canopy and 20% in the live canopy region. A subcanopy maximum occurs near 3 m height and a region of minimum wind speed occurs near 6 m height. Thus, some error is introduced by assuming a homogeneous vertical wind profile. Jarvis et al. (1976) discussed other studies of wind speed profiles in conifer canopies.

The data derived from the AGA Thermovision on July 15-16 were not reduced to absolute temperatures due to several technical difficulties. However, the black and white Polaroid photographs derived from the system were utilized to document relative trends which occurred within the lodgepole pine canopy. The photographs show several interesting trends. Figure 11-A shows the canopy at 0700. Some of the needles and small branches tend to heat up due to solar heating; however, this phenomenon is very heterogeneous in nature due to the heterogeneous distribution of sun-flecks within the canopy as discussed by Ross (1976). This phenomenon is supported by the erratic contact thermister

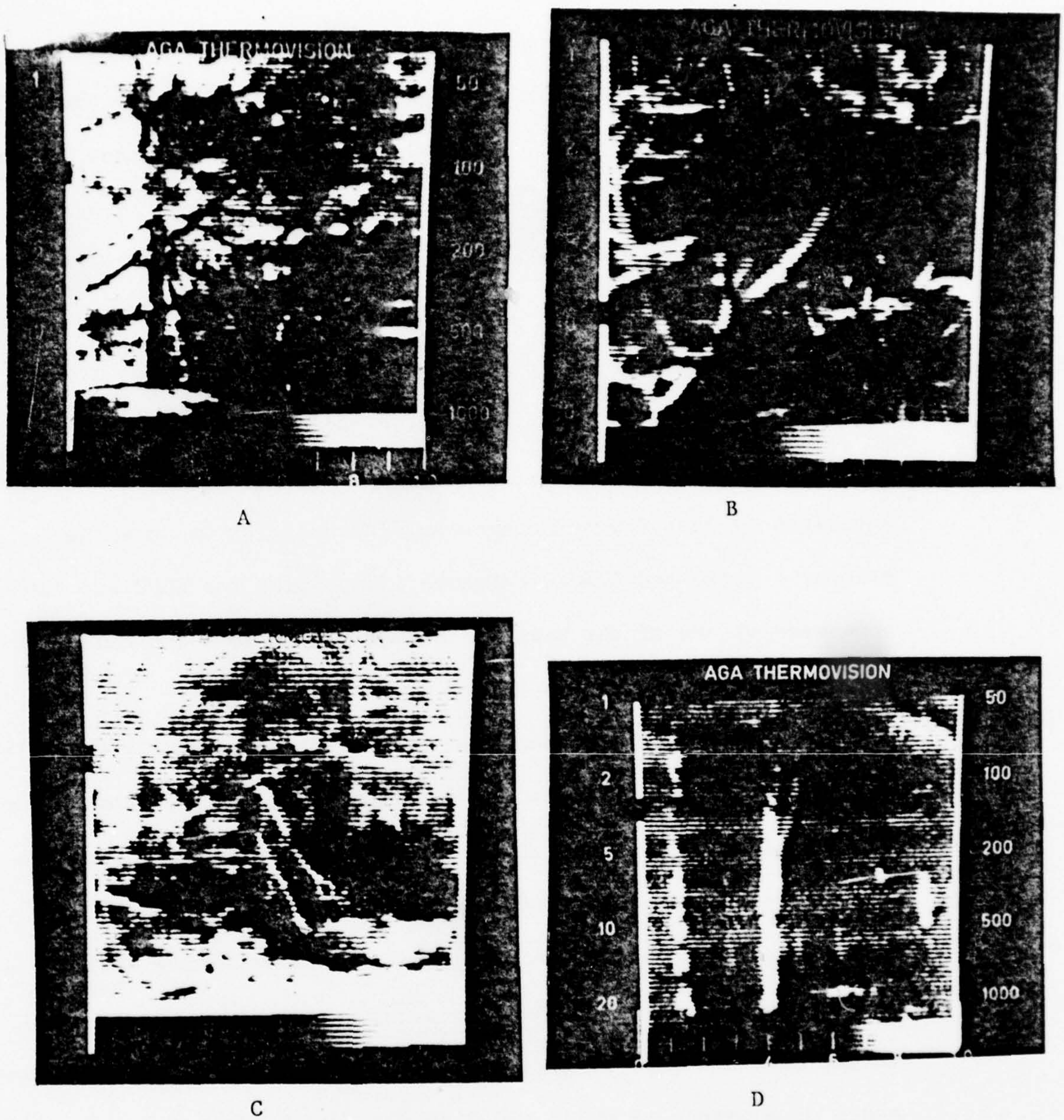

Figure 11. AGA Thermovision black and white Polaroid photographs of the modeling trees at Standard Times of 0700(A), 1100(B), 1300(C), and 0400(D) on July 15-16, 1977.

measurements of the three branch tips in Layers 1, 2, and 3, respectively, during the day. In addition, the bole and larger branches tend to be relatively cool due to the relatively large mass (Figure 11-A); and thus, the steady-state assumption of energy exchange may not be appropriate for these elements. This heterogeneity is important, especially in the design of the field measurements used to validate the simulated results. The AGA photographs show at 0900 that the boles and larger branches are still relatively cooler than the other canopy elements. During the morning the above trends are supported by Heat Spy measurements. The Heat Spy measurements of 4 branch, 7 bole, and 5 needle-branch tip samples for 0800 and 1000 show mean values of the branch and bole ERT to be 1-4°C cooler than the mean needle-branch tip ERT.

However, by 1100 the branches (Figure 11-B) generally tended to be warmer than the other canopy elements. Figure 11-C shows a close-up of a group of branches at 1300. The branches generally have a higher total solar absorption coefficient (Kimes and Smith, 1979), and they do not possess the high degree of convectional exchange and transpirational exchange that the needles experience due to their larger mass and physiology. During the afternoon the Heat Spy measurements of 4 branch, 7 bole, and 5 needle-branch tip samples for 1200 and 1400 show mean values of the branch ERT to be 6 to 8°C warmer than the needle-branch tip ERT. And the mean bole ERT was 2°C cooler and 1°C warmer than the needle-branch tip ERT, respectively, for the two times.

Figure 11-D shows that in the early morning hours the boles, which have a high heat capacity, are still relatively warm. The ERT of the

mean branch and needle-branch tip samples were equal and the mean bole ERT was 3°C warmer.

The majority of photographs derived from the AGA Thermovision did not include the uppermost crowns. Thus, it is difficult to compare trends of mean layer temperature as a function of height within the canopy for both simulated and measured data. The photographs largely emphasize Layers 2 and 3 of the canopy. As can be seen in Figure 11, the simulated results for Layers 2 and 3 are very close in absolute temperature, and the photographs (Figure 11-A,B) do not demonstrate any clear trends of mean element temperature as a function of height.

At night the simulated results (Figure 9) suggest that under clear sky conditions the mean temperature of Layer 1 will be approximately 2°C cooler than the other layers due to a high net thermal radiant loss to the sky. However, several photographs taken at night tend to show a portion of Layer 1. A trend of cooler canopy elements with increasing canopy height can be seen in Figure 11-D.

The 11-A photograph suggests another source of error. The TCSM assumes canopy layers of infinite extent; however, in the cluster of four modeling trees, solar heating of the edges of the canopy system does occur.

All simulated results for July 15-16 were validated against the mean Heat Spy ERT measurements of the 4 stake positions. It was believed that these measurements were the best ground truth available in regards to the modeling criteria. However, these measurements were not taken for the October 14-15 date, and the mean ERT of 5 needle-branch tips (Figure 8) was utilized for validation.

The simulated mean element surface temperatures for October 14-15 are presented in Figure 12 along with the mean Heat Spy ERT's from 5 branch tips occurring in Layers 1 and 2. The global irradiance, air temperature, and wind speed measured at the M1 site are presented in Figures 13 and 14. The accuracy of prediction is relatively good except at night when a deviation of approximately 3°C consistently occurs. A possible explanation of this deviation is as follows.

Only the air temperature probe in the meadow opening (M1 site) was available during the October 14-15 date. As discussed previously, the air temperature in the meadow (M1 site) was approximately 2°C lower at night than in the canopy (M3 site) during two July dates. This discrepancy could explain some of the deviation between simulated and measured results during the night period in Figure 12. In addition, as discussed previously, it is believed that the ERT's of the needle-branch tips may bias the average element temperature to be high which would also explain some of the deviations seen in Figure 12.

Figures 12 and 13 show that the simulated temperatures of Layers 1, 2, and 3 closely follow air temperature during the day. Unlike the July simulation, Layer 1 temperature does not deviate significantly from Layers 2 and 3 during high solar irradiance. This is due to the relatively high wind velocity and thus high convectional exchange which occurs during the October simulation.

To recapitulate, the TCSM, which incorporates the geometric structure of a vegetation canopy and predicts the thermal response of the canopy under various environmental conditions, was developed. The TCSM is designed to be instantaneous in nature, e.g., all canopy elements are under steady-state conditions and no heat storage may

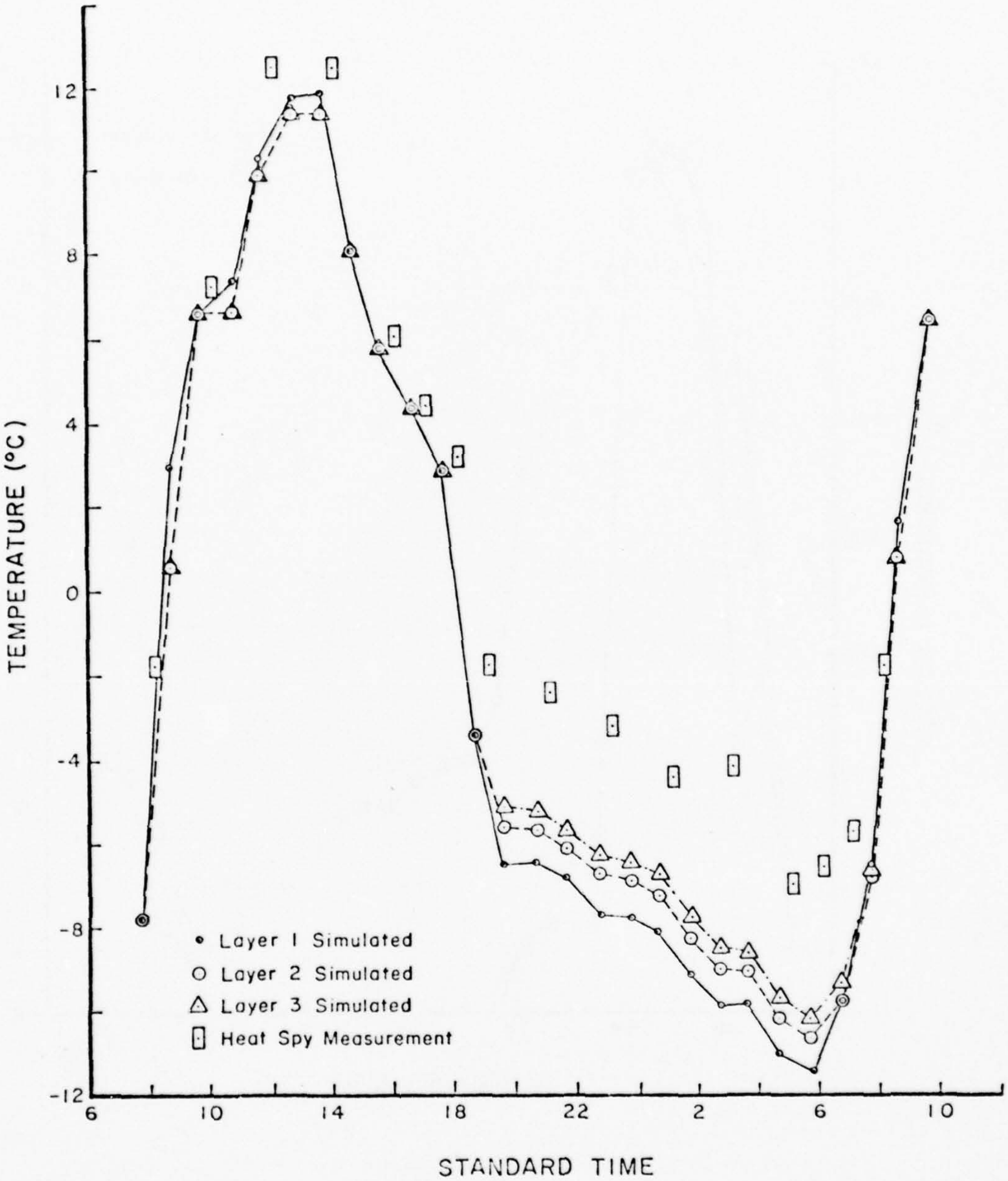

Figure 12. Simulated versus measured lodgepole pine canopy temperatures for October 14-15, 1977. Measured temperatures are the mean of five point ERT's of Layer 2 as measured by the Heat Spy. Air temperature was recorded in the meadow opening (M1 site).

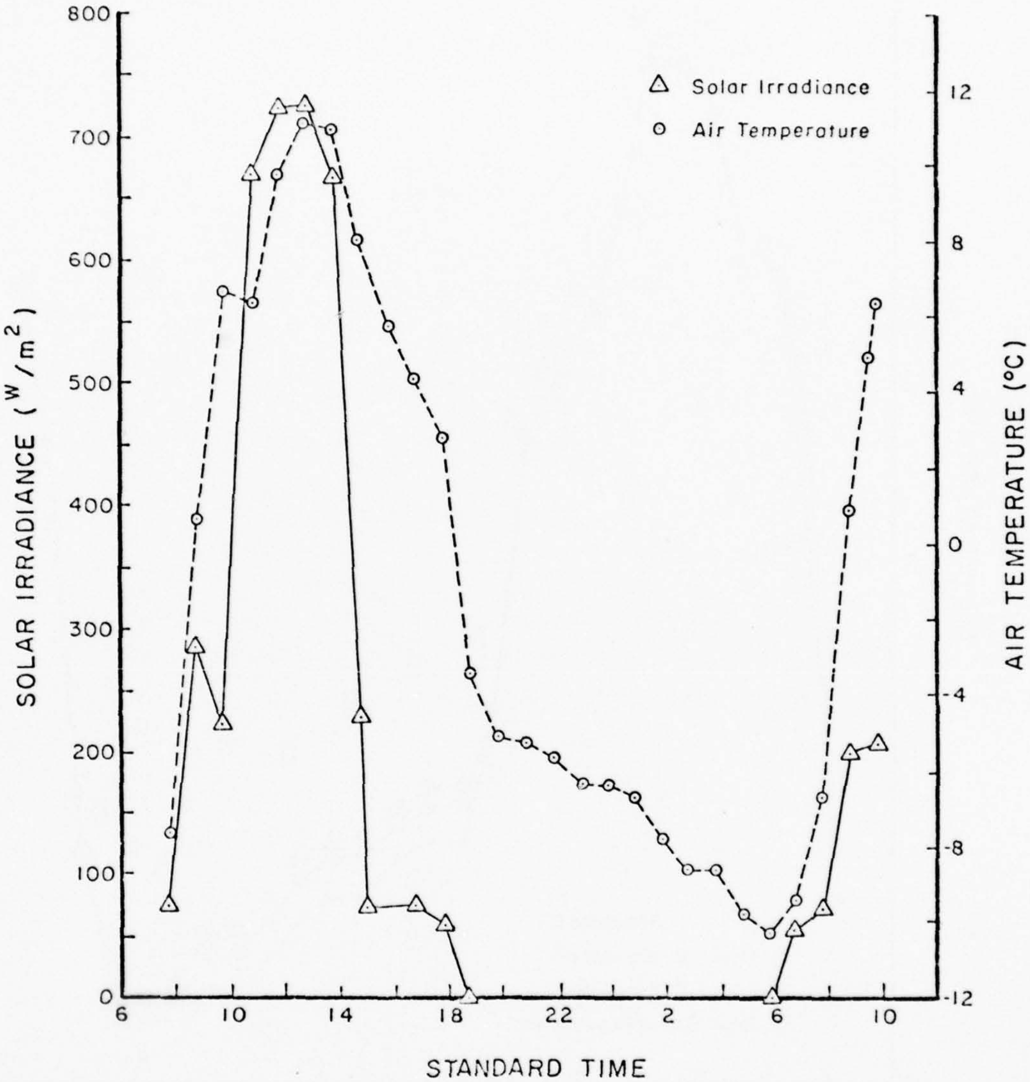

Figure 13. Measured global solar irradiance (highest value of M1 and M2 sites) and air temperature (M1 site) for October 14-15, 1977.

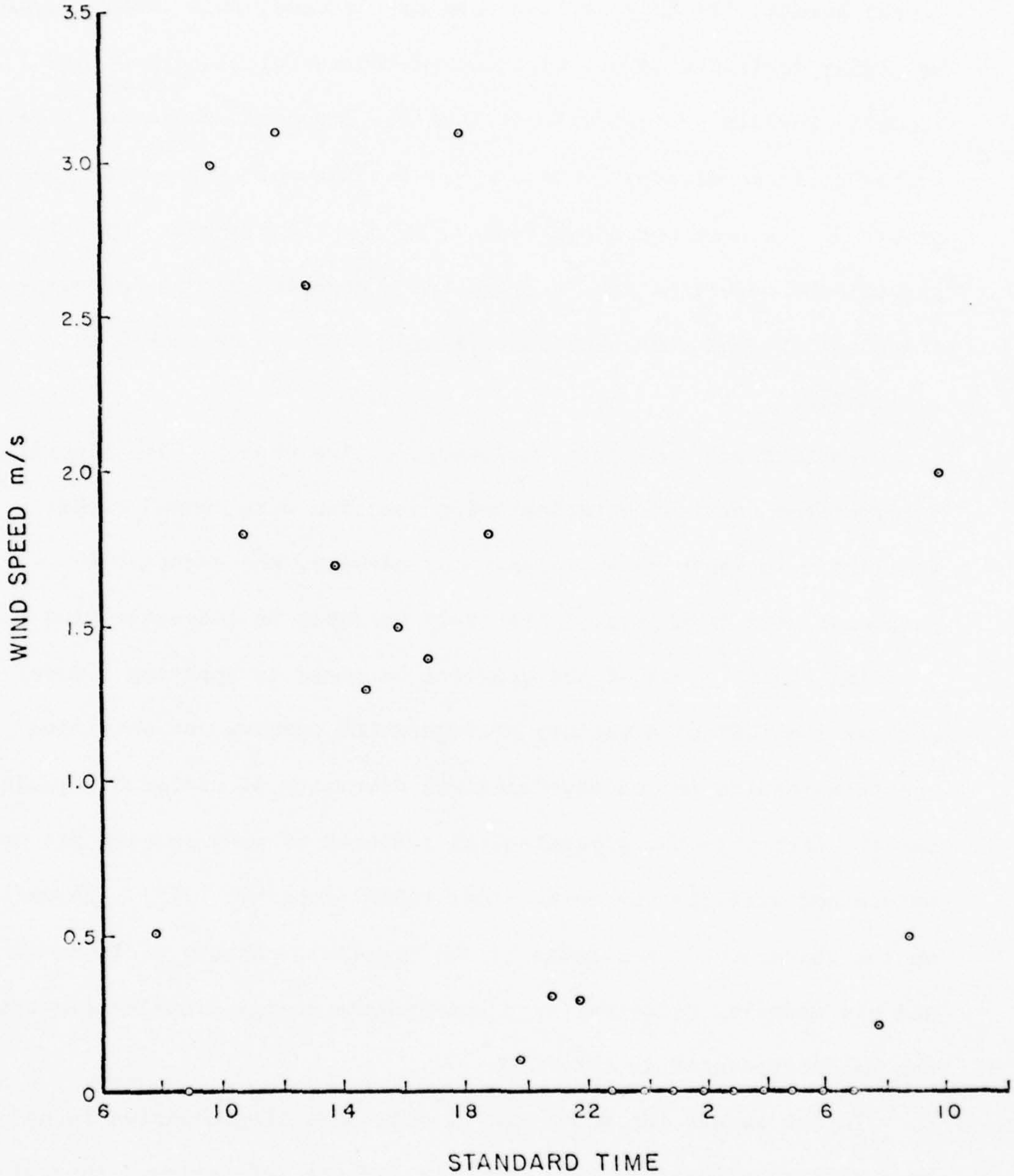

Figure 14. Wind speed as measured in the meadow opening (M1 site) for October 14-15, 1977.

occur. Therefore, the model is independent of all previous environmental events. In many applications of the model this feature would be highly desirable (e.g., when the environmental history is not known). However, to approximate the time dependent phenomena (non-steady-state conditions), one can use a series of incremental changes of steady-state energy flows (Gates, 1975). In branches and boles a significant amount of heat storage and conduction may be operating (Gates, 1975), and the above modifications may be desirable in some applications.

The TCSM was applied to a lodgepole pine canopy. The algorithms incorporated for transpiration and convection were indeed rather simplistic in their assumptions. For example, the constant R_l parameter used in this study is truly variable in lodgepole pine (Running, 1978). One of the greatest barriers in applying a model such as the TCSM to a variety of vegetation species and obtaining accurate results is the physiological diversity of different species, and the fact that the physiological response of many species are not understood sufficiently to be predictable (Running, 1978). Depending on the researcher's knowledge of the vegetation canopy of interest and his modeling criteria, more appropriate energy transfer algorithms can be incorporated in the TCSM.

In the future the model can be made more comprehensive in nature by including algorithms for: thermal radiant reflections; thermal spectral radiance of the sensor; time difference equations which account for energy dynamic and heat storage of the soil profile and the tree boles; wind profiles within the canopy; air temperature profiles; and canopy water relations. In addition, it is anticipated that the model will be applied to a variety of vegetation canopy types which do not closely approximate air temperature as was the case for the lodgepole pine canopy.

Conclusions

During the July simulation the differentials between the simulated versus measured horizontal effective radiant temperatures for a lodgepole pine canopy were, in general, less than 2°C. The simulated average layer temperatures for all three layers were generally within 2°C of air temperature, except for Layer 1 during periods of high solar irradiance in July. It is believed this discrepancy is due to erroneous values of the internal leaf resistance to water vapor diffusion (R_l). The simulated results suggest that for needle-bearing forest canopies, average element temperatures deviate significantly above air temperature only during periods of relatively high solar irradiance, low wind velocities, and low transpiration.

The effect of canopy geometry (element inclination distribution) on thermal radiation transfers, to and from the individual layers within the canopy, seems to be minimal. However, the canopy geometry clearly has an effect on the contribution of thermal radiation from each layer to the sensor above the canopy as a function of view angle. It is believed that for certain canopy element inclination distributions, canopy LAI, and environmental conditions, the sensor inclination angle will affect the sensor response greatly; and this phenomenon has important implications on the optimum view angle for making inferences about the target of interest.

The surface temperatures of canopy elements are very heterogeneous, especially during direct solar irradiance conditions. The mean of several point measurements (contact thermisters and Heat Spy on branch tips) biases the measured average canopy temperatures, but a horizontal ERT which includes a cross section of canopy elements is believed to be the least biased of the measurements taken in this study.

Both air temperature and wind speed variations, as a function of location within the canopy, introduce error in the simulated results. In addition, the assumption of a constant R_l introduces error. The assumption of instantaneous heat exchange may not be accurate for branches and boles.

Due to the large heat capacity of the ground and net thermal radiant loss to the clear night sky, the average element temperature increases as one proceeds from Layer 1 to Layer 3 as demonstrated by both simulated and measured results.

Model simulations showed that the total global irradiance absorbed by the lodgepole pine canopy system is relatively constant with solar zenith angle. However, the proportion of total global irradiance absorbed by individual canopy layers varies as a function of solar zenith angle.

The TCSM provides a modeling framework which may be useful to a variety of research interests. Specific energy transfer algorithms, which are best suited to the researcher's modeling criteria, can be incorporated in the TCSM. The TCSM is unique in that the framework incorporates the geometric structure in radiation transfer algorithms.

References

Allen W.A., and J.A. Richardson. 1968. Interaction of Light with a Plant Canopy. J. Opt. Soc. Am. 58(8):1023-1028.

Bergen, J.D. 1971. Vertical Profiles of Windspeed in a Pine Stand. Forest Sci. 17:314-321.

Bergen, J.D. 1974. Variation of Windspeed with Canopy Cover within a Lodgepole Pine Stand. U.S.D.A. Forest Service Research Note RM-252. 4 p.

Berry, J.K. 1976. Extracting Scene Feature Vectors Through Modeling. Ph.D. Dissertation, Colorado State University, Fort Collins, Colorado. 169 p.

Blaxter, K.L. 1967. The Energy Metabolism of Ruminants. 2nd Edition. Hutchinson, London. 332 p.

Brown, K.M. 1969. A Quadratically Convergent Newton-like Method Based upon Gaussian Elimination. SIAA Journal on Numerical Analysis, 6(4):560-569.

Brown, K.M., and J.E. Dennis, Jr. 1971. On the Second Order Convergence of Brown's Derivative-free Method for Solving Simultaneous Nonlinear Equations. Yale University, Department of Computer Science, Technical Report 71-7.

deWit, C.T. 1965. Photosynthesis of Leaf Canopies. Agr. Res. Rept. 663. Wageningen, Netherlands. Chap. 4, p. 11.

Gary, H.L. 1976. Crown Structure and Distribution of Biomass in a Lodgepole Pine Stand. U.S.D.A. Forest Service Res. Pap. RM-165, Rocky Mountain Forest and Range Experiment Station, Fort Collins, Colorado. 20 p.

Gates, D.M. 1966. Transpiration and Energy Exchange. Quart. Rev. Biol. 41:353-364.

Gates, D.M. 1968. Energy Exchange in the Biosphere. Harper and Row, Inc., New York. 151 p.

Gates, D.M. 1975. Introduction: Biophysical Ecology. In: Perspectives of Biophysical Ecology (D.M. Gates and R.B. Schmerl, eds.) Springer-Verlag, New York. p. 1-28.

Heilman, J.L., E.T. Kanemasu, and N.J. Rosenberg. 1976. Thermal Scanner Measurement of Canopy Temperatures to Estimate Evapotranspiration. Remote Sensing of Environment 5(2):137.

Hinckley, T.M., J.P. Lassoie, and S.W. Running. 1978. Temporal and Spatial Variations in the Water Status of Forest Trees. Forest Science Monograph 20. 72 p.

Idso, S.B., and C.T. deWit. 1970. Light Relations in Plant Canopies. Applied Optics 9(1):177-184.

Idso, S.B., D.G. Baker, and B.L. Blad. 1969. Relations of Radiation Fluxes over Natural Surfaces. Quart. J. Roy. Meteorol. Soc. 95:244.

IMSL Library 3, Edition 6, 1977. (Fortran) CDC 6000/7000, CYBER / 170 Series, International Mathematical and Statistical Libraries, Inc., 1977.

Kimes, D.S., K.J. Ranson, J.A. Kirchner, and J.A. Smith. 1978. Modeling Descriptions and Terrain Modules. Final Report. Environmental Laboratory, U.S. Army Engineers Waterways Experiment Station, DACW 39-77-C-0073. 125 p.

Kimes, D.S., and J.A. Smith. 1979. Mathematical Simulation of Absorbed Solar Radiation in Vegetation Canopies. To be submitted for publication.

Kimes, D.S., J.A. Smith, and J.K. Berry. 1979. Determining Forest Canopy Geometry. To be submitted for publication.

Kondrat'yev, K. YA. 1965. Actinometry. Translation of "Aktinometriya" Gidrometeorologicheskoye Izdatel' stvo, Leningrad, 1965. National Aeronautics and Space Administration, Washington, D.C. November 1965, NASA TT F-9712.

Lansberg, J.J., and M.M. Ludlow. 1969. A Technique for Determining Resistance to Mass Transfer Through the Boundary Layers of Plants with Complex Structure. J. Appl. Ecol. 7:187-192.

Lee, R., and D.M. Gates. 1964. Diffusion Resistance in Leaves as Related to Their Stomatal Anatomy and Micro-structure. Am. J. Bot. 51(9):963-975.

Leeman, V., D. Earing, R.K. Vincent, and S. Ladd. 1971. The NASA Earth Resources Spectral Information System: A Data Compilation. Infrared and Optics Laboratory, Willow Run Laboratories, University of Michigan, NASA CR-WRL-31650-24-T.

Miller, P., and D.M. Gates. 1967. Transpiration Resistance of Plants. Am. Midl. Natural. 77:77-85.

Monteith, J.L. 1965. Light Distribution and Photosynthesis in Field Crops. Ann. Bot. 29(133):17-37.

Monteith, J.L. 1973. Principles of Environmental Physics. American Elsevier Publ. Co., Inc., New York. 241 p.

National Bureau of Standards. 1978. Self Study Manual on Optical Radiation Measurements. Parts 1, 2, 3. Optical Physics Division, Institute for Basic Standards, Washington, D.C.

Nilson, T. 1970. A Theoretical Analysis of the Frequency of Gaps in Plant Stands. Agr. Meteorol. 7:25-38.

Oliver, R.E., and J.A. Smith. 1973. Vegetation Canopy Reflectance Models, Final Report, U.S. Army Research Office - Durham, DA-ARO-D-31-124-71-6165. 82 p.

Oliver, R.E., and J.A. Smith. 1974. A Stochastic Canopy Model of Diurnal Reflectance. Final Report, U.S. Army Research Office, Durham, North Carolina, DAH C04-74-60001. 105 p.

Ranson, K.J., J.A. Kirchner, and J.A. Smith. 1978. Scene Radiation Dynamics, Vol. II. Final Report, Environmental Laboratory, U.S. Army Engineer Waterways Experiment Station. DACW 39-77-C-0073. 74 p.

Ross, J. 1976. Radiative Transfer in Plant Communities. In: Vegetation and the Atmosphere, Vol. I Principles (J.L. Monteith, ed.) Academic Press, London.

Running, S.W. 1978. An ET Model Controlled by Physiological Processes for Coniferous Forests. In press for Proceedings of the 14th Conference on Agriculture and Forest Meteorology, April 2-6, 1979. Published by Am. Meteor. Soc., Boston, Mass.

Rutter, A.J. 1975. The Hydrological Cycle in Vegetation. In: Vegetation and the Atmosphere (J.L. Monteith, ed.) Academic Press, London.

Stone, L.R., E.T. Kanemasu, and M.L. Horton. 1975. Grain Sorghum Canopy Temperature as Influenced by Clouds. Remote Sensing of Environment 4:177-181.

Suits, G.H. 1972. The Calculation of Directional Reflectance of a Vegetation Canopy. Remote Sensing of Environment 2:117-125.

Tan, C.S., T.A. Black, and J.V. Nnyamah. 1978. A Simple Diffusion Model of Transpiration Applied to a Thinned Douglas-fir Stand. To be published in Ecology.

Tenhunen, J.D., and D.M. Gates. 1975. Light Intensity and Leaf Temperature as Determining Factors in Diffusion Resistance. In: Perspectives of Biophysical Ecology (D.M. Gates and R.B. Schmerl, eds.) Springer-Verlag, New York.

Tibbals, E.C., E.K. Carr, D.M. Gates, and F. Kreith. 1964. Radiation and Convection in Conifers. Am. J. Bot. 51(5):529-538.

The University of Michigan. 1969. Target Temperature Modeling. Evaluation of Contract F30602-68-C-0099, Defense Documentation Center.

Warren Wilson, J. 1965. Stand Structure and Light Penetration, I. Analysis by Point Quadrats. J. Appl. Ecol. 2:383-390.

Watson, Kenneth. 1971. A Thermal Model for Analysis of Infrared Images. In: NASA Third Annual Earth Resources Aircraft Program Review. NASA, Houston, Texas.

Watson, K., L.E. Rowan, and T.W. Offield. 1971. Application of Thermal Modeling in the Geologic Interpretation of IR Images. Proceedings of the Seventh International Symposium on Remote Sensing of Environment, Ann Arbor, Michigan, May 1971. p. 2017-2041.

West, H.W., and H.M. Floyd. 1976. An Automated System for Collecting, Processing, and Displaying Environmental Baseline Data. Mobility and Environment Systems Laboratory, U.S. Army Engineer Waterways Experiment Station, Vicksburg, Mississippi, Tech. Report M-76-11.

Wiebelt, J.A., and J.B. Henderson. 1977. Techniques and Analysis of Thermal Infrared Camouflage in Foliated Backgrounds. Final Report, U.S. Army Mobility Equipment Research and Development Command, Fort Belvoir, Virginia. DAAG53-76-C-0134. 63 p.

4.0 CONCLUSIONS AND RECOMMENDATIONS

The thermal canopy signature model (TCSM), Chapter 3, together with the absorption calculations performed by ABSORPT, Chapter 2, provide a modeling framework for simulating energy transfers within vegetation canopies of specific geometric structure. The thermal modeling approach is unique in that it incorporates detailed geometric canopy structure to define the radiant transfers occurring within the canopy system. The model predicts the radiometric temperatures as a function of look angle. In addition, a radiometric temperature height profile of the canopy is calculated. The model was successfully applied to a lodgepole pine (Pinus contorta) canopy which indicated that, except for specific environmental and physiological conditions, mean element temperatures closely approximate air temperature. The model suggests, however, that canopy structure can have significant effects on the response of a thermal sensor above the canopy. The angular thermal exitance prediction capability of the TCSM recommends it as a useful tool for defining optimum sensor view angle and environmental conditions for target/background discrimination studies.

The research described in this report also addressed the development of methods for determining forest canopy geometry, particularly needle and branch angle frequency distributions. It was found that these distributions strongly influence the absorption of solar radiation within the canopy. Solar radiant absorption, in turn, affects the overall thermal equilibrium within the canopy layers. A description of the geometry techniques has been submitted and accepted by the appropriate journals (Appendix A).

There are many broad areas of potential application of the modeling approaches described depending on a user's orientation. Some of these applications might focus on the vegetation canopy itself as the primary scene of interest, as in agricultural or forest water relation studies. Others might focus on the surface beneath the canopy, as in geological or snow cover estimation problems. A detailed exploration and description of such applications is beyond the scope of this report. However, with regard to the modeling approach itself, the authors make the following recommendations.

First, and most importantly, how well does the TCSM perform when applied to a wide variety of vegetation types and terrain conditions? The model needs to be validated for other situations than the lodgepole canopy simulated here. Undoubtedly, specific energy transfer algorithms presently incorporated in the model will need modification. The application of the model to closed versus open canopies will also need to be systematically addressed.

Secondly, what is the tradeoff in model precision or accuracy versus the availability of model parameters? A related question is the relative advantage, under different conditions, of employing a detailed model such as the TCSM which meticulously accounts for all energy transfers and incorporates complete canopy geometry to that of employing more simple models?

In summary, the terrain feature models described in this report provide a basic framework which can be adapted or utilized to study a large number of research interests. For many design problems relative to predicting background electromagnetic behavior of natural features, the present models should prove useful. However, further validation and appropriate modification of model processes is recommended before the model is applied generally.

APPENDIX A: Abstracts of Submitted Papers

A Monte Carlo Calculation of the Effects of Canopy Geometry on PhAR Absorption

D. S. Kimes,* K. J. Ranson and J. A. Smith

College of Forestry and Natural Resources
Colorado State University
Fort Collins, Colorado 80523, U.S.A.

ABSTRACT

The ability of vegetation canopies to absorb photosynthetically active radiation (PhAR) is known to be a function of the canopy geometry. A Monte Carlo model was used to estimate relative PhAR absorption in theoretical vegetation canopies of different structure. The relatively simple single component, multilayer simulations adequately describe the empirically established trends reported by a wide variety of investigators. Absorption trends for erectophile (mostly vertical leaves) and planophile (mostly horizontal leaves) canopies are indicated with respect to leaf area index (LAI) and solar zenith angle. Generally, our model results show that erectophile canopies are more efficient at absorbing PhAR under medium to high LAI and all ranges of zenith angle. Planophile canopies show increased absorption at lower LAI's.

*Present Address
Earth Resources Branch
NASA/Goddard Space Flight Center
Greenbelt, Maryland 20771, U.S.A.

Extension of the Optical Diffraction Analysis Technique for Estimating Forest Canopy Geometry

D.S. Kimes[A], J.A. Smith[A], and J.K. Berry[B]

[A]College of Forestry and Natural Resources, Colorado State University, Fort Collins, Colorado 80523, U.S.A.

[B]School of Forestry and Environmental Studies, Yale University, New Haven, Connecticut 06511, U.S.A.

Abstract

Optical diffraction analysis of *in situ* ground photographs has previously been utilized to estimate foliage angle distributions in grassland canopies. These canopies are typically characterized by a single component, leaves, and the foliage is highly linear in nature. In this paper, the diffraction technique is extended to a multi-component forest canopy containing needles and branches. Additional convolution and coordinate transformations are derived to estimate the branch and needle angle frequency distributions for top, middle, and base sections of two lodgepole pine (*Pinus contorta*) trees. The resulting distributions show that the branch inclination angles tend to increase as one proceeds to the tree tops. The needle inclination angle distribution was relatively constant for all layers, and it is believed that this distribution is characteristic of a large class of needle bearing species.

Aust. J. Bot., 1979, 27, 123-33

Optical Diffraction Analysis for Estimating Foliage Angle Distribution in Grassland Canopies

J. A. Smith[A] *and J. K. Berry*[B]

[A] College of Forestry and Natural Resources, Colorado State University, Fort Collins, Colo. 80523, U.S.A.
[B] School of Forestry and Environmental Studies, Yale University, New Haven, Conn. 06511, U.S.A.

Abstract

A non-destructive, rapid technique utilizing horizontal *in situ* ground photographs for estimating foliage angle distributions is discussed. Optical diffraction patterns generated from orthogonal photographs are analysed for angular bias by wedge sampling. Probability distributions for planar projections of foliage orientations are derived from these measurements and mathematically convoluted to determine the actual three-space probability distribution function for foliage angles. The method is particularly appropriate for dense canopies which are difficult to measure by other techniques. The diffraction technique is evaluated for abstract canopies and for a canopy of Western wheat grass (*Agropyron smithii*). It also yields physically consistent interpretations for the phenological development of domestic Satanta wheat (*Triticum aestivum*).

Introduction

Foliage angle distribution functions for grassland canopies have traditionally been estimated by point quadrat techniques such as discussed by Wilson (1960, 1963) and Philip (1965). Other recent techniques involving photographic or photocell measurements of foliage gap frequency which can be related to the foliage angle distribution include the methods discussed by Norman and Tanner (1969) and Bonhomme and Chartier (1972). The present authors described another photographic procedure for grassland canopies in an earlier paper (Smith *et al.* 1977) whereby off-angle photographs are used to record gap frequency and a Fredholm integral equation is solved which relates foliage angles to gap frequency.

The point quadrat technique offers practical difficulties in the amount of field time required to obtain the measurements. The photographic and photocell methods are an improvement in this regard, but they are difficult to apply in canopies with dense foliage cover. The Fredholm technique, for example, cannot be applied to dense canopies in which canopy closure at most view angles is complete.

In this paper we present an alternative approach applicable to dense canopies which utilizes optical diffraction pattern analysis of field photographs. Planar distributions of foliage angles are determined from orthogonal ground photographs obtained in the vertical plane of the plant canopy. These orthogonal distributions are then mathematically convoluted to estimate the actual plant canopy foliage angle distribution. This diffraction technique is also a simple and rapid *in situ* measurement method.

Aust. J. Bot., 1977, **25**, 545–53

A Comparison of two Photographic Techniques for Estimating Foliage Angle Distribution

J. A. Smith[A], *R. E. Oliver*[AB], *and J. K. Berry*[AC]

[A] Department of Earth Resources, Colorado State University, Fort Collins, Colorado 80523, U.S.A.
[B] Present address: IBM Corporation, Houston, Texas, U.S.A.
[C] Present address: School of Forestry and Environmental Studies, Yale University, New Haven, Connecticut, U.S.A.

Abstract

There is an increasing interest in theoretical models which describe the interaction of solar radiation with vegetation canopies. Common to these models is a need to describe mathematically the geometric structure of the plant canopy. The amount of radiation reflected or absorbed by the canopy is primarily determined by the distribution of gaps in the foliage with respect to the radiation source. A measure of canopy geometry related to gap frequency at various view angles is the distribution of leaf angles. Two methods for measuring the distribution of leaf angles are discussed. The first method is to project orthogonally and photograph individual plants and relate the measured leaf angles in the projections to the canopy distribution of angles. The second method is a rapid *in situ* method based on ground level multiple view angle photography. A Fredholm integral equation relating foliage angles to the proportion of gap in the canopy as a function of view angle is then solved. Comparisons of the results using the two methods are made for a canopy of Western wheat grass (*Agropyron smithii*).

Introduction

Mathematically, a homogeneous vegetation canopy may be described given the following information:

(1) Inclination angle distribution of the foliage elements.

(2) Azimuthal angle distribution of the foliage elements.

(3) Leaf area index (ratio of the one-sided leaf area to a unit area of underlying soil surface).

(4) A relation describing the three-dimensional dispersion of the leaf area within the canopy.

The situation becomes more complex if the canopy is heterogeneous in either composition or structure. Heterogeneity usually implies that the canopy must be stratified into layers and the above information determined for each layer. Stratification may be determined either from a height distribution (Oliver and Smith 1973) or from the apparent morphology characteristics of the vegetation under study.

The foliage inclination angle distributions for various typical classes of stand geometry are shown in Fig. 1 (de Wit 1965). Horizontal leaves are most frequent in planophile canopies, and vertical leaves in erectophile canopies. The leaves in plagiophile canopies are most frequent at oblique inclinations of greater than 45°, those in extremophile canopies at oblique inclinations of less than 45°. Interpretations of the cumulative frequency distribution function may be made as above and their

Reprinted from Optical Engineering © 1978 Society of Photo-Optical Instrumentation Engineers, Bellingham, Washington 98225 USA

A Portable Instrument for Simultaneous Recording of Scene Composition and Spectral Reflectance

Joseph K. Berry
Formerly Graduate Research Associate
Department of Earth Resources, Colorado State University
Now with School of Forestry and Environmental Studies
Yale University

Frederick J. Heimes
Graduate Research Assistant, Department of Earth Resources
Colorado State University, Fort Collins, Colorado 80523

James A. Smith
Associate Professor, Department of Earth Resources
Colorado State University, Fort Collins, Colorado 80523

Abstract

A battery-powered scene recording radiometer system has been developed for relating spectral variability and target composition. A remote controlled filter wheel radiometer is interfaced with a Hasselblad 500 EL camera, so that the silicon detector is directed toward the camera's viewing glass. Signal detection at discrete wavelength bands is achieved by successively rotating interchangeable interference filters that interdict the view of the detector. Filter positioning is controlled by coding holes drilled in the filter wheel disk which are interpreted by a bank of opposing light emitting diodes and phototransistors. Upon obtaining a photographic record of the scene, the camera is automatically advanced.

Introduction

A recurring problem in applying remote sensing technology to natural resources is the difficulty in correctly classifying a resolution element which contains a mixture of materials. This problem is particularly acute in natural vegetation communities such as those encountered in the West, where a great deal of heterogeneity occurs within the resolution element. A machine-assisted classification rule, however, is forced into one of two choices: (1) identifying the resolution element as a single material when, in fact, it may contain only a small percentage of the material; or (2) leaving the resolution element unclassified. This problem of mixtures is closely related mathematically to the problem of signature extraction, which describes the difficulty of determining a typical spectral response for materials when the underlying data distributions are heterogeneous.

There are two broad approaches to the mixtures problem. These include a least squares approach, and a parameter estimation technique using maximum likelihood procedures. Pace and Detchmendy[1] as well as Hallum[2] discuss the former approach. The maximum likelihood procedure is described by Horwitz et al[3] and Guseman[4]. Both approaches have as their fundamental assumption the hypothesis that there is a linear relationship between measured spectral response from a resolution element and the proportions of materials contained within the resolution element. This assumption has never been clearly evaluated through empirical data. The primary reason for this omission appears to be the fact that most spectrometers measure the total response from a resolution element without the capability of providing a registered record of the composition of the resolution element. One exception is the system reported by Dana[5] as used in determining aircraft reflectance measurements in which a bore-sighted camera is used in conjunction with a radiometer.

The instrument described in this paper was developed to provide a method for obtaining a direct and simultaneous measurement of both scene composition and spectral response, using a common field of view. The instrument has been used by the authors for investigating mixture effects in a lodgepole pine (*Pinus contorta*) community in the central Colorado mountains. The age of the stand studied was between 30 and 50 years with average height of the stand approximately 20 ft. Canopy density was variable ranging from approximately 80% crown closure to a completely open, grass-covered clearing. The majority of the understory within denser regions of the lodgepole stand was similar to that of the meadow opening. In this application an aerial tramway system was required to suspend the instrument.

Physical Features

The scene recording radiometer is essentially a remote controlled filter wheel radiometer interfaced to a Hasselblad EL 500 camera. A schematic of the instrument is shown in Figure 1. A remote readout and control station are utilized in conjunction with the instrument. The functions of the system are five-fold: (1) signal detection, (2) partitioning of the signal into discrete wavelength bands, (3) control of filter wheel position, (4) photographing the scene, and (5) remote system control and signal readout.

The radiometer system uses a silicon detector directed toward the viewing glass of the camera. The optics of the camera define the instrument's field of view. This allows adjustment of the radiometer field of view by varying the camera's lens system. Sharp definition of the field of view of the instrument is achieved by overlaying a circular mask on the viewing glass. The diameter of the mask was constructed to be slightly smaller than the physically constrained field of view of the detector when interdicted by an interference filter. This constrained field of view was measured by mounting the instrument on a goniometer and rotating it about the optical axis of the camera, while exposing it to a narrow beam of light. An interference filter centered at 6328 Å was used to accommodate a helium neon gas laser light source.

1427 received March 22, 1977.

Scene Radiation Dynamics

ABSTRACT

These reports are a two-volume Final Report Series for Project DACW 39-77-C-0073 issued by the Environmental Laboratory of the U.S. Army Engineer Waterways Experiment Station. The period covered is from 11 August, 1977 to 30 September, 1978. Overall objectives of this one year study were to develop a comprehensive optical and thermal signature data base and to evaluate or develop optical and thermal canopy radiation models. A variety of vegetation terrain features were studied including coniferous trees (*Pinus contorta*), deciduous trees (*Elaeagnus augustifolia*), shrubs (*Potentilla*) and grasses (*Festuca*). In order to synthesize the scene radiation dynamics with the use of models, accompanying geometric and meteorological parameters were also obtained.

Volume I presents the optical and thermal modeling descriptions and includes terrain data modules for coniferous, deciduous, and grass terrain features. The optical SRVC (Solar Radiation Vegetation Canopy Model) developed under previous U.S. Army Research Office sponsorship is evaluated against these terrain modules. A thermal leaf model and an initial thermal canopy signature model are described and compared against field measurements. Both optical and thermal signature models are infinite plane terrain approximations to a three-layer stratified canopy. Source and view angle dependencies of the exitance are predicted. In addition, the thermal model predicts the temperature distribution of the vegetation layers.

Volume II contains the optical reflectance data listings and includes descriptive information for the experimental sites. The data

types and data reduction methods are enumerated. Finally, an analysis of optical data dispersions is given including seasonal and diurnal variability and two-spectral space scatter plots. The applicability of a Tasseled Cap type of transformation is evident.

Evaluation of Illumination and Terrain Geometry Effects on Spectral Response in Mountain Terrain

ABSTRACT

An extensive analysis of terrain geometric effects on the optical scattering properties of natural resource scene in mountainous terrain has been performed. Spectral reflectance measurements were obtained for lodgepole pine, *Pinus contorta*, ponderosa pine, *Pinus ponderosa*, Russian olive, *Eleaegnus angustifolia*, grass species, *Agropyron sp.*, and *Bromus sp.*, and snow. Sensor platforms included ground-based measurements using aerial tramways, aircraft radiometric observations, and satellite (Landsat) measurements. A wide range of effective view and source illumination angles were recorded for the various target/sensor combinations.

Regression analyses and photometric plots were made from the data in order to test the Lambertian assumption for the various material types. In addition a process-oriented radiative transfer model was applied to the data. This model was also used to evaluate initial effects of background topographic variations.

Results of this study indicate that, particularly in the chlorophyll absorption band all materials exhibit non-Lambertian behavior for effective zenith sensor or source angles greater than 60 degrees, but that for effective angles less than 40 degrees, the Lambertian assumption may be valid. For stable atmospheric conditions and constant phase angle the Minnaert relationship may be applied to quantify scene radiance properties. The canopy reflectance model was found to follow the general trends of the field measurements but overestimates infrared response. In order to adequately model topographic influences or spectral response, canopy density variations must be included.

APPENDIX B: Supporting Material for Monte Carlo Calculations of Absorbed Solar Radiation in Vegetation Canopies

Diffuse/Direct Ratio Sensitivity Analysis

Element Transmission Sensitivity Analysis

Vertical Reflection Validation

SRVC Simulated Absorption Coefficients

Program Listing for ABSORPT

APPENDIX B

The following topics present in full detail the results of the data analysis and computer programs mentioned in the main text of Chapter III.

Diffuse/Direct Ratio Sensitivity Analysis

Figures 1 and 2 present the proportion of absorbed spectral solar irradiance for a wavelength of high canopy reflectance (ρ = .50, τ = .05 for all canopy elements) with a solar zenith angle of 0° and 72°, respectively. Figures 3 and 4 present the proportion of absorbed spectral solar irradiance for a low canopy reflectance (ρ = .05, τ = .001 for all canopy elements) with a solar zenith angle of 0° and 72°, respectively.

Element Transmission Sensitivity Analysis

Figures 5 and 6 show the simulated proportion of absorbed spectral solar irradiance for a wavelength of high canopy reflectance (ρ = .50 for all canopy elements) as a function of canopy element transmission coefficient for a solar zenith angle of 0° and 72°, respectively.

Vertical Reflection Validation

The measured versus simulated vertical spectral canopy reflectance of the modeling trees for three time periods are presented in Figures 7, 8, and 9.

SRVC Simulated Absorption Coefficients

The Simulated $\alpha_{\lambda,i,z}$ absorption coefficients for various mean canopy element reflectances and for a solar angle of 47° are shown in Figure 10.

Program ABSORPT

The Fortran program ABSORPT calculates the spectral and total absorption within the canopy system using the interpolation and integration techniques described in Chapter III.

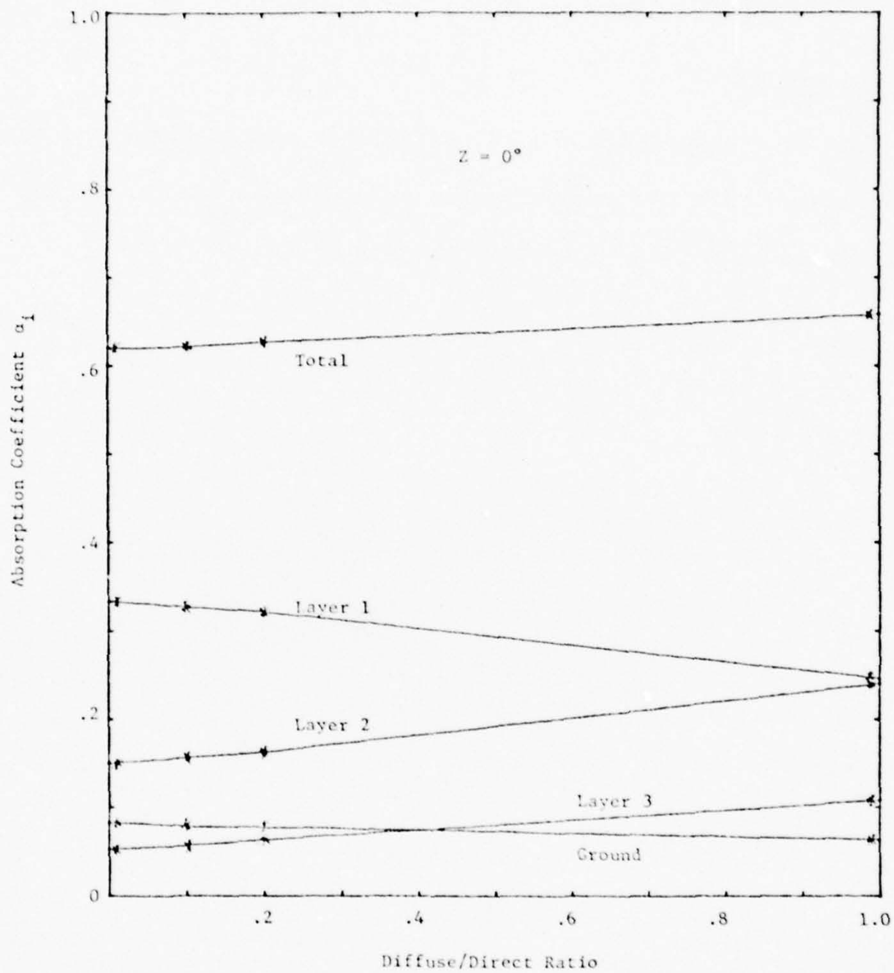

Figure 1. The simulated proportion of absorbed spectral solar irradiance for a wavelength of high canopy reflectance (ρ = .50, τ = .05 for all canopy elements) with a solar zenith angle (Z) of 0°. The proportion absorbed (α_i) by each canopy layer is shown as well as the total canopy absorption.

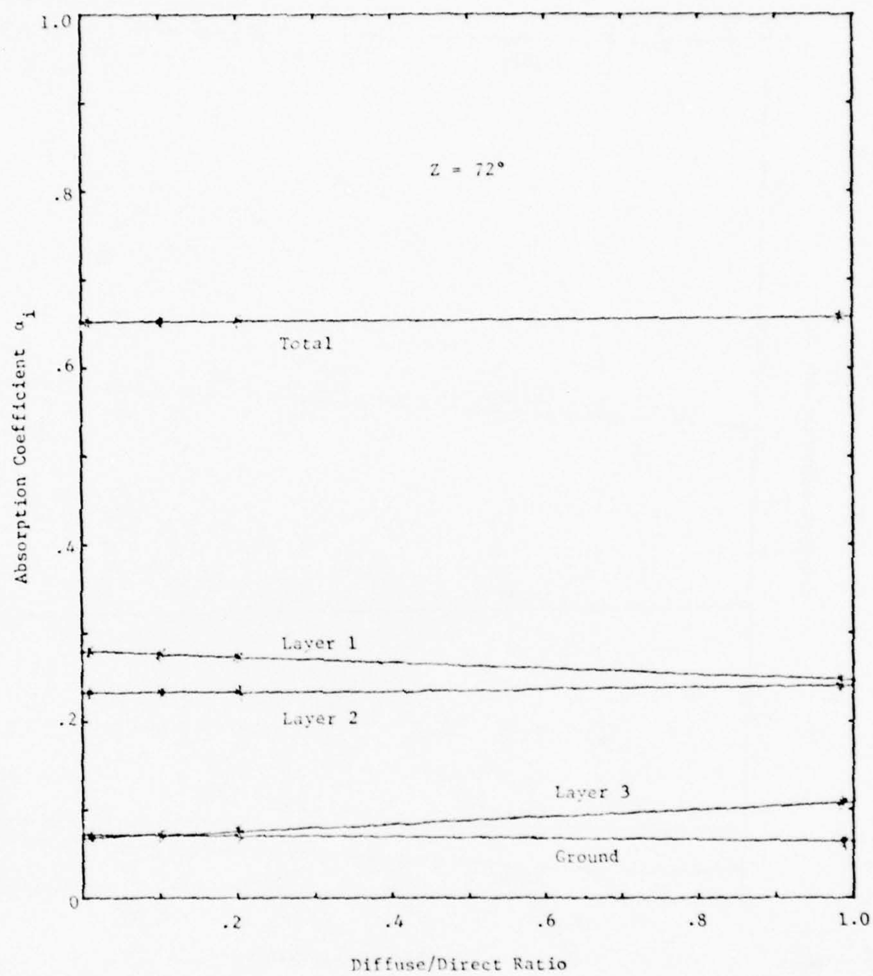

Figure 2. The simulated proportions of absorbed solar irradiance for a wavelength of high canopy reflectance (ρ = .50, τ = .05 for all canopy elements) with a solar *zenith angle* (Z) of 72°. The proportion absorbed (α_i) by each canopy layer is shown as well as the total canopy absorption.

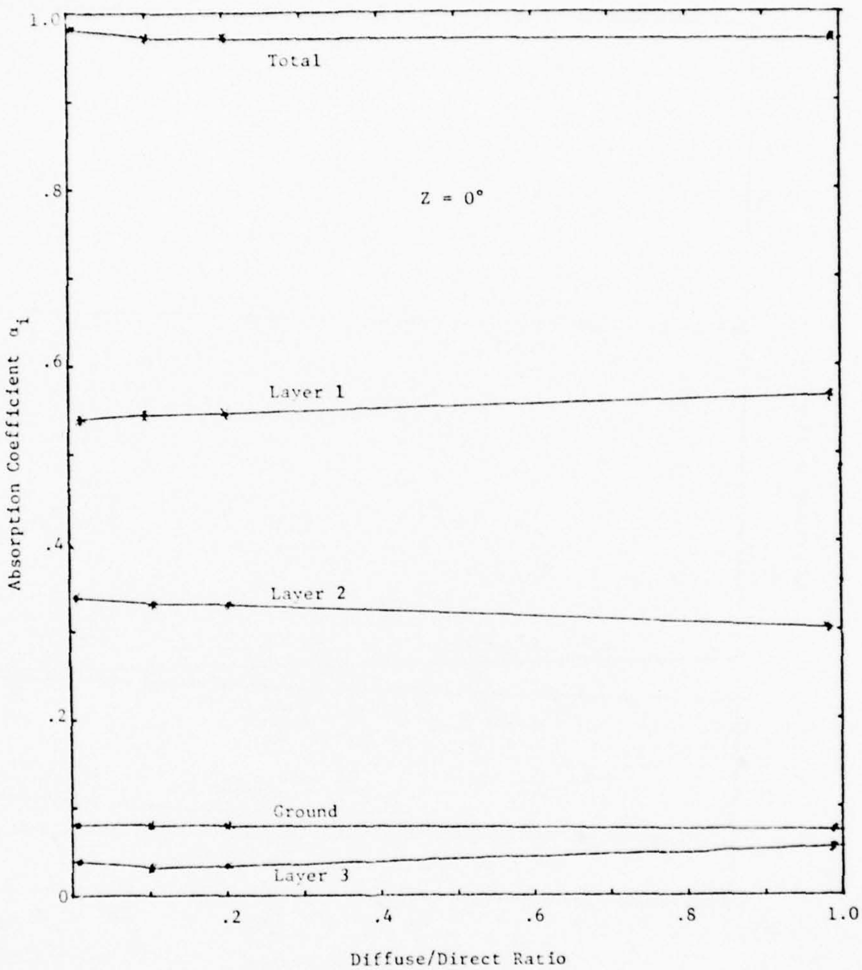

Figure 3. The simulated proportion of absorbed spectral solar irradiance for a wavelength of low canopy reflectance (ρ = .05, τ = .001 for all canopy elements) with a solar zenith angle of 0°. The proportion absorbed (α_i) by each canopy layer is shown as well as the total canopy absorption.

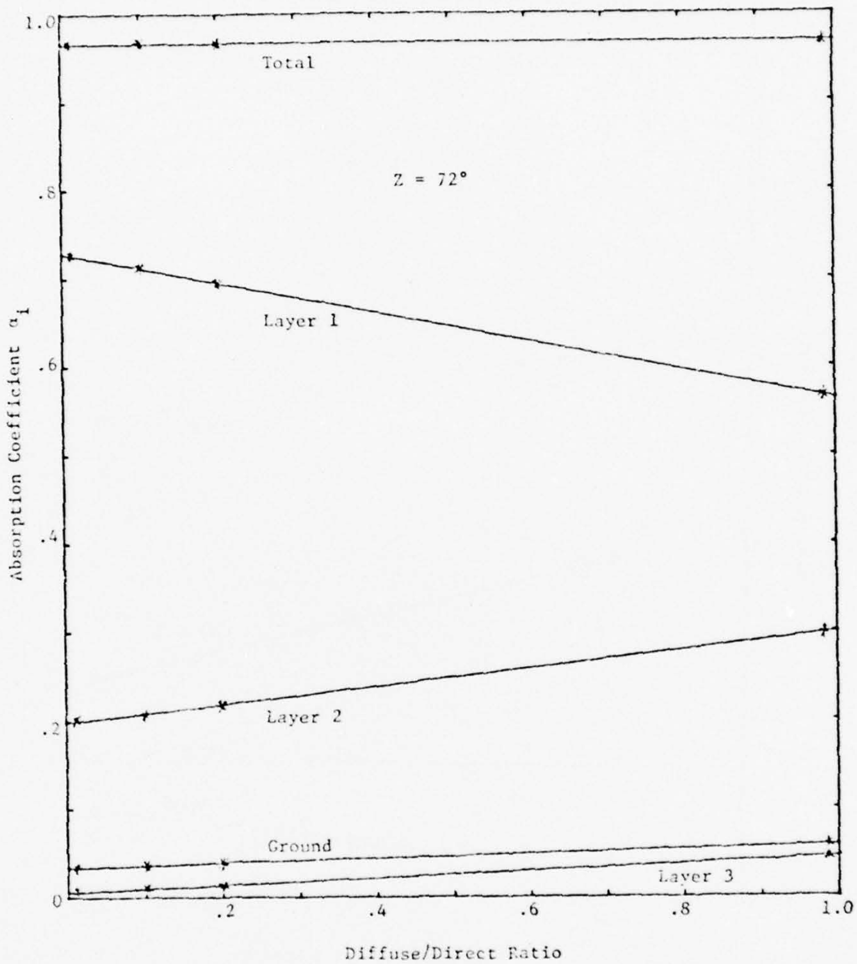

Figure 4. The simulated proportion of absorbed spectral solar irradiance for a wavelength of low canopy reflectance (ρ = .05, τ = .001 for all canopy elements) with a solar zenith angle of 72°. The proportion absorbed (α_i) by each canopy layer is shown as well as the total canopy absorption.

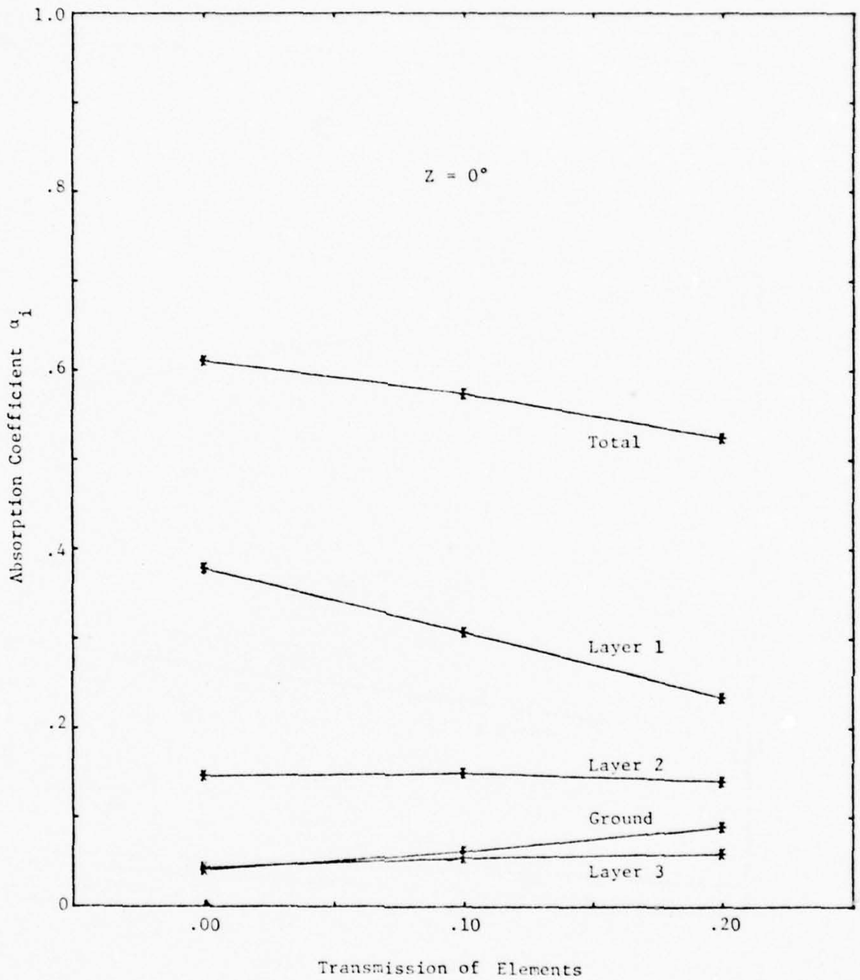

Figure 5. The simulated proportion of absorbed spectral solar irradiance for a wavelength of high canopy reflectance (ρ = .50 for all canopy elements) for four canopy element transmission coefficients and for a solar zenith angle of 0°. The proportion absorbed (α_i) for each canopy layer is shown as well as the total canopy absorption.

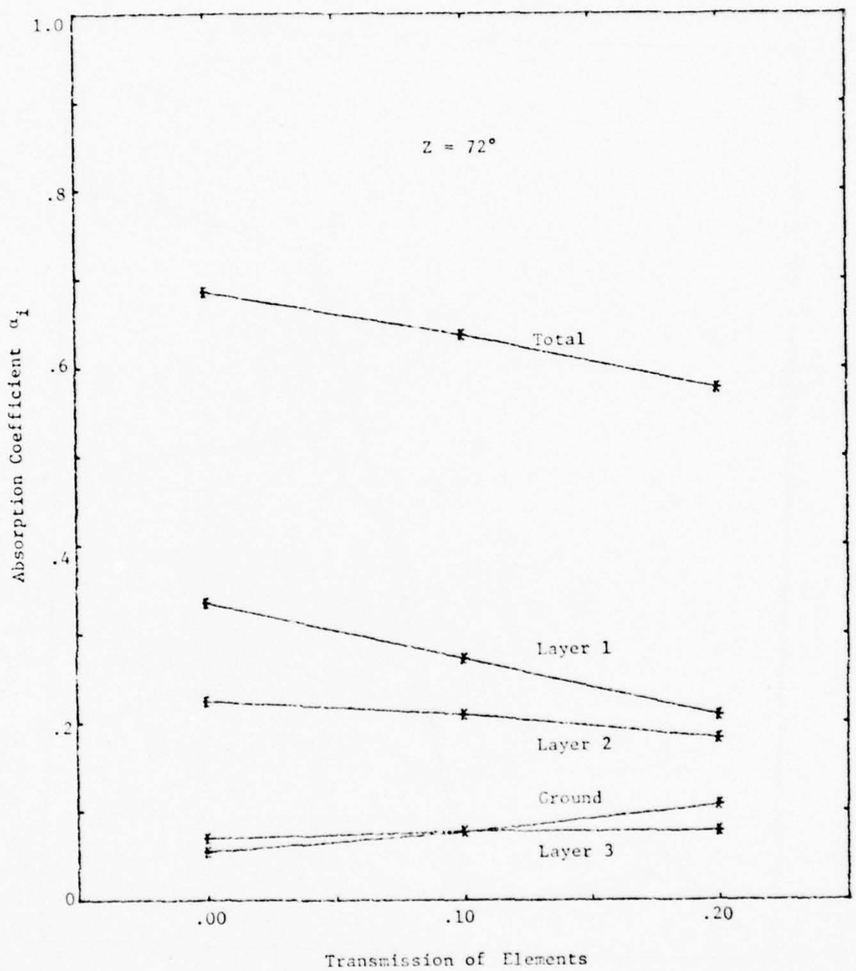

Figure 6. The simulated proportion of absorbed spectral solar irradiance for a wavelength of high canopy reflectance (ρ = .50 for all canopy elements) for four canopy element transmission coefficients and for a solar zenith angle of 72°. The proportion absorbed (α_i) for each canopy layer is shown as well as the total canopy absorption.

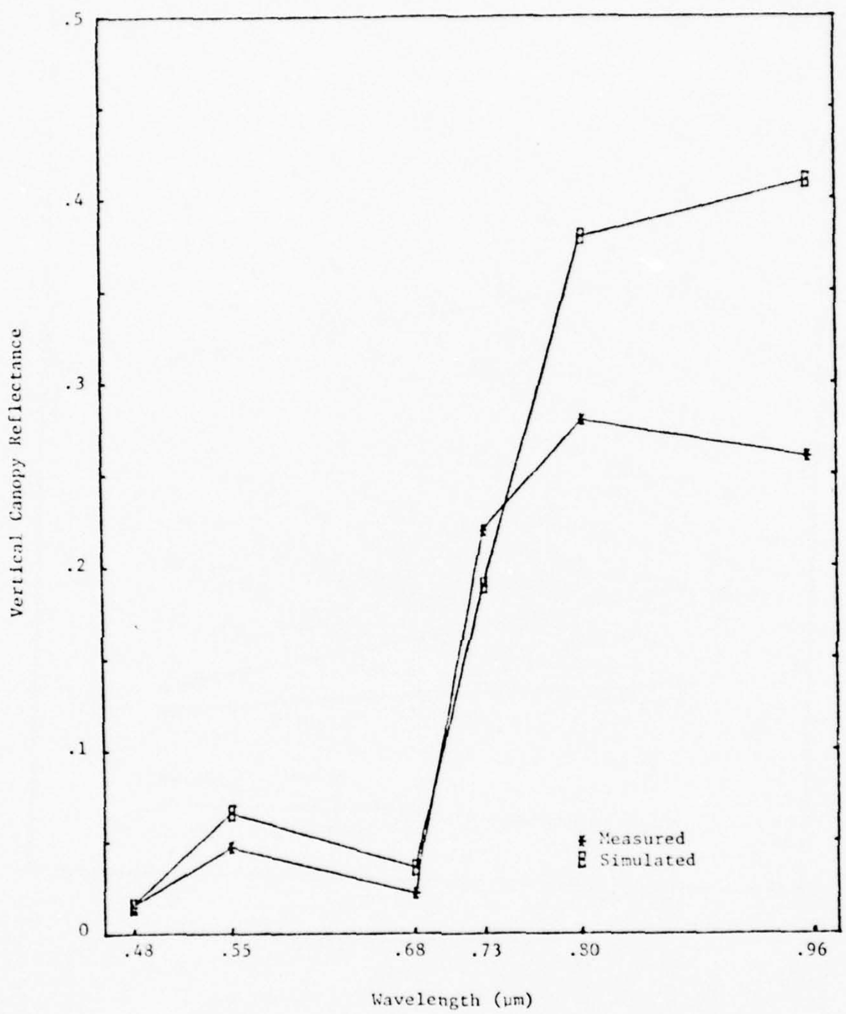

Figure 7. Measured versus simulated vertical spectral canopy reflectance for May 24, 1978, 0800 Standard Time.

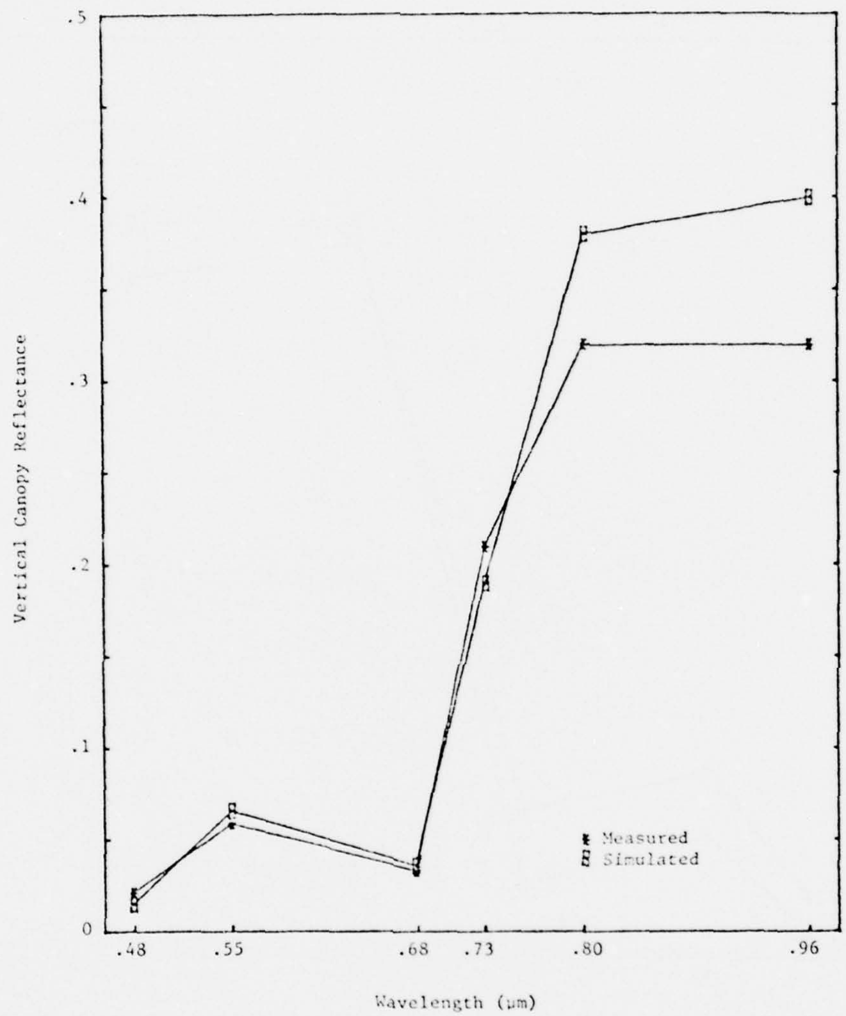

Figure 8. Measured versus simulated vertical spectral canopy reflectance for July 1, 1977, 1000 Standard Time.

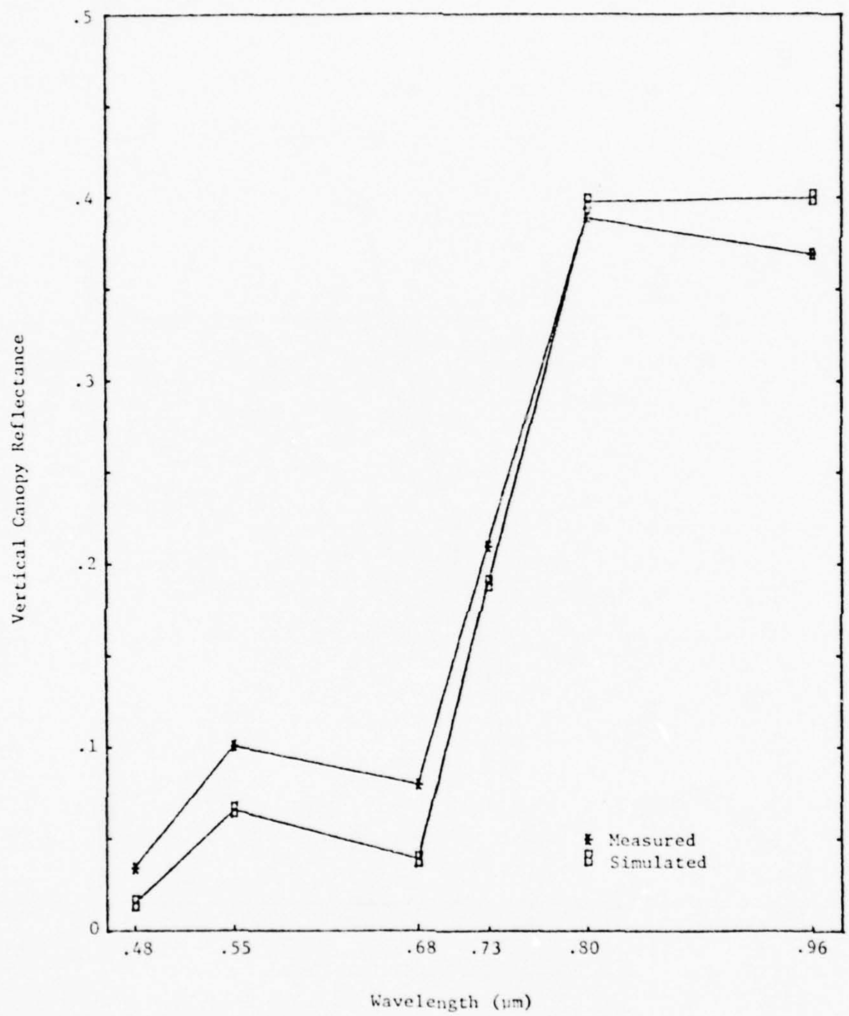

Figure 9. Measured versus simulated vertical spectral canopy reflectance for October 14, 1977, 1200 Standard Time.

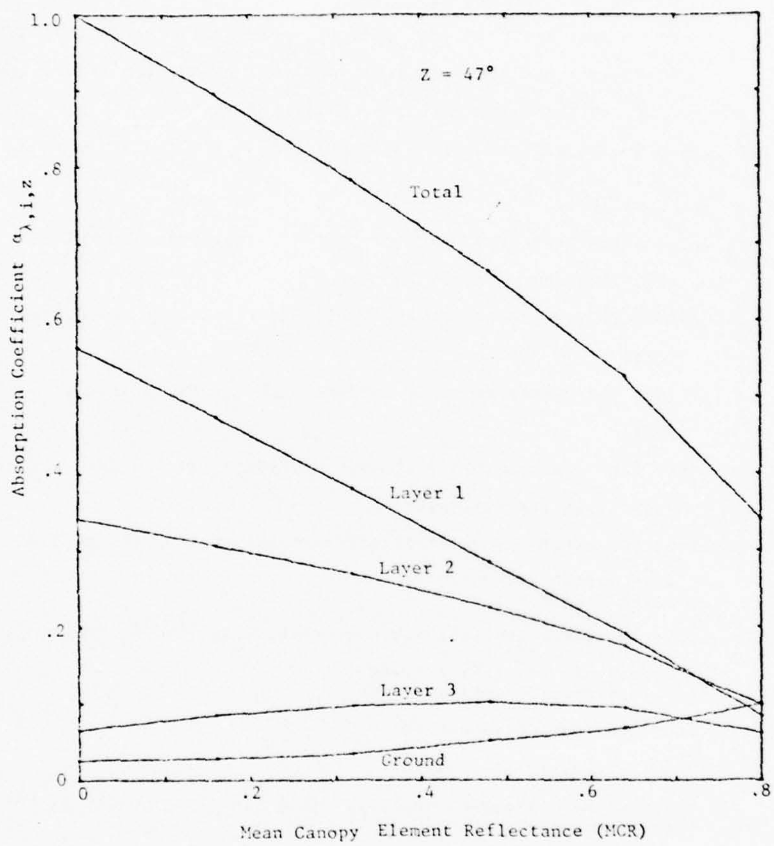

Figure 10. SRVC simulated $\alpha_{\lambda,i,z}$ absorption coefficients for various mean canopy element reflectances and for a solar zenith angle of 47°. The $\alpha_{\lambda,i,z}$ for each canopy layer is presented as well as the total proportion of the spectral irradiance absorbed.

```
      PROGRAM ABSORPT (INPUT,OUTPUT,TAPE5=INPUT,TAPE6=OUTPUT)
C
C...PROGRAM ABSORP CALCULATES THE TOTAL ABSORBED SOLAR RADIATION (W/M**2) IN
C    LAYER I (I=1,2,3) GIVEN NN NORMALIZED SPECTRAL IRRADIANCE CURVES, THE TOTAL
C    IRRADIANCE (W/M**2), AND THE SRVC INTERPOLATION FUNCTIONS. COLORADO STATE
C    UNIVERSITY , D.S. KIMES , AUGUST/78.
C
      COMMON/A1/ LAT,PL,LONG,     LAI(4), DEC, E, TIME(100), IRRAD(100),
     +   X(100), ZNN(20),  SCURV(20,100),  UVIR(20,100),  Z,
     +  CURVE2(100),  ABSORB(20,100),  F(20,100),  SUM1(4),  SUM2(4),
     +  TOTAL(4),  INT(100),  TNN(100),  SURV(20,100)
      COMMON /A2/ ZUVIR(100)
      COMMON/A3/ SUM
      COMMON/A4/ R(100),T(100),AB(100),ABE(100),R2(20),T2(20),AB2(20),
     + ABE2(20)
      COMMON/ALPHA1/ ALPHAI(4,5,6),ZALPH(4), XALPH(6),  ZTEMP(4,6)
     + ,TTEMP(6), ABSORB1(5,50), ABSORB2(5,50)
      REAL LAT,IRRAD(100),PL,LONG,LAI(4),INT(100)
C
C...READ THE NUMBER OF DESIRED SIMULATIONS
C
      READ(5,10)NS
   10 FORMAT(I10)
C
C...READ THE NUMBER OF NORMALIZED SPECTRAL IRRADIANCE CURVES
C
      READ(5,10) NN
C
C...ASSIGN THE NUMBER OF POINTS TO USE THE TRAPAZOIDAL RULE ON.
C
      I1=31
C
C...ASSIGN THE NUMBER OF EXTRA INTERVALS IN THE UV,IR RANGES
C
      I2=3
C
C...READ THE TOTAL (2SIDED + ROUNDED SURFACES) LAI FOR THE 4 LAYERS
C
      READ(5,20) (LAI(I),I=1,4)
C
C...READ THE LATITUDE,LONGITUDE,DECLINATION,AND EQUATION OF TIME
C
      READ(5,20) LAT,LONG,DEC,E
   20 FORMAT (8F10.5)
C
C...READ THE TIME, AND IRRADIANCE VECTORS, NOTE TIME IS IN STANDARD TIME..
C
      READ(5,20) (TIME(I),I=1,NS)
      READ(5,20) (IRRAD(I),I=1,NS)
C
C...READ THE WAVELENGTH VALUES
C
      READ(5,20) (X(I),I=1,I1)
C
C...READ THE NN NORMALIZED SPECTRAL SOLAR CURVES OF THE I1 POINTS AND THE
C    CORRESPONDING ZENITH ANGLES.
C
      DO 30 J=1,NN
      READ (5,20) ZNN(J)
      READ(5,20) (SCURV(J,I),I=1,I1)
      READ(5,20) (UVIR(J,I),I=1,I2)
```

```
   30 CONTINUE
C
C...READ THE REFLECTION AND TRANSMISSION COEFFICIENTS OF THE AVERAGE COMPONENT
C    FOR THE CURVE OF I1 AND I2 POINTS
C
      READ (5,20) (R(I),I=1,I1)
      READ(5,20) (R2(I),I=1,I2)
      READ(5,20) (T(I),I=1,I1)
      READ(5,20) (T2(I),I=1,I2)
C
C...READ THE SRVC ABSORPTION INTERPOLATION COEFFICIENTS.
C
C
C.......READ THE NUMBER OF ALPHAI CURVES.
C
      READ(5,10) NALPH
C
C.......READ THE SIMULATED WAVELENGTHS (MEAN CANOPY COMPONENT REFLECTANCE
C          OF THE ALPHAI CURVES)
C
      READ(5,20) (YALPH(I),I=1,6)
C
C.......READ THE ZENITH ANGLE AND THE CURVES OF THE 4 LAYERS
C         AND THE TOTAL CURVE FOR EACH NALPH.
C
      DO 501 I=1,NALPH
      READ(5,20) ZALPH(I)
      DO 502 M=1,5
      READ(5,20) (ALPHAI(I,M,J),J=1,6)
  602 CONTINUE
  501 CONTINUE
      CALL XMAIN (NS,NN,I1,I2,NALPH)
      STOP
      END
```

```
      SUBROUTINE XMAIN(NS,NN,I1,I2,NALPH)
C
C...PROGRAM XMAIN PREFORMS ALL THE MAJOR CALCULATIONS.
C
      COMMON/A1/ LAT,PL,LONG,    LAI(4), DEC, E, TIME(100), IRRAD(100),
     +  X(100), ZNN(20),  SCURV(20,100),  UVIR(20,100),  Z,
     +  CURVE2(100),  ABSORB(20,100),  F(20,100),  SUM1(4),  SUM2(4),
     +  TOTAL(4),  INT(100),  TNN(100),  SURV(20,100)
      COMMON /A2/ ZUVIR(100)
      COMMON/A3/ SUM
      COMMON/A4/ R(100),T(100),AB(100),ABE(100),R2(20),T2(20),AB2(20),
     + ABE2(20)
      COMMON/ALPHA1/ ALPHA1(4,5,6),ZALPH(4), XALPH(6),  ZTEMP(4,6)
     + ,TTEMP(6), ABSORB1(5,50), ABSORB2(5,50)
      REAL LAT,IRRAD(100),PL,LONG,LAI(4),INT(100)
      REAL  TTOTAL(5)
      WRITE(6,199)
  199 FORMAT(/////,' THE CONSTANT PARAMETERS FOR THIS RUN ARE AS FOLLOWS
     +',///)
      WRITE (6,200) LAT,LONG,DEC,E,(LAI(I),I=1,4)
  200 FORMAT (1X,'LATITUDE=',F8.3,3X,'LONGITUDE=',F8.3,3X,'DECLINATION='
     +,F8.3,3X,'TIME EQN',F8.3,3X,'TOTAL LAI(1-4)=',4F8.3)
C
C...THE MAIN LOOP PREFORMES  ALL THE MAJOR CLCULATIONS FOR EACH SIMULATION
C
      WRITE (6,201)
  201 FORMAT (1X,' THE SIMULATIONS WERE AS FOLLOWS',///)
      DO 155 K=1,NS
C
C...CALCULATE THE CORRECT ZENITH ANGLE AND PATH LENGTH FOR THE PRESENT
C   SIMULATION TIME.
C     TIME
C
      INDEX=K
      CALL ZENITH (NS,NN,I1,I2,INDEX)
C
C...RATHER THAN EXTRAPOLATING BEYOND 85 DEGREES SET X .GT. 85 TO 85.
C
      IF(Z.GE.85.) Z=84.9
C
C...USING LINEAR INTERPOLATION CALCULATE THE NORMALIZED SPECTRAL SOLAR CURVE AND
C   UVIR PROPORTIONS FOR THE PRESENT ZENITH ANGLE
C
      CALL INTERP (NS,NN,I1,I2)
C
C
C...CALCULATE THE TOTAL ABSORPTION COEFFICIENTS FOR THE AVERAGE COMPONENT.
C
      DO 73 I=1,I1
      AB(I)=1.-(R(I)+T(I))
   73 CONTINUE
      DO 74 I=1,I2
      AB2(I)=1.-(R2(I)+T2(I))
   74 CONTINUE
      DO 76 I=1,I1
      ABE(I)=AB(I)*CURVE2(I)
   76 CONTINUE
      DO 77 I=1,I2
      ABE2(I)=AB2(I)*ZUVIR(I)
   77 CONTINUE
      ADD=0.0
```

```
      MM=I1-1
      DO 78 I=1,MM
      ADD=((ABE(I)+ABE(I+1))/2.)*(X(I+1)-X(I))+ADD
   78 CONTINUE
      ADD2=0.0
      DO 79 I=1,I2
      ADD2= ABE2(I)+ADD2
   79 CONTINUE
      ADD=ADD+ADD2
C...USING INTERPOLATION TECHNIQUES CALCULATE THE SOLAR ABSORPTION COEFFICIENTS
C   FOR THE I1 POINTS AND THE I2 POINTS.
C
      CALL ALPHA (NS,NN,I1,I2,NALPH)
C
C...CALCUALTE THE TOTAL ABSORBED SOLAR RADIATION (W/M**2) IN LAYER I.
C
C
C.................MULTIPLY THE VARIABLES.
C
      DO 110 I=1,I1
      DO 110 M=1,4
      F(M,I)= CURVE2(I)*IRRAD(K)*ABSORB1(M,I)
  110 CONTINUE
C
C...INTEGRATE THE ABOVE CURVE
C
      DO 991 I=1,4
      SUM1(I)=0.0
  991 CONTINUE
      MM=I1-1
      DO 25 I=1,MM
      DO 25 M=1,4
      SUM1(M)=((F(M,I )+F(M,I+1))/2.)*(X(I+1)-X(I)) + SUM1(M)
   25 CONTINUE
C
C...CALCULATE THE ABSORBED SOLAR IRRADIANCE FOR LAYER J IN THE UV AND IR BANDS.
C
      DO 992 I=1,4
      SUM2(I)=0.0
  992 CONTINUE
      DO 120 J=1,4
      DO 120 I=1,I2
      SUM2(J)=ZUVIR(I)*IRRAD(K)*ABSORB2(J,I) + SUM2(J)
  120 CONTINUE
C
C....SUM THE 2 COMPONENTS OF ABSORBED SOLAR IRRADIANCE FOR EACH LAYER,
C
      DO 130 I=1,4
      TOTAL(I)= SUM1(I)+SUM2(I)
  130 CONTINUE
C
C...DIVIDE BY THE LAI OF EACH LAYER TO ESTIMATE THE ABSORBED W/M**2 OF CANOPY
C   COMPONENT AREA.
C
      DO 131 I=1,4
      TTOTAL(I)= TOTAL(I)/LAI(I)
  131 CONTINUE
      WRITE(6,202)
  202 FORMAT(//,'.........................................................
     *...................',//)
      WRITE (6,203) TIME(K),IRRAD(K),Z,PL
```

```
  203 FORMAT (1X,*TIME=*,F8.3,3X,*IRRADIANCE=*,F8.3,3X,*ZENITH ANGLE*,F8
     *.3,*AND PATH LENGTH=*,F8.3)
      WRITE(6,204)
  204 FORMAT (1X,* THE INTERPOLATED NORMALIZED SOLAR IRRADIANCE CURVE IS
     * (X AND F(X))*)
      DO 394 I=1,I1
      WRITE(6,205) X(I),CURVE2(I)
  205 FORMAT(1X,F10.5,3X,F10.5)
  394 CONTINUE
      WRITE(6,209)
  209 FORMAT(//,* THE INTERPOLATED NORMALIZED PROPORTIONS FOR THE UV AND
     * IR BANDS ARE*)
      WRITE(6,206) (ZUVIR(I),I=1,I2)
  206 FORMAT (1X,3F10.5)
      WRITE (6,701) SUM
  701 FORMAT (1X,//,* THE INTEGRAL OF THE SPECTRAL CURVE IS *,F10.5)
      WRITE(6,351) AOD
  351 FORMAT (1X,//,* THE TOTAL ABSORPTION OF THE MEAN CONPONENT IS *,
     * F10.5)
C
C....WRITE THE SOLAR  ABSORPTION  COEFFICIENTS FOR THIS  PARTICULAR ZENITH
C    ANGLE , 4 LAYERS, AND  FOR  WAVELENGTH OCCURING IN THE X VECTOR.
C
C
      WRITE(6,500)
  500 FORMAT(1X,////,* THE ABSORPTION COEFFICIENTS FOR THE 6 MEAN COMPON
     *ENT REFLECTANCES ARE (REFL., LAYER 1,2,3,4)*,/)
      DO 501 I=1,6
      WRITE(6,502) XALPH(I),(ZTEMP(L,I),L=1,4)
  502 FORMAT(1X,F10.3,4(3X,F10.3))
  501 CONTINUE
      WRITE(6,503)
  503 FORMAT(1X,//,* THE TOTAL PROPORTIONS ABSORBED FOR EACH OF THE 6 ME
     *AN COMPONENT REFLECTANCES ARE (REF,TOTAL)*,/)
      DO 504 I=1,6
      WRITE(6,505) XALPH(I),TTEMP(I)
  505 FORMAT(1X,2(3X,F10.3))
  504 CONTINUE
      WRITE(6,973) (TOTAL(I),I=1,4)
  973 FORMAT (1X,* THE TOTAL SOLAR ENERGY ABSORBED FOR LAYER1-4 *,4F8.3)
      SYSTOT=0.0
      DO 770 I=1,4
      SYSTOT= SYSTOT + TOTAL(I)
  770 CONTINUE
      WRITE(6,771) SYSTOT
  771 FORMAT(1X,//,* THE TOTAL ENERGY ABSORBED BY THE CANOPY SYSTEM IS *
     *,F10.5)
      AASORB= SYSTOT/IRRAD(K)
      WRITE(6,772) AASORB
  772 FORMAT (1X,//,* THE TOTAL PROPORTION OF SOLAR IRRADIANCE ABSORBED
     *BY THE CANOPY IS *,F10.5)
      AASORB= 1.-AASORB
      WRITE(6,773) AASORB
  773 FORMAT(1X,//,* THE TOTAL PROPORTION OF SOLAR IRRADIANCE REFLECTED
     *BY THE CANOPY IS *,F10.5)
C
      DO 208 I=1,4
      II=I
      WRITE(6,207)II,TTOTAL(I)
  207 FORMAT (//,* THE WATS PER METER SQUARE SURFACE AREA OF CANOPY
     * COMPONENT IN LAYER *,I1,* IS *,F10.5)
  208 CONTINUE
  155 CONTINUE
      RETURN
      END
```

```
      SUBROUTINE ZENITH (NS,NN,I1,I2,INDEX)
C
C...SUBROUTINE ZENITH CALCULATES THE ZENITH ANGLE AND PATH LENGTH GIVEN THE
C   LATITUDE, LONGITUDE, DECLINATION, TIME, AND EQUATION OF TIME.
C
      COMMON/A1/ LAT,PL,LONG,    LAT(4), DEC, E, TIME(100), IRRAD(100),
     *   R(100), ZNN(20), SCURV(20,100), DVIP(20,100), Z,
     *  CURVE2(100), ABSORB(20,100), F(20,100), SUM1(4), SUM2(4),
     *  TOTAL(4), IST(100), TNN(100), SUMV(20,100)
      COMMON /A2/ TWVIP(100)
      COMMON/A3/ SUM
      REAL LAT,IRRAD(100),PL,LONG,LAT(4),IST(100)
C
C...GEOMETRIC FORMULA FOR CALCULATING SOLAR ZENITH ANGLE AND PATH LENGTH.
C   EQUATION OF TIME USES STANDARD TIME..
C
      TIMESN=12.+E+((LONG-105.)/15.)
      HOUR= ABS((TIMESN-TIME(INDEX))*15.0*3.1416/180.
       IF(INDEX.GT.1) GO TO 50
      LAT=LAT*3.1416/180.
      DEC=DEC*3.1416/180.
   50 CONTINUE
      COSZ=SIN(LAT)*SIN(DEC)+COS(LAT)*COS(DEC)*COS(HOUR)
      Z= ACOS(COSZ)*180./3.1416
      PL=1./COS(Z*3.1416/180.)
      RETURN
      END
```

```
      SUBROUTINE INTERP (NS,NN,I1,I2)
C
C...SUBROUTINE INTERP LINEAR INTERPOLATES THE NORMALIZED SPECTRAL SOLAR CURVES
C    FOR  THE PRESENT ZENITH ANGLE.
C
      COMMON/A1/ LAT,PL,LONG,     LAT(4), DEC, F, TIME(100), IRRAD(100),
     +   X(100), ZNN(20),  SCURV(20,100),  UVIR(20,100),  Z,
     +  CURVE2(100),  ABSORB(20,100),  F(20,100),  SUM1(4),  SUM2(4),
     +  TOTAL(4),  INT(100),  TNN(100),  SURV(20,100)
      COMMON /A2/ ZUVIR(100)
      COMMON/A3/ SUM
      COMMON/A4/ R(100),T(100),AB(100),ABE(100),R2(20),T2(20),AB2(20),
     + ABE2(20)
      COMMON/ALPHA1/ ALPHA1(4,5,6),ZALPH(4), YALPH(6),  ZTEMP(4,6)
     + ,TTEMP(6), ABSOR1(5,50), ABSORB2(5,50)
      REAL LAT,IRRAD(100),PL,LONG,LAT(4),INT(100),ZUVIR(100)
C
C...THE ZENITH ANGLES ARE USED TO INTERPOLATE ON.
C
C
C...CALCUALTE THE ZENITH INTERVAL OF THE NORMALIZED CURVES THAT THE PRESENT
C    Z FALLS INTO.
      NNM1=NN-1
      DO 10 I=1,NNM1
      IP1=I+1
      IF(ZNN(I).LE.Z.AND.Z.LT.ZNN(IP1)) GO TO 20
      GO TO 10
   20 ZPROP=(ZNN(I)-Z)/(ZNN(I)-ZNN(I+1))
      ZPROP=ABS(ZPROP)
      ID=I
      GO TO 30
   10 CONTINUE
   30 CONTINUE
C
C...CALCULATE PRESENT NORMALIZED CURVE
C
      DO 40 M=1,I1
      J=ID
      JJ=ID+1
       CURVE2(M)=(SCURV(JJ,M)-SCURV(J,M))*ZPROP + SCURV(J,M)
   40 CONTINUE
C
C...CALCULATE THE PRESENT PROPORTIONS OF THE UV AND IR BANDS
C
      DO 50 M=1,I2
      JJ=J+1
      ZUVIR(M)=(UVIR(JJ,M)-UVIR(J,M))*ZPROP + UVIR(J,M)
   50 CONTINUE
C
C...CHECH TO SEE IF THE CURVES ARE STILL RELATIVELY NORMALIZED.
C..........INTEGRATE
C
      SUM3=0.0
      DO 60 I=1,I2
      SUM3=ZUVIR(I)+SUM3
   60 CONTINUE
      SUM=0.0
      MM=I1-1
      DO 61 I=1,MM
      SUM=((CURVE2(I)+CURVE2(I+1))/2.)*(X(I+1)-X(I))+SUM
   61 CONTINUF
      SUM=SUM+SUM3
      RETURN
      END
```

```
      SUBROUTINE ALPHA(NS,NN,I1,I2,NALPH)
C
C...SUBROUTINE ALPHA CALCULATES THE PROPORTION OF INCOMENG SOLAR SPECTRAL
C   IRRADIANCE ABSORBED IN ANY GIVEN LAYER. THE INTERPOLATION PROCEDURE IS
C   BASED ON THE MEAN CANOPY COMPONENT REFLECTANCE CURVE.
C
      COMMON/A1/ LAT,PL,LONG,    LAI(4), DEC, E, TIME(100), IRRAD(100),
     +  Y(100), ZNN(20),  SCURV(20,100),  UVIR(20,100),  Z,
     +  CURVE2(100),  ABSORB(20,100),  F(20,100),  SUM1(4),  SUM2(4),
     +  TOTAL(4),  INT(100),  TNN(100),  SURV(20,100)
      COMMON /A2/ ZUVIR(100)
      COMMON/A3/ SUM
      COMMON/A4/ R(100),T(100),AB(100),ABE(100),R2(20),T2(20),AB2(20),
     + ABE2(20)
      COMMON/ALPHAI/ ALPHAI(4,5,6),ZALPH(4), YALPH(6),  ZTEMP(4,6)
     + ,TTEMP(6), ABSORB1(5,50), ABSORB2(5,50)
      REAL LAT,IRRAD(100),PL,LONG,LAI(4),INT(100)
C
C...THE ZENITH ANGLES ARE USED TO INTERPOLATE ON.
C
C...CALCULATE THE ZENITH INTERVAL OF  THE ALPHAI CURVES THAT THE  PRESENT Z
C   FALLS INTO.
C
      M=NALPH-1
      DO 10 I=1,M
      IP1=I+1
      IF(ZALPH(I).LE.Z.AND.Z.LT.ZALPH(IP1))  GO TO 20
      GO TO 10
   20 ZPROP= (ZALPH(I)-Z)/(ZALPH(I)-ZALPH(I+1))
      ZPROP=ABS(ZPROP)
      ID=I
      GO TO 30
   10 CONTINUE
   30 CONTINUE
C
C...CALCULATE THE PRESENT 6 POINT ABSORPTION CURVES FOR EACH ANOPY LAYER
C
      DO 40 M=1,6
      J=ID
      JJ=ID+1
      DO 40 K=1,4
      ZTEMP(K,M)= (ALPHAI(JJ,K,M)-ALPHAI(J,K,M))*ZPROP+ALPHAI(J,K,M)
   40 CONTINUE
C
C...NORMALIXE THE ABOVE ZTEMP ARRAY SO THAT FOR EACH OF THE 6 REFLECTANCE VALUES
C   THE SUM OF ALL 4 LAYERS IS EQUAL TO THE TOTAL.
C
C
C.......FIND THE INTERPOLATED TOTAL FOR EACH TO THE 6 WAVELENGTHS  FOR THE
C         PRESENT ZENITH,
C
      DO 50 M=1,6
      J=ID
      JJ=ID+1
      TTEMP(M)=(ALPHAI(JJ,5,M)-ALPHAI(J,5,M)) * ZPROP + ALPHAI(J,5,M)
   50 CONTINUE
C
C.......NOW NORMALIZE
C
      DO 60 M=1,6
      SSUM=0.0
```

```
      DO 51 K=1,4
      SSUM= ZTEMP(K,M) + SSUM
   51 CONTINUE
      DO 52 I=1,4
      ZTEMP(I,M)= ZTEMP(I,M)*(TTEMP(M)/SSUM)
   52 CONTINUE
   60 CONTINUE
C
C...CALCULATE THE ALPHA COEFFICIENTS FOR ALL WAVELENGHTS (I1,I2) BASED ON THE
C    MEAN CANOPY REFLECTANCE CURVE.
C
C
C.......FIND THE MEAN CANOPY COMPONENT REFLECTANCE INTERVAL THAT EACH I1 POINT
C         FALLS INTO AND CALCULATE THE APPROPRIATE ABSORPTION COEFFICIENT.
C
      DO 70 I=1,I1
      DO 80 M=1,5
      IP1=M+1
      IF(XALPH(M).LE.R(I).AND.R(I).LT.XALPH(IP1)) GO TO 90
      GO TO 80
   90 XPROP=(XALPH(M)-R(I))/(XALPH(M)-XALPH(M+1))
      XPROP=ABS(XPROP)
      ID=M
      GO TO 100
   80 CONTINUE
  100 CONTINUE
      DO 105 L=1,4
      J=ID
      JJ=ID+1
      ABSORB1(L,I)= (ZTEMP(L,JJ)-ZTEMP(L,J))*XPROP+ZTEMP(L,J)
  105 CONTINUE
   70 CONTINUE
      DO 200 I=1,I2
      DO 210 M=1,5
      IP1=M+1
      IF(XALPH(M).LE.R2(I).AND.R2(I).LT.XALPH(IP1))  GO TO 220
      GO TO 210
  220 XPROP= (XALPH(M)-R2(I)) / (XALPH(M)-XALPH(M+1))
      XPROP=ABS(XPROP)
      ID=M
      GO TO 230
  210 CONTINUE
  230 CONTINUE
      DO 235 L=1,4
      J=ID
      JJ=ID+1
      ABSORB2(L,I)= (ZTEMP(L,JJ)-ZTEMP(L,J))*XPROP+ZTEMP(L,J)
  235 CONTINUE
  200 CONTINUE
      RETURN
      END
```

APPENDIX C: Supporting Material for Thermal Exitance Vegetation Canopy Model

Data Reduction and Initial Analysis

Day and Night Input and Output

Sensitivity Analysis

Air Temperature Variations

Program Listing for TCSM

APPENDIX C

The following topics present in full detail the data, analyses and computer programs mentioned in the main text of Chapter IV.

Data Reduction and Initial Analysis

Figures 1 and 2 present the measurements of air temperature (M1 Site), the contact thermister and the Heat Spy on two branch tips for October 14-15, 1977. Figure 3 shows the simulated TCSM results for October 14-15 versus the three contact thermister measurements.

Day and Night Input and Output

The TCSM input and output for 0930 and 0330 Standard Times for July 15-16, 1977, are presented in Figures 4 and 5. The input data for the day and night environmental conditions are the fixed parameters used for the sensitivity analysis.

Sensitivity Analysis

Figures 6, 7, 8, and 9 show the emissivity and internal resistance to water vapor diffusion sensitivity results for the day and night environmental conditions.

Air Temperature Variations

Figures 10 and 11 show the air temperature measurements for M1, M2, and M3 Sites for July 14 and July 15-16, 1977. Figure 12 presents the simulated versus measured horizontal ERT's for July 15-16. The air temperature was recorded in the meadow opening (M1 Site) and is presented in Figure 13.

Program TCSM

The Fortran program TCSM is the thermal canopy signature model, as presented in Chapter IV. The required inputs are described in Subroutine Inputda. The program ZSYSTM of the International Mathematical and Statistical Library (1977) must be attached.

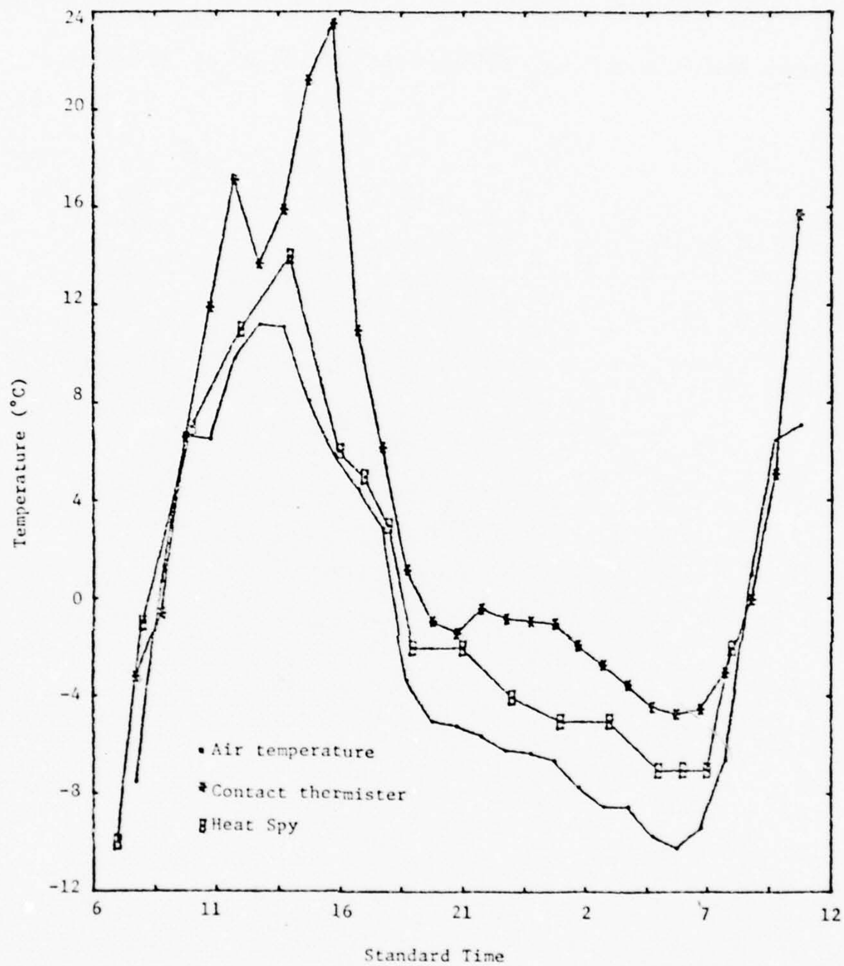

Figure 1. Measured contact thermister and Heat Spy data for a branch tip in Layer 2, and air temperature at the M1 Site for October 14-15, 1977.

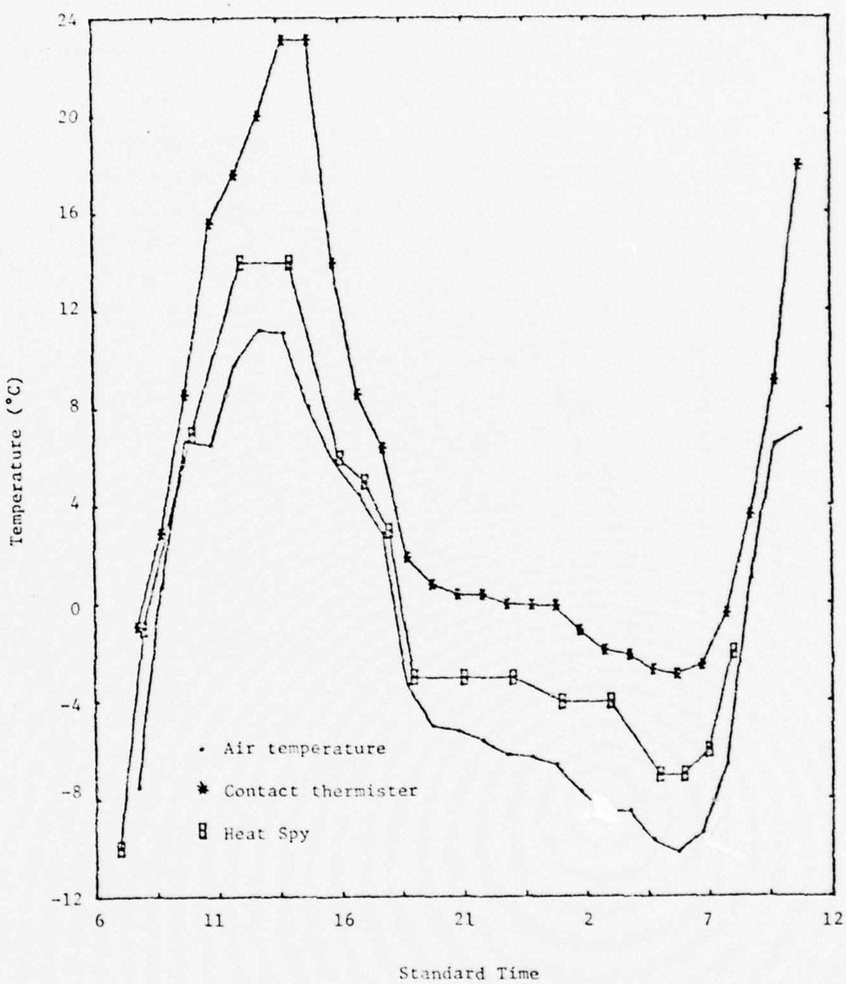

Figure 2. Measured contact thermister and Heat Spy data for a branch tip in Layer 1, and air temperature at the M1 Site for October 14-15, 1977.

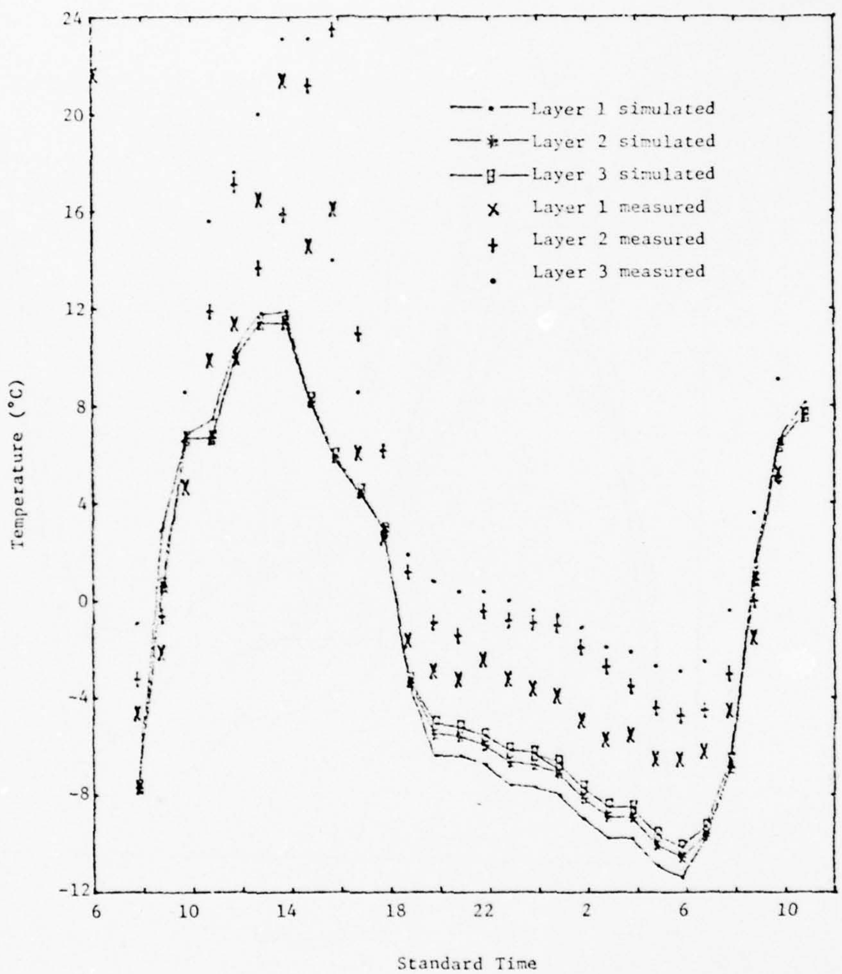

Figure 3. Simulated mean canopy layer temperature versus the data from three contact thermisters in branch tips of Layers 1, 2, and 3 for October 14-15, 1977. Air temperature was recorded at the M1 Site.

* Time = 0930

* Emissivity (Layers 1-4) = 1.0, 1.0, 1.0, 1.0

* Solar irradiance = 855 w/m^2

* Air temperature = 14.6°C

* Ground temperature = 11.7°C

* Wind velocity = 10.0 cm/s

* Relative humidity = .20

* Leaf resistance to water vapor diffusion = 0.66 min/cm

Average element temperatures (Layers 1-3) = 20.4, 16.6, 16.3°C

Ground thermal exitance = 372 w/m^2

Sky thermal exitance = 302 w/m^2

* Mean absorbed solar flux density for elements Layers 1-3 = 144, 49, 46 w/m^2

Emitted thermal flux density for the average elements (1-3) = 420, 399, 397 w/m^2

Absorbed thermal flux density for the average elements (1-3) = 375, 387, 384 w/m^2

Energy gain by convection for the average elements (1-3) = -90, -31, -26 w/m^2

Energy loss by transpiration for the average elements (1-3) = 9, 7, 7 w/m^2

The thermal exitance and ERT above the canopy for the various viewing angles are:

Inclination (degrees)	Exitance (w/m^2)	ERT (°C)
5	419	20.3
15	413	19.2
25	410	18.6
35	408	18.4
45	408	18.2
55	407	18.1
65	407	18.1
75	407	18.1
85	407	18.1

The thermal exitance and ERT for the horizontal view are:

Layer	Exitance (w/m^2)	ERT (°C)
1	420	20.4
2	399	16.6
3	397	16.3

Figure 4. Environmental and simulated conditions for 0930 (day environmental conditions) July 15, 1977. Input parameters are denoted by asterisks.

* Time = 0330

* Emissivity (Layers 1-4) - 1.0, 1.0, 1.0, 1.0

* Solar irradiance = 0.0 w/m^2

* Air temperature = 0.4°C

* Ground temperature = 5.0°C

* Wind velocity = 10 cm/s

* Relative humidity = 0.85

* Leaf resistance to water vapor diffusion = 0.66 min/cm

Average element temperatures (Layers 1-3) = -1.0, 0.0, 0.5°C

Ground thermal exitance = 399 w/m^2

Sky thermal exitance = 234 w/m^2

* Mean absorbed solar flux for Layers 1-3 = 0.0, 0.0, 0.0 w/m^2

Emitted thermal flux density for the average elements (1-3) = 310, 315, 317 w/m^2

Absorbed thermal flux density for the average elements (1-3) = 288, 309, 320 w/m^2

Energy gain by convection for the average elements (1-3) = 22, 7, -2 w/m^2

Energy loss by transpiration for the average elements (1-3) = 0.2, 0.4, 0.5 w/m^2

The thermal exitance and ERT above the canopy for the various viewing angles are:

Inclination (degrees)	Exitance (w/m^2)	ERT (°C)
5	310	-1.0
15	311	-0.6
25	313	-0.4
35	314	-0.2
45	314	-0.1
55	314	-0.1
65	315	-0.1
75	315	-0.1
85	315	-0.1

The thermal exitance and ERT for the horizontal view are:

Layer	Exitance (w/m^2)	ERT (°C)
1	310	-1.0
2	315	0.0
3	317	0.5

Figure 5. Environmental and simulated conditions for 0330 July 16, 1977. Input parameters are denoted by asterisks.

66

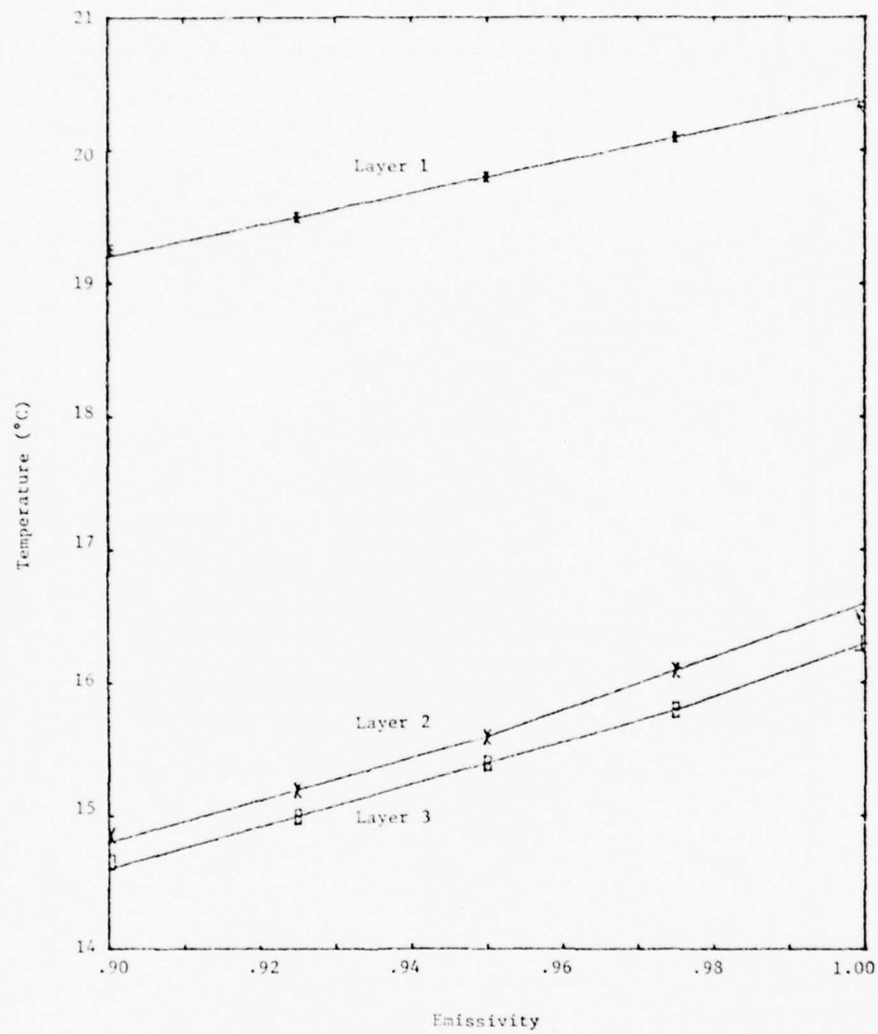

Figure 6. Sensitivity analysis of average element emissivity versus average element temperature of the three canopy layers for the day environmental conditions.

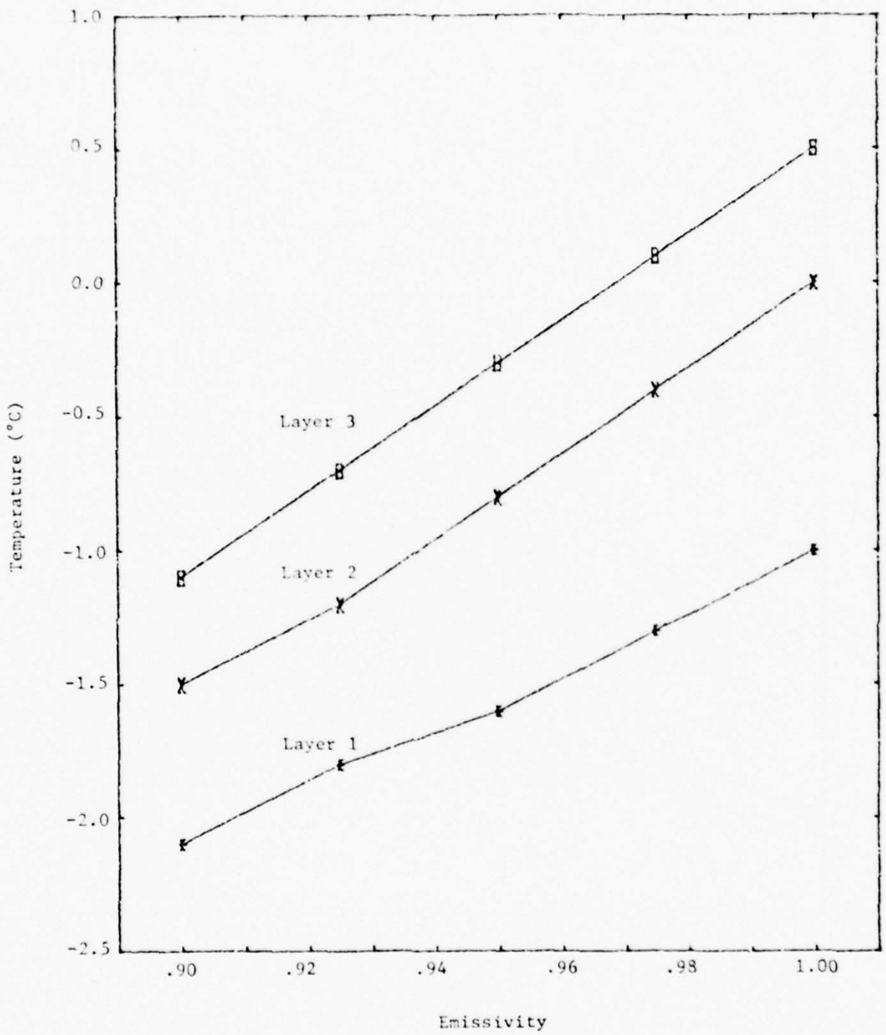

Figure 7. Sensitivity analysis of average element emissivity versus average element temperature of the three canopy layers for the night environmental conditions.

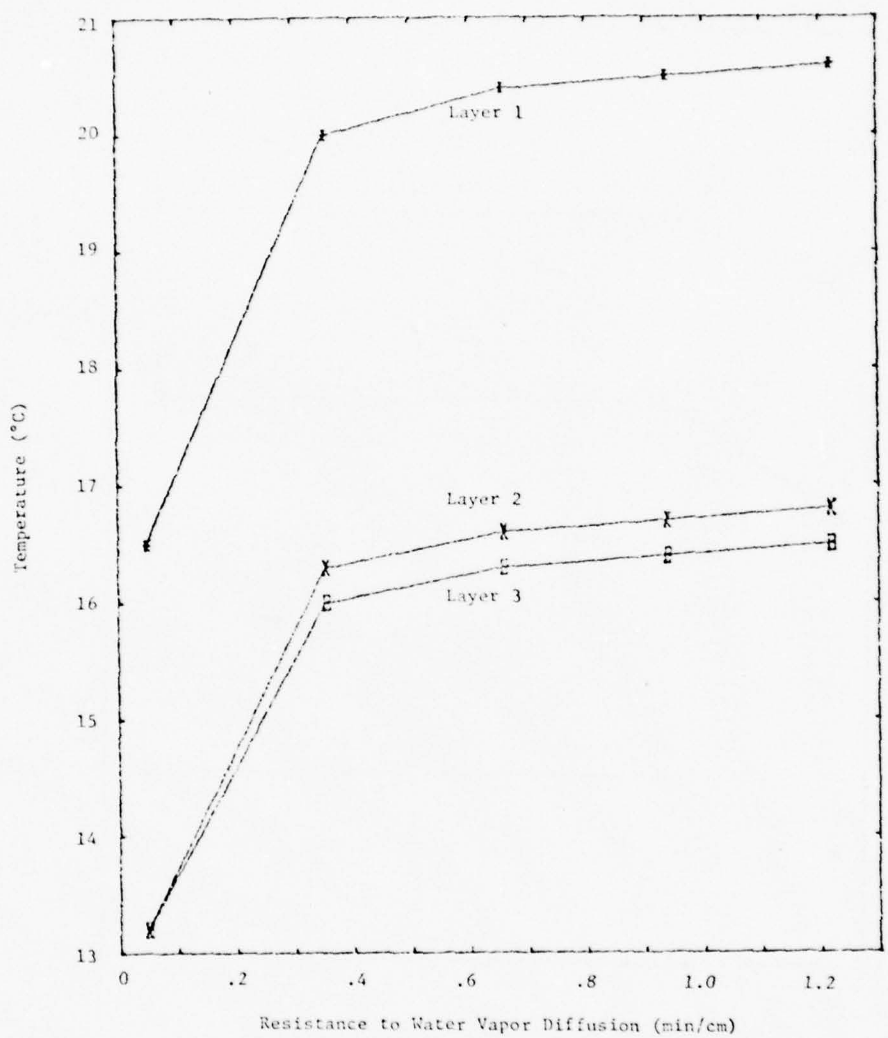

Figure 8. Sensitivity analysis of average element resistance to water vapor diffusion versus average element temperature of the three canopy layers for the day environmental conditions.

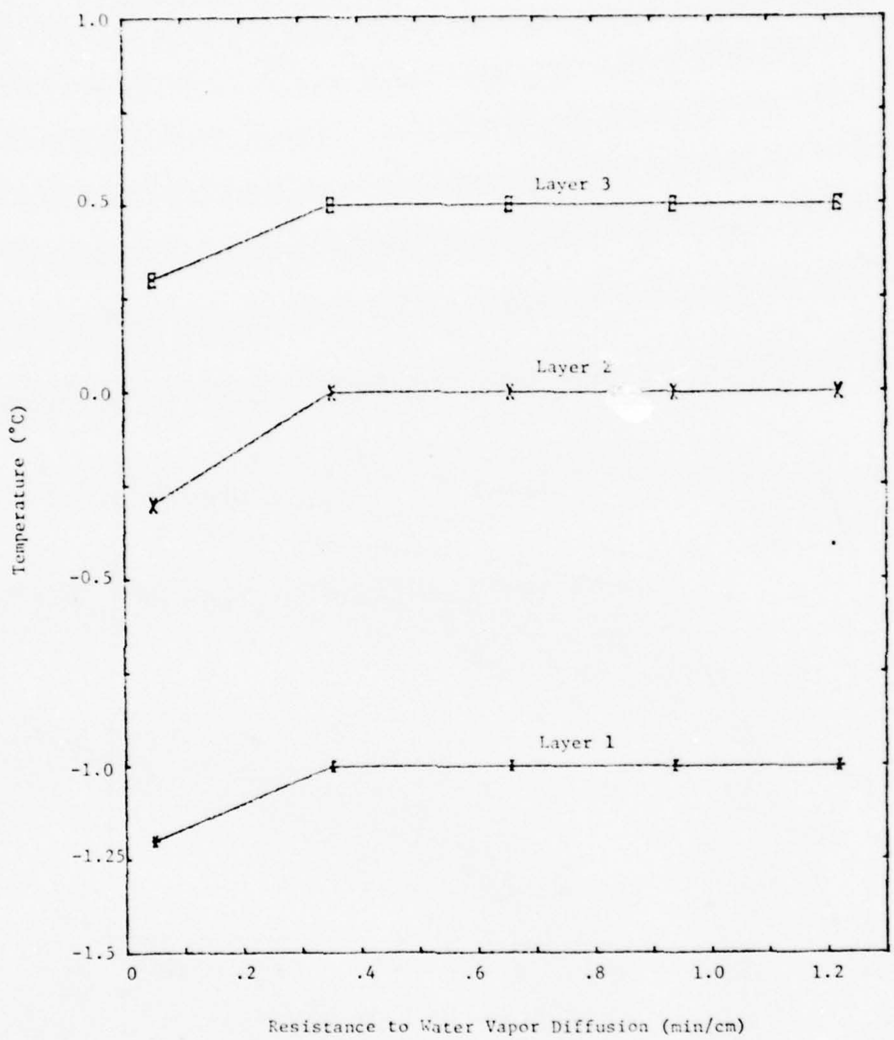

Figure 9. Sensitivity analysis of average element resistance to water vapor diffusion versus average element temperature of the three canopy layers for the night environmental conditions.

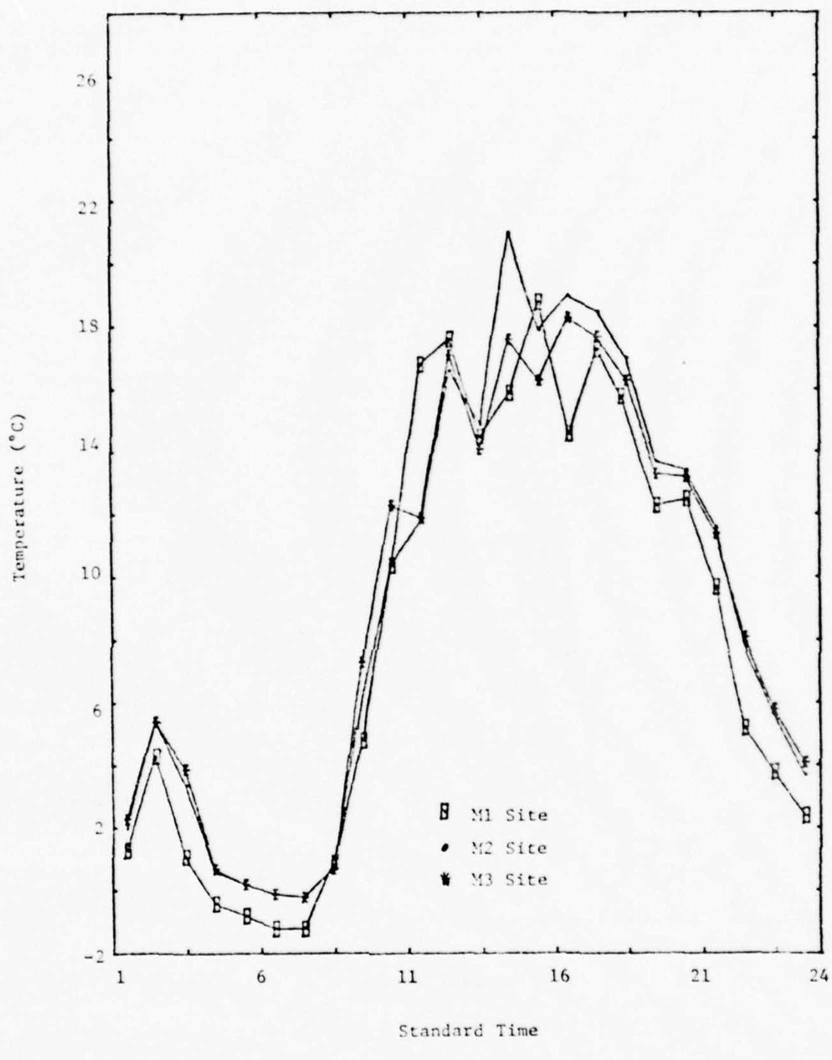

Figure 10. Air temperature measurements at the M1, M2, and M3 Sites for July 14, 1977.

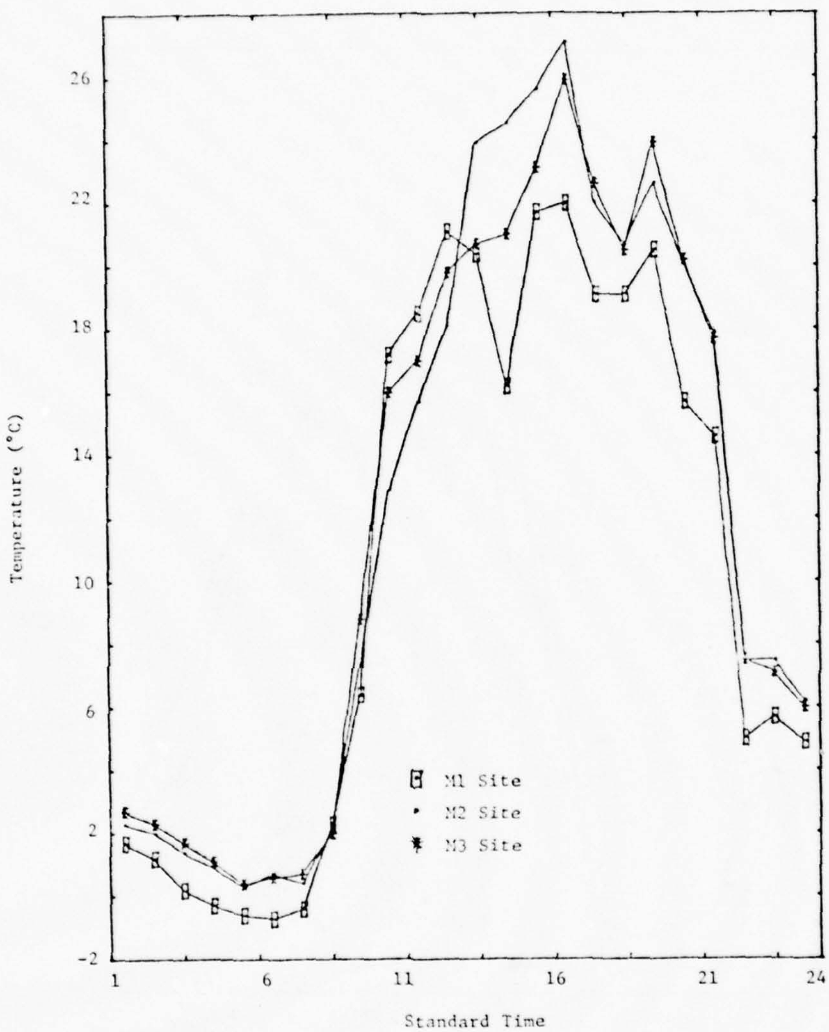

Figure 11. Air temperature measurements at the M1, M2, and M3 Sites for July 16, 1977.

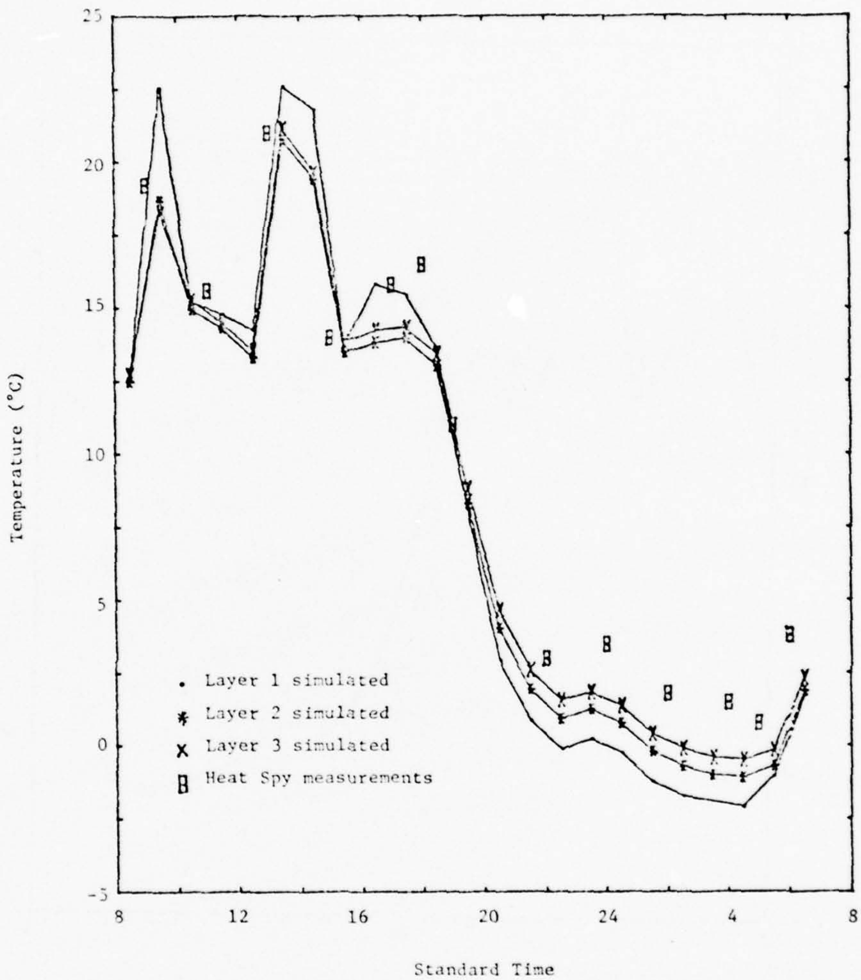

Figure 12. Simulated versus measured lodgepole pine canopy horizontal effective radiant temperatures (ERT) for July 15-16, 1977. Measured ERT's are the mean of 4 horizontal ERT's of the middle layer as measured by the Heat Spy. Air temperature was recorded at the M1 Site.

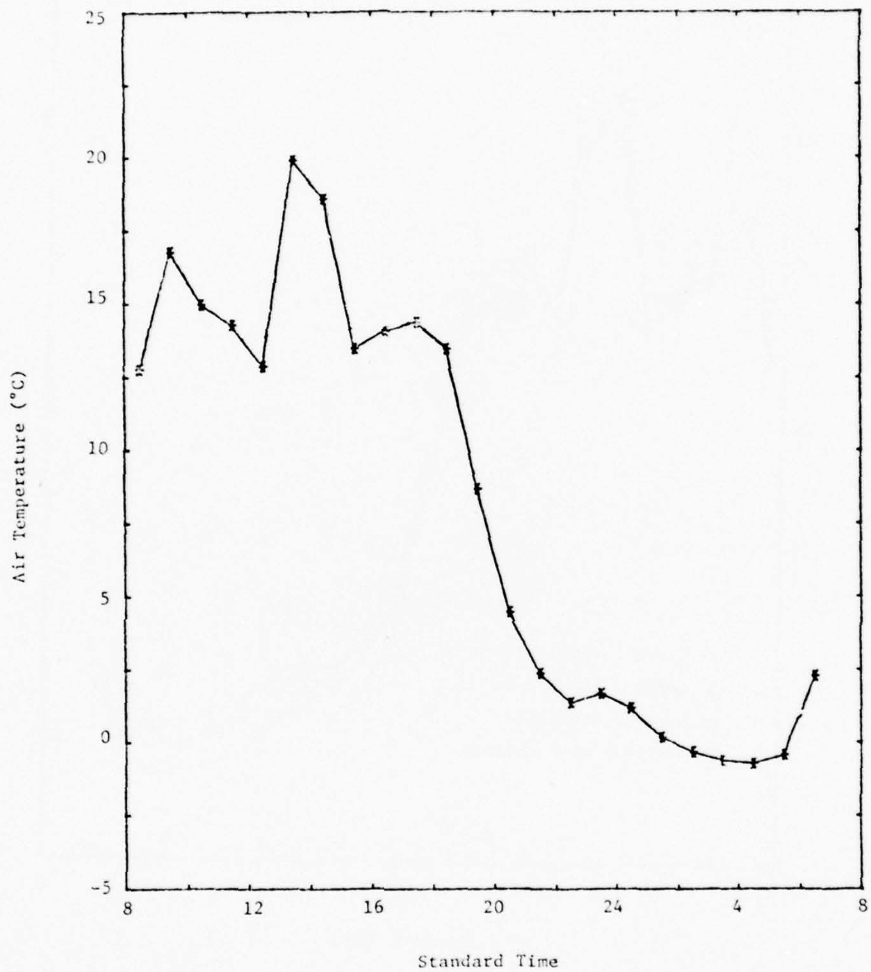

Figure 13. Measured air temperature at the M1 Site for July 15-16, 1977.

```
      PROGRAM TCSM    (INPUT,OUTPUT,TAPE5=INPUT,TAPE6=OUTPUT)
C
C
C...PROGRAM CANTEMP IS A MATHEMATICAL MODEL FOR THE PREDICTION OF THE THERMAL
C   BEHAVIOR OF A VEGETATION CANOPY. INPUTS AND OUTPUTS ARE DESCRIBED IN
C   SUBROUTINE INPUTDA AND OUTDAT RESPECTIVELY
C   (DANIEL S. KIMES, COLORADO STATE UNIVERSITY, 6/16/78)
C
C
      COMMON /A/ WV,RH,RI,D(3)
      COMMON /B/ PGAP(3,9), PHIT(3,9),PGAP2(3,9), PHIT2(3,9),STEF
      COMMON/C/COSTA(9,9,18),EMISSV(4),ABSORB(3), ESKY, EGRD, SECTAR(9)
      COMMON/D/CONT(3,5,9),C(3,5,9), SUMT(3,9), KELV, GT, NUSIM, ITIME
      COMMON/E/AT,THETA(9),PHI(18),XLF(9), YLF(9), ZLF(9), XS(9,18)
      COMMON/F/YS(9,18),ZS(9), CENTR, R, FREQD(9,3) , WA(15),EPS
      COMMON/G/NSIG,N, ITMAX
      COMMON /H/ INDEX1
      COMMON /I/ X(3)
      COMMON /J/ THERM,THMLEX,CONVEC,TRANS
      COMMON/S/ ABSOL(3)
C
C...READ AND ASSIGN THE INPUT DATA
C
      NUSIM=-1
      INDEX1=0
   76 IF(INDEX1.EQ.NUSIM)STOP
      CALL INPUTDA
      IF(INDEX1.GT.1) GO TO 95
C
C...CALCULATE THE CANOPY GEOMETRY COEFFICIENTS
C
      CALL CANGEOM
C
C...CALCULATE THE SIN THETA FACTORS FOR ALL SOURCE ANGLE-LEAF ANGLE
C   PURMUTATIONS.
C
      CALL DEVANG
C
C...CALCULATE THE NORMALIZING FACTOR FOR THE RELATIVE SIZES OF SOURCE SECTORS
C
      CALL SECTOR
   95 CONTINUE
C
C...CALCULATE THE THERMAL SKY EXITANCE
C
      CALL SKYEX
C
C...CALCULATE THE THERMAL GROUND EXITANCE
C
      CALL GRONDEX
C
C...CALCULATE THE THERMAL RADIATION COEFFICIENTS
C
      CALL SETUP
C
C...CALCULATE THE AVERAGE LEAF TEMPERATURE WITHIN EACH LAYER.
C
      CALL NONLIN(X,WA,EPS,NSIG,  ITMAX,IER)
C
C...CALCULATE THE THERMAL EXITANCE AND EBT ABOVE THE CANOPY FOR THE 9
C   INCLINATION AND 3 HORIZONTAL SENSOR ANGLES.

C
      CALL SENSOR
C
C...DISPLAY THE OUTPUT
C
      CALL OUTDAT
      GO TO 76
      END
```

```
      SUBROUTINE INPUTDA
C
C
C...SUBROUTINE INPUTDA READS AND ASSIGNS THE INPUT DATA
C
C
      COMMON/GEO/ PHITI(3,9),FLAI(3,1),SLAI(3,1),AXLFA(19,3),AYLFA(19,3)
      COMMON /A/ WV,PH,PL,D(3)
      COMMON /B/ PGAP(3,9), PHIT(3,9),PGAP2(3,9), PHIT2(3,9),STEF
      COMMON/C/COSTA(9,9,18),EMISSV(4),ABSORB(3), ESKY, EGRD, SECTAR(9)
      COMMON/D/CONT(3,5,9),C(3,5,9), SUMT(3,9), KELV, GT, NUSIM, ITIME
      COMMON/E/AT,THETA(9),PHI(18),XLF(9), YLF(9), ZLF(9), XS(9,18)
      COMMON/F/YS(9,18),ZS(9), CEDTP, B, FREQD(9,3) , WA(15),EPS
      COMMON/G/NSIG,N, ITMAX
      COMMON /H/ INDEX1
      COMMON /I/ X(3)
      COMMON /J/ THERM,THMLEX,CONVEC,TRANS
      COMMON /N/ STOR(3)
      COMMON/S/ ABSOL(3)
C
C...TEST FOR THE SIMULATION NUMBER AND SKIP TO THE APPROPRIATE INPUT DATA
C
      IF (INDEX1.EQ.0) GO TO 99
      IF(INDEX1.GT.0.AND.INDEX1.LT.NUSIM) GO TO 90
      IF(INDEX1.EQ.NUSIM) STOP
   99 CONTINUE
C
C...ASSIGN THE STEFAN BOLTZMANN CONSTANT WATTS/M**2*K**4
C
      STEF=5.6686E-8
C
C...ASSIGN THE CONVERSION FACTOR FOR KELVIN-DEGREES
C
      B= 273.0
C
C...READ THE AVERAGE THERMAL EMISSIVITY COEFFICIENTS FOR THE 3 VEGETAION LAYERS
C    (1,2,3) AND THE GROUND(4).
C
      READ(5,10)(EMISSV(I),I=1,4)
   10 FORMAT (8F10.5)
C
C...READ THE AVERAGE THERMAL ABSORPTION COEFFICIENTS FOR THE 3 VEGETATION LAYERS
C
      READ(5,10)(ABSORB(I),I=1,3)
C
C
C...READ THE ZSYSTM SUBPROGRAM PARAMETERS (IMSL LIBRARY). ZSYSTM SOLVES FOR THE
C    AVERAGE LEAF TEMPERATUR WITHIN EACH LAYER.
C     EPS    FIRST STOPPING CRITERION . A ROOT X(1),.....,X(N) IS ACCEPTED IF THE
C            MAXIMUM ABSOLUTE VALUE OF F(X,K,PAR) IS LESS THAN OR EQUAL TO EPS,
C            WHERE K=1,.....,N. (INPUT)
C      NSIG SECOND STOPPING CRITERION. A ROOT IS ACCEPTED IF TWO SUCCESSIVE
C            APPROXIMATIONS TO A GIVEN ROOT AGREE IN THE FIRST NSIG DIGITS,(INPUT)
C            NOTE. IF EITHER OR BOTH OF THE STOPPING CRITERIA ARE FULFILLED THE
C            ROOT IS ACCEPTED.
C      N     THE NUMBER OF EQUATIONS (= NUMBER OF UNKNOWNS) (INPUT)
C      X     THE VECTOR OF LENGTH N, AS INPUT, IS THE INITIAL GUESS TO THE ROOT.
C            AS OUTPUT, IT IS THE COMPUTED SOLUTION.
C      ITMAX ON INPUT=THE MAXIMUM ALLOWABLE NUMBER OF ITERATIONS AND ON OUTPUT=
C            THE NUMBER OF ITERATIONS USED IN FINDING THE COMPUTED SOLUTION.
C      WA    AN ARRAY WORK AREA OF SIZE ((N+2)*(N-1))/2+3*N SUPPLIED BY THE USER.
```

```
C       PAR  PAR CONTAINS A PARAMETER SET (POSSIBLY A FUNCTION NAME) WHICH IS
C            PASSED TO THE USER SUPPLIED FUNCTION F. PAR MAY BE USED TO PASS ANY
C            AUXILIARY PARAMETERS NECESSARY FOR COMPUATION OF THE FUNCTION F.
C       IER  ERROR PARAMETER      TERMINAL ERROR=128+N
C                                 N=1 INDICATES FAILURE TO CONVERGE WITHIN ITMAX
C                                                                     ITERATIONS
C                                 N=2 SINGULAR SYSTEM (JACOBIAN)
C
C
C
      READ(5,11) EPS , NSIG, N, ITMAX
   11 FORMAT(E20.8,3I10)
C
C
C...READ THE CANOPY GEOMETRY FREQUENCY DISTRIBUTIONS OF THE ELEMENTS
C    IN LAYERS 1,2,3. AYLEA REPRESENTS THE INCLINATION ANGLES 0-90
C    (5 DEGREE INTERVALS) AND AYLEA REPRESENTS THE CORRESPONDING
C    FREQUENCY. SLAI AND FLAI ARE EACH LAYERS S PARAMETER AND LAI
C    RESPECTIVELY.
C
C
      DO 190 I=1,3
      READ(5,101)(AYLEA(M,I),AYLEA(M,I),M=1,19)
      READ(5,101)SLAI(I,1),FLAI(I,1)
  190 CONTINUE
  101 FORMAT (8F10.5)
C
C...STORE THE ZSYSTM PARAMETERS FOR OUTPUT.
C
      STOR(1)=EPS
      STOR(2)=NSIG
      STOR(3)=ITMAX
      READ(5,12) (X(I),I=1,3)
   12 FORMAT (4E20.8)
C
C...READ THE LEAF DIAMETERS FOR EACH LAYER
C
      READ(5,51) (D(I),I=1,3)
   51 FORMAT(3F10.5)
C
C...READ THE NUMBER OF SIMULATION RUNS DESIRED
C
      READ(5,13) NUSIM
   13 FORMAT(I10)
C
C...READ THE NEW TIME,AIRTEMP,TRUEGOUND TEMP,WINDVELOCITY,RELATIVE HUMIDITY, AND
C    LEAF RESISTANCE FOR THE NEXT DESIRED SIMULATION.
C
   90 INDEX1=INDEX1 + 1
      READ (5,40) TTIME,AT,GT,WV,RH,RL
   40 FORMAT (I4,7F10.5)
C
C...READ THE AVERAGE ABSORBED SOLAR FLUX IN LAYERS 1,2,3. THESE VALUES
C    ARE OBTAINED FROM THE MODIFIED SRVC MODEL.
C
      READ(5,120) (ABSOL(I),I=1,3)
  120 FORMAT(3F10.5)
C
C...REINITIALIZE THE ZSYSTM PARAMETERS SINCE THEY ARE CHANGED INTERNALLY
C    AFTER EACH SIMULATION.
C
      EPS=STOR(1)
      NSIG=STOR(2)
      ITMAX=STOR(3)
      RETURN
      END
```

```
      SUBROUTINE OUTPAT
C
C
C...SUBROUTINE OUTPUT FORMATS THE DATA TO BE DISPLAYED.
C
C
      COMMON/SENS/  FLAYT(9),FLAYH(3),FRTT(9),FRTH(3)
      COMMON/GEO/ PHIT1(3,9),FLAI(3,1),SLAI(3,1),AXLFA(19,3),AYLFA(19,3)
      COMMON /A/ WV,RH,RL,D(3)
      COMMON /B/ PGAP(3,9), PHIT(3,9),PGAP2(3,9), PHIT2(3,9),STEF
      COMMON/C/COSTA(9,3,19),EMISSV(4),ABSORB(3), ESKY, EGRD, SECTAR(9)
      COMMON/D/CONT(3,5,9),C(3,5,9), SUMT(3,9), KELV, CT, NUSIM, ITIME
      COMMON/E/AT,THETA(9),PHI(18),XLF(9), YLF(9), ZLF(9), XS(9,18)
      COMMON/F/YS(9,18),ZS(9), CEDTR, R, FREQD(9,3) , WA(15),EPS
      COMMON/G/NSIG,N, ITMAX
      COMMON /H/ INDEX1
      COMMON /I/ X(3)
      COMMON /J/ THERM,THMLEX,CONVEC,TRANS
      COMMON /K/ TT1(3),TT2(3),TT3(3),TT4(3)
      COMMON /N/ STOR(3)
      COMMON /L/ TEMP(3)
      COMMON/S/ ABSOL(3)
      IF(INDEX1.GT.1) GO TO 109
C
C...WRITE THE TITLE FOR CONSTANT PARAMETERS
C
      WRITE(6,100)
  100 FORMAT(//////,* THE CONSTANT PARAMETERS FOR THIS SERIES OF RUNS AR
     +E AS FOLLOWS *,//////)
C
C...WRITE THE ZSYSTM PARAMETERS
C
      WRITE(6,102)(STOR(J),J=1,3)
  102 FORMAT(1X,* THE EPS,NSIG,AND ITMAX PARAMETES FOR ZSYSTM ARE= *,
     +3F10.5,/)
C
C...WRITE THE LAYERS EMISSIVITY
C
      WRITE(6,201) (EMISSV(I),I=1,4)
  201 FORMAT(1X,* THE AVERAGE EMISSIVITIES FOR THE 3 LAYERS(1-3) AND
     +GROUND ARE= *,4F10.4,/)
C
C...WRITE THE LEAF DIAMETERS FOR EACH LAYER
C
      WRITE(6,203) (D(I),I=1,3)
  203 FORMAT(1X,* THE LEAF DIAMETERS IN CM FOR LAYER1-3 ARE= *,3F10.5,
     +//)
C
C...WRITE THE CALCULATED GEOMETRY FOR EACH LAYER
C
      DO 319 I=1,3
      WRITE(6,320) I
  320 FORMAT (///,* THE COMPONENT ANGLE COMPUTATIONS FOR LAYER *,I1,/)
      WRITE(6,321) FLAI(I,1),SLAI(I,1)
  321 FORMAT ( * LAI = *,F4.2,4X,* S= *,F4.2,/)
      WRITE(6,322) (AXLFA(M,I),AYLFA(M,I),M=1,19)
  322 FORMAT( * XLFA,YLFA *,/,(2X,16F8.3))
      WRITE(6,323) (PGAP(I,M),M=1,9)
  323 FORMAT(//,* PGAP FOR 1-9 INCLINATION INTERVALS*,9F8.3)
  319 CONTINUE
C
```

```
C...WRITE THE CALCULATED THERMAL CONTRIBUTIONS COEFFICIENTS
C
      WRITE(6,302)
  302 FORMAT(1X,//////,* THE PROPORTION OF RADIANCE AREA CONTRIBUTED BY
     $A SECTOR OF THE 9 BANDS(1-9) DIVIDED BY 19 (SECTORS) ARE=*,/)
      WRITE(6,303)(SECTAR(I),I=1,9)
  303 FORMAT(10X,9F10.5,////////)
      WRITE(6,40)
   40 FORMAT (1X,//,* THE BAND-RGAP-PHIT-COEFFICIENTS FOR THE THERMAL RA
     +DIATION TRANSFERS ARE =*,/)
      DO 39 I=1,3
      WRITE(6,41) I
   41 FORMAT (1X,* THE 9 BAND COEFFICIENTS TO LAYER *,I1,* ARE*)
      DO 39 J=1,5
      WRITE (6,42) J,(CONT(I,J,M),M=1,9)
   42 FORMAT(8X,* FROM LAYER*,I1,2X,9F6.4)
   39 CONTINUE
      WRITE(6,50)
   50 FORMAT (1X,////,* THE FINAL THERMAL RADIATION COEFFICIENTS ARE AS FOLLOWS
     +*,/)
      DO 51 I=1,3
      WRITE(6,52) I
   52 FORMAT (1X,* THE THERMAL RADIATION CONTRIBUTION TO LAYER *,I1,* FO
     +R EACH OF THE 9 LEAF INCLINATIONS ARE*)
      DO 51 J=1,5
      WRITE (6,53)J,(C(I,J,M),M=1,9)
   53 FORMAT (8X,* FROM LAYER*,I1,2X,9F10.3)
   51 CONTINUE
      WRITE(6,154)
  154 FORMAT(1X,////,* THE COS(THETA) FACTORS ARE AS FOLLOWS *,/)
      DO 101 I=1,9
      WRITE(6,108) I
  108 FORMAT(1X,* THE 19 SECTOR FACTORS FOR A LEAF INCLINATION OF *,I1,*
     + ARE*)
      DO 101 J=1,9
      WRITE (6,103) J,(COSTA(I,J,M),M=1,19)
  103 FORMAT(8X,* SOURCE FROM BAND*,I1,19F5.3)
  101 CONTINUE
C
C...WRITE THE TITLE FOR THE SIMULATIONS MADE
C
      WRITE(6,104)
  104 FORMAT(1X,/////,*...........THE FOLLOWING SIMULATIONS WERE MADE...
     +....................................*,///)
  109 CONTINUE
C
C...WRITE THE CONSTANT PARAMETERS FOR EACH SIMULATION
C
      WRITE(6,105) ITIME,AT,GT,WV,RH,RL
  105 FORMAT(1X,* TIME=*,I4,* AIR TEMP=*,F7.2,* GROUND TEMP=*,F7.2,*
     +WIND VELOCITY=*,F7.2,* REL HUMIDITY=*,F7.2,* LEAF RES VAP DIFF=*,F
     +7.2)
C
C...WRITE THE SIMULATED AVERAGE LAYER TEMPERATURES
C
      WRITE(6,300)(TEMP(I),I=1,3)
  300 FORMAT(1X,//,* THE AVERAGE SIMULATED LAYER TEMPERATURES (1-3) ARE
     +*,3F10.2,//)
C
C...WRITE THE CALCULATED GROUND THERMAL EXITANCE
C
```

```
      WRITE(6,250) EGRD
  250 FORMAT(1X,/,' THE GROUND THERMAL EXITANCE IS ',F8.2)
C
C...WRITE THE CALCULATED SKY THERMAL EXITANCE
C
      WRITE(6,251) ESKY
  251 FORMAT(1X,' THE SKY THERMAL EXITANCE IS ',F8.2)
      DO 121 I=1,3
      CALL STHERM(TEMP,I,TOTAL)
      TT2(I)=THMLEX
      TT3(I)=CONVEC
      TT4(I)=TRANS
      TT1(I)=THERM
  121 CONTINUE
C
C...WRITE THE ABSORBED SOLAR RADIATION FOR EACH LAYER
C
      WRITE(6,119) (ABSOL(I),I=1,3)
  119 FORMAT(1X,' THE AVERAGE ABSORBED SOLAR FLUX FOR LAYERS 1-3 ARE ',
     *3F10.5)
C
C...WRITE THE EMITTED THERMAL RADIATION FOR THE AVERAGE LEAVES
C
      WRITE(6,120) (TT2(I),I=1,3)
  120 FORMAT(1X,' THE EMITTED THERMAL RADIATION FOR THE AVERAGE LEAVES
     *(LAYERS 1-3) ARE', 3F10.5)
C
C...WRITE THE ABSORBED THERMAL RADIATION FOR THE AVERAGE LEAVES.
C
      WRITE(6,122) (TT1(I),I=1,3)
  122 FORMAT (1X,' THE ABSORBED THERMAL RADIATION FOR THE AVERAGE LEAVES
     + (LAYERS 1-3) ARE',3F10.5 )
C
C...WRITE THE ENERGY GAINED BY CONVECTION FOR THE AVERAGE LEAVES
C
      WRITE(6,123) (TT3(I),I=1,3)
  123 FORMAT(1X,' THE ENERGY GAIN BY CONVECTION FOR THE AVERAGE LEAVES
     +ARE',3F10.5)
C
C...WRITE THE ENERGY LOSS BY TRANSPIRATION FOR THE AVERAGE LEAVES.
C
      WRITE(6,124) (TT4(I),I=1,3)
  124 FORMAT (1X,' THE ENERGY LOSS BY TRANSPIRATION FOR THE AVERAGE
     + LEAVES ARE', 3F10.5)
C
C...WRITE THE EXITANCE AND ERT ABOVE AND WITHIN THE CANOPY.
C
      WRITE (6,60)
   60 FORMAT (1X,//,' THE THERMAL EXITANCE AND ERT ABOVE THE CADPY FOR
     / 5-85 DEGREE INCLINATIONS ARE ')
      DO 59 M=1,9
      WRITE (6,61) ELAYT(M),ERTT(M)
   61 FORMAT (3X,F10.5,' W/M**2',3X,F10.5,' CENTIGRADE')
   59 CONTINUE
      WRITE  (6,62)
   62 FORMAT ( ' THE THERMAL EXITANCE AND ERT (HORIZONTAL VIEW) FOR THE
     / 3 LAYERS ARE  ')
      DO 58 M=1,3
      WRITE(6,63) ELAYH(M),ERTH(M)
   63 FORMAT (3X,F10.5,' W/M**2',3X,F10.5,' CENTIGRADE')
   58 CONTINUE
      WRITE(6,400)
  400 FORMAT(1X,////,'...................................................
     *.........................................................',///
     */)
      RETURN
      END
```

```
      SUBROUTINE SETUP
C
C
C...SUBROUTINE SETUP PRE-CALCULATES AND PRE-ARRANGES MANY OF THE THERMAL
C   COEFFICIENTS NEEDED FOR THE FINAL ENERGY BUDGETS WHICH ARE PLACED INTO THE
C   ZSYSTM ROUTINE.
C
C
      COMMON /A/ WV,PH,PL,D(3)
      COMMON /B/ PGAP(3,9), PHIT(3,9),PGAP2(3,9), PHIT2(3,9),STEF
      COMMON/C/COSTA(9,3,18),EMISSV(4),ABSORB(3), ESKY, EGRD, SECTAR(9)
      COMMON/D/CONT(3,5,9),C(3,5,9), SUMT(3,9), KELV, GT, NUSIM, ITIME
      COMMON/E/AT,THETA(9),PHI(18),XLF(9), YLF(9), ZLF(9), XS(9,18)
      COMMON/F/YS(9,18),ZS(9), CEDTR, R, FREQD(9,3) , WA(15),EPS
      COMMON/G/NSIG,N, ITMAX
      COMMON /H/ INDEX1
C
C
C...FOR EACH LAYER CALCULATE THE BAND*PGAP-PHIT COEFFICIENTS NEEDED FOR EACH
C   LAYERS THERMAL RADIATION CONTRIBUTION TO A  SPECIFIC LAYER.
C
C
      DO 20 I=1,9
C
C
C...CONTRIBUTION COEFFICIENTS TO LAYER 1
C
C
C.....FROM SKY
C
      CONT(1,1,I)= PGAP2(1,I)
C
C.....FROM LAYER 1
C
      CONT(1,2,I)= 2.*PHIT2(1,I)
C
C.....FROM LAYER 2
C
      CONT(1,3,I)= PGAP2(1,I)-PGAP2(1,I)*PGAP(2,I)
C
C.....FROM LAYER 3
C
      CONT(1,4,I)= PGAP2(1,I)*PGAP(2,I)-PGAP2(1,I)*PGAP(2,I)*PGAP(3,I)
C
C.....FROM GROUND
C
      CONT(1,5,I)= PGAP2(1,I)*PGAP(2,I)*PGAP(3,I)
C
C
C...CONTRIBUTION COEFFICIENTS TO LAYER 2
C
C
C.....FROM SKY
C
      CONT(2,1,I)= PGAP(1,I)*PGAP2(2,I)
C
C.....FROM LAYER 1
C
      CONT(2,2,I)= PGAP2(2,I)-PGAP2(2,I)*PGAP(1,I)
C
C.....FROM LAYER 2
```

```
C
      CONT(2,3,I)= 2.*PHIT2(2,I)
C
C.....FROM LAYER 3
C
      CONT(2,4,I)= PGAP2(2,I)-PGAP2(2,I)*PGAP(3,I)
C
C.....FROM GROUND
C
      CONT(2,5,I)= PGAP2(2,I)*PGAP(3,I)
C
C
C...CONTRIBUTION COEFFICIENTS TO LAYER 3
C
C
C.....FROM SKY
C
      CONT(3,1,I)= PGAP(1,I)*PGAP(2,I)*PGAP2(3,I)
C
C.....FROM LAYER 1
C
      CONT(3,2,I)= PGAP2(3,I)*PGAP(2,I)-PGAP2(3,I)*PGAP(2,I)*PGAP(1,I)
C
C.....FROM LAYER 2
C
      CONT(3,3,I)= PGAP2(3,I)-PGAP2(3,I)*PGAP(2,I)
C
C.....FROM LAYER 3
C
      CONT(3,4,I)= 2.*PHIT2(3,I)
C
C.....FROM GROUND
C
      CONT(3,5,I)= PGAP2(3,I)
   20 CONTINUE
C
C
C...NOW FORM THE EQUATION COEFFICIENTS FOR THE CONTRIBUTED THERMAL RADIANT
C   ENERGY TO EACH LAYER AND FOR EACH LEAF INCLINATION ANGLE WITHIN A LAYER.
C
C
      CALL SETO3(C,3,5,9)
C
C...THERMAL RADIATION CONTRIBUTION TO LAYER N
C
      DO 30 N=1,3
C
C...FOR EACH LEAF INCLINATION ANGLE INTERVAL
C
      DO 30 I= 1,9
C
C...SUM EACH SECTORS RADIATION CONTRIBUTION (9 BANDS CONTAINING 18 SECTORS)
C
      DO 30 J=1,9
      DO 30 K=1,18
C
C...ABSORBED THERMAL RADIATION CONTRIBUTED BY SKY
C
      C(N,1,I)= C(N,1,I) + SECTAR(J)*CONT(N,1,J)*ESKY*ABSORB(N)*COSTA
     + (I,J,K)
C...ABSORBED THERMAL RADIATION CONTRIBUTED BY LAYER 1
C
      C(N,2,I)= C(N,2,I) + SECTAR(J)*CONT(N,2,J)*STEF*EMISSV(1)*ABSORB(N
     + )*COSTA(I,J,K)
C
C...ABSORBED THERMAL RADIATION CONTRIBUTED BY LAYER 2
C
      C(N,3,I)= C(N,3,I) + SECTAR(J)*CONT(N,3,J)*STEF*EMISSV(2)*ABSORB(N
     + )*COSTA(I,J,K)
C
C...ABSORBED THERMAL RADIATION CONTRIBUTED BY LAYER 3
C
      C(N,4,I)= C(N,4,I) + SECTAR(J)*CONT(N,4,J)*STEF*EMISSV(3)*ABSORB(N
     +)*COSTA(I,J,K)
C
C...ABSORBED THERMAL RADIATION CONTRIBUTED BY THE GROUND
C
      C(N,5,I)= C(N,5,I) + SECTAR(J)*CONT(N,5,J)*EGRD*
     + ABSORB(N)*COSTA(I,J,K)
   30 CONTINUE
      RETURN
      END
```

```
      SUBROUTINE NONLIN(X,WA,EPS,NSIG,ITMAX,IER)
C
C
C...SUBROUTINE NONLIN IS SIMPLY A CALLING PROGRAM FOR THE ZSYSTM ALGORITHIM ON
C   THE IMSL LIBRARY. ZSYSTM DETERMINES THE ROOTS OF A SYSTEM OF N SIMULTANEOUS
C   NONLINEAR EQUATIONS IN N UNKNOWNS, F(X)=0 , IN VECTOR FORM. FUNCTION
C   F IS CALLED BY ZSYSTM TO FURNISH THE VALUES OF THE FUNCTIONS WHICH DEFINE
C   THE SYSTEM OF EQUATIONS BEING SOLVED.
C
C
      COMMON /J/ THERM,THMLEX,CONVEC,TRANS
      COMMON /L/ TEMP(3)
      COMMON/S/ ABSOL(3)
      DIMENSION X(3),WA(15),PAR(1)
      DIMENSION TT1(3),TT2(3),TT3(3),TT4(3)
      EXTERNAL F
C
C...CALL ZSYSTM FOR SOLVING THE SYSTEM OF NONLINEAR EQUATIONS
C
      CALL ZSYSTM (F,EPS,NSIG,3,X,ITMAX,WA,PAR,IER)
C
C...TEST FOR SYSTEM FAILURES
C
      IF(IER.EQ.0) GO TO 50
      IF(IER.EQ.2) GO TO 60
      IF(IER.GT.2) GO TO 100
      WRITE(6,70)
   70 FORMAT( *FAILURE TO CONVERGE WITHIN ITMAX ITERATIONS*)
      GO TO 50
   60 WRITE (6,90)
   90 FORMAT( * SINGULAR SYSTEM (JACOBIAN)*)
      GO TO 80
   50 CONTINUE
      DO 54 L=1,3
      TEMP(L)=X(L)
   54 CONTINUE
      GO TO 80
  100 WRITE(6,101)
  101 FORMAT( *TERMINAL ERROR*)
   80 CONTINUE
      RETURN
      END
```

```
      FUNCTION F (X,K,PAR)
C
C
C...FUNCTION F SETS UP THE TOTAL ENERGY BUDGET EQUATION FOR LAYER 1,2, AND 3.
C   THERMAL RADIATION CONTRIBUTION TO EACH LAYER. FUNCTION F IS THEN USED BY
C   ZSYSTM TO CALCULATE EACH ITERATE.
C
C
      DIMENSION X(3)
      DIMENSION PAR(1)
C
C   CALCULATE THE ENERGY BUDGET FOR THE NEXT ITERATE FOR LAYER 1,2, OR 3.
C
      GO TO (1,2,3) K
C
C...ENERGY BUDGET FOR LAYER 1
C
    1 CALL STHERM (X,K,TOTAL)
      F= TOTAL
       RETURN
C
C...ENERGY BUDGET FOR LAYER 2
C
    2 CALL STHERM (X,K,TOTAL)
      F= TOTAL
       RETURN
C
C...ENERGY BUDGET FOR LAYER 3
C
    3 CALL STHERM (X,K,TOTAL)
      F= TOTAL
      RETURN
      END
```

```
      SUBROUTINE STHERM (X,K,TOTAL)
C
C
C...SUBROUTINE STHERM CALCULATES IN FINAL FORM THE THERMAL CONTRIBUTION
C   (ITERATE) TO EACH LAYER AND THE THERMAL EXITANCE, CONVECTIONAL,
C   TRANSPIRATIONAL, AND SOLAR RADIATION EXCHANGES. FOR EACH LAYER THERE ARE 9
C   EQUATIONS. EACH EQUATION IS WEIGHTED BY THE FREQUENCY OF OCCURENCE FOR THE
C   CORRESPONDING INCLINATION ANGLE INTERVAL.
C
C
      COMMON /A/ WV,RH,RL,D(3)
      COMMON /B/ PGAP(3,9), PHIT(3,9),PGAP2(3,9), PHIT2(3,9),STEF
      COMMON/C/COSTA(9,9,18),EMISSV(4),ABSORB(3), ESKY, EGRD, SECTAR(9)
      COMMON/D/CONT(3,5,9),C(3,5,9), SUMT(3,9), KELV, GT, NUSIM, ITIME
      COMMON/E/AT,THETA(9),PHI(18),XLF(9), YLF(9), ZLF(9), XS(9,18)
      COMMON/F/YS(9,18),ZS(9), CEDTR, B, FREQD(9,3) , WA(15),EPS
      COMMON/G/NSTG,N, ITMAX
      COMMON /J/ THERM,THMLEX,CONVEC,TRANS
      COMMON/S/ ABSOL(3)
      DIMENSION X(3)
      REAL LE
C
C...SUM SKY AND GROUND THERMAL RADIATION CONTRIBUTIONS TO THE DESIGNATED LAYER
C   (K) AND EACH INCLINATION CLASS
C
      DO 10 I=1,9
      SUMT(K,I)= C(K,1,I) + C(K,5,I)
   10 CONTINUE
C
C...ALSO SUM EACH LAYERS THERMAL RADIATION CONTRIBUTION  TO EACH RECEIVING LAYER
C
      DO 20 I=1,9
      DO 20 J=1,3
      SUMT(K,I)= C(K,J+1,I)*(X(J)+B)**4  +  SUMT(K,I)
   20 CONTINUE
C
C...APPLY THE WEIGHTING COEFFICIENT FOR THE PROBABILITY OF OCCURENCE OF EACH
C   LEAF INCLINATION INTERVAL WITHIN THE APPROPRIATE LAYER (K).
C
      THERM=0.0
      DO 30 I=1,9
      THERM= SUMT(K,I)*FREQD(I,K) + THERM
   30 CONTINUE
C
C...DIVIDE THE THERMAL RADIANT ENERGY (THERM) CONTRIBUTED TO LAYER K BY 2.0.
C   THIS FACTOR ACCOUNTS FOR THE FACT THAT THERMAL ENERGY INTERACTS BOTH WITH
C   THE TOP AND BOTTOM SURFACES OF THE LEAF AND ALL ENERGY CALCULATIONS ARE DONE
C   ON A PER UNIT AREA BASIS.
C
       THERM = THERM/2.0
C
C...FUNCTION CONVEC CALCULATES THE CONVECTIONAL LOSS OR GAIN FROM THE AVERAGE
C   LEAF IN LAYER K.
C
      IF(WV.LE.30.0) GO TO 110
      GO TO 120
  110 CONVEC= (20.4+0.2*(WV**0.97))*(.001)*(697.76)
      CONVEC= CONVEC*(-1.)
      CONVEC=CONVEC*(X(K)-AT)
      GO TO 130
  120 CONVEC= (0.95*WV**0.97)*(.001)*(697.76)
```

```
      CONVEC= CONVEC*(-1.)
      CONVEC=CONVEC*(X(K)-AT)
  130 CONTINUE
C
C...FUNCTION THMLEX CALCULATES THE EMITTED THERMAL ENERGY FROM THE AVERAGE LEAF
C   IN LAYER K.
C
      THMLEX= STEF*EMISSV(K)*(X(K)+3)**4
C
C...FUNCTION TRANS CALCULATES THE ENERGY LOSS FROM THE AVERAGE LEAF IN LAYER K
C   BY TRANSPIRATION.
C
      LE= -0.566*Y(K) + 597.3
      SDL= (5.2342*EXP(0.056715*Y(K))) *1.0E-6
      SDA= RH*(5.2342*EXP(0.056715*AT))*1.0E-6
      RA= (0.04+1.27*(1./WV**0.5))/50.
      TRANS=LE*(SDL-SDA)/(RL+RA)
      TRANS=697.75 * TRANS
C
C...SUM ALL THE ENERGY LOSSES AND GAINS OF THE AVERAGE LEAF IN LAYER K.
C
      TOTAL= THERM-THMLEX+CONVEC-TRANS+ABSOL(K)
      RETURN
      END
```

```
      SUBROUTINE DEVANG
C
C
C...SUBROUTINE DVANG CALCULATES THE COS(ANGLE) DEVIATION
C   ANGLE OF ALL LEAF INCLINATIONS SOURCE ORIENTATIONS PERMUTATIONS. THE THEORY
C   IS BASED ON THE EXISTENCE OF PLANE ELEMENTS AS USED IN THE SPVC MODEL.
C
C
      COMMON /A/ WV,PH,RL,D(3)
      COMMON /B/ PGAP(3,9), PHIT(3,9),PGAP2(3,9), PHIT2(3,9),STEF
      COMMON/C/COSTA(9,9,18),EMISSV(4),ABSORB(3), ESKY, EGRD, SECTAR(9)
      COMMON/D/CONT(3,5,9),C(3,5,9), SUMT(3,9), KELV, GT, NUSIM, ITIME
      COMMON/E/AT,THETA(9),PHI(18),XLF(9), YLF(9), ZLF(9), XS(9,18)
      COMMON/F/YS(9,18),ZS(9), CEDTR, B, FREQD(9,3) , WA(15),EPS
      COMMON/G/NSIG,N, ITMAX
      INTEGER S8,SS
      CEDTR= 0.017453293
C
C...CALCULATE INCLINATIN ANGLES IN RADIANS
C
      THETA(1)= 5. * CEDTR
      DO 10 I=1,8
      THETA(I+1)= THETA(I) + 10.0 * CEDTR
   10 CONTINUE
C
C...CALCULATE AZIMUTH ANGLES IN RADIANS
C
      PHI(1)= 10.*CEDTR
      DO 20 I=1,17
      PHI(I+1)= 20.*CEDTR+PHI(I)
   20 CONTINUE
C
C...CALCULATE ALL THE DIRECTION COSINES OF SOURCE SECTORS
C
      DO 40 I=1,9
      ZS(I)=SIN(THETA(I))
      DO 40 J=1,18
      XS(I,J)=COS(THETA(I))*COS(PHI(J))
      YS(I,J)= COS(THETA(I))*SIN(PHI(J))
   40 CONTINUE
C
C...CALCULATE THE DIRECTION COSINES FOR THE NORMAL VECTOR OF ALL PLANAR LEAF
C   INCLINATION ANGLES ASSUMING THAT THE AZIMUTH ANGLE IS EQUAL TO ZERO DEGREES.
C
      DO 30 I= 1,9
      XLF(I)= -SIN(THETA(I))
      YLF(I)= 0.0
      ZLF(I)= COS(THETA(I))
   30 CONTINUE
C
C...CALCULATE THE ABSOLUTE VALUE OF THE DOT PRODUCTS OF ALL SOURCE-LEAF
C   ANGLE PERMUTATIONS. THIS VALUE IS EQUAL TO THE COSINE FACTOR DESIRED.
C
      DO 50 LI=1,9
      DO 50 S8=1,9
      DO 50 SS= 1,18
      DOT= (XLF(LI)*XS(S8,SS)+YLF(LI)*YS(S8,SS)+ZLF(LI)*ZS(S8))
      COSTA(LI,S8,SS)= ABS (DOT)
   50 CONTINUE
      RETURN
      END


      SUBROUTINE GRONDEX
C
C
C...SUBROUTINE GRONDEX CALCULATES THE THERMAL GROUND EXITANCE GIVEN THE TRUE
C   GROUND SURFACE TEMPERATURE.
C
C
      COMMON /A/ WV,PH,RL,D(3)
      COMMON /B/ PGAP(3,9), PHIT(3,9),PGAP2(3,9), PHIT2(3,9),STEF
      COMMON/C/COSTA(9,9,18),EMISSV(4),ABSORB(3), ESKY, EGRD, SECTAR(9)
      COMMON/D/CONT(3,5,9),C(3,5,9), SUMT(3,9), KELV, GT, NUSIM, ITIME
      COMMON/E/AT,THETA(9),PHI(18),XLF(9), YLF(9), ZLF(9), XS(9,18)
      COMMON/F/YS(9,18),ZS(9), CEDTR, B, FREQD(9,3) , WA(15),EPS
      COMMON/G/NSIG,N, ITMAX
C
      EGRD= EMISSV(4)*STEF*(GT+B)**4
C
      RETURN
      END
```

```
      SUBROUTINE SKYEX
C
C
C...SUBROUTINE SKYEX CALCULATES THE THERMAL EXITANCE FROM THE SKY.
C
C
      COMMON /A/ WV,PH,PL,D(3)
      COMMON /B/ PGAP(3,9), PHIT(3,9),PGAP2(3,9), PHIT2(3,9),STEF
      COMMON/C/COSTA(9,9,19),EMISSV(4),ABSORB(3), ESKY, EGRD, SECTAR(9)
      COMMON/D/CONT(3,5,9),C(3,5,9), SUMT(3,9), KELV, GT, NUSIM, ITIME
      COMMON/E/AT,THETA(9),PHI(19),XLF(9), YLF(9), ZLF(9), XS(9,18)
      COMMON/F/YS(9,18),ZS(9), CEDTR, B, FREQD(9,3) , WA(15),EPS
      COMMON/G/NSIG,N, ITMAX
C
      F= 1.0-0.261*EXP(-7.77E-4*(AT)**2)
      ESKY=STEF*(AT+B)**4*F
C
      RETURN
      END
```

```
      SUBROUTINE CANGEOM
C
C
C...SUBROUTINE CANGEOM CALCULATES THE CANOPY GEOMETRY COEFFICIENTS.
C...THE SUBROUTINE CANGEOM CALLS SUBROUTINE SRVCMOD WHICH IS A MODIFIED
C   PORTION OF THE SRVC MODEL THAT CALCULATES THE CANOPY GEOMETRY
C   PARAMETERS.
C
C
C
      COMMON/GEO/ PHIT1(3,9),FLAI(3,1),SLAI(3,1),AXLFA(19,3),AYLFA(19,3)
      COMMON /A/ WV,PH,PL,D(3)
      COMMON /B/ PGAP(3,9), PHIT(3,9),PGAP2(3,9), PHIT2(3,9),STEF
      COMMON/C/COSTA(9,9,19),EMISSV(4),ABSORB(3), ESKY, EGRD, SECTAR(9)
      COMMON/D/CONT(3,5,9),C(3,5,9), SUMT(3,9), KELV, GT, NUSIM, ITIME
      COMMON/E/AT,THETA(9),PHI(19),XLF(9), YLF(9), ZLF(9), XS(9,18)
      COMMON/F/YS(9,18),ZS(9), CEDTR, B, FREQD(9,3) , WA(15),EPS
      COMMON/G/NSIG,N, ITMAX
      CALL SRVCMOD
      DO 10 I=1,3
      DO 10 M=1,9
C
C...TRANSFER IDENTICAL ARRAYS PHIT AND PHIT1. PHIT CONTAINS THE
C   PROBABILITY OF HIT COEFFICIENTS FOR EACH VIEW ANGLE AND LAYER
C   PERMUTAION
C
      PHIT(I,M)=PHIT1(I,M)
C
C...CALCULATE THE PROBABILITY OF GAP (PGAP) FOR ALL PERMUTATIONS.
C
      PGAP(I,M)=1.-PHIT(I,M)
C
C...CALCULATE THE PROBABILITY OF GAP AND HIT FOR THE HALF LAYERS(PGAP2,PHIT2)
C   FOR ALL PERMUTATIONS.
C
      PGAP2(I,M)= SQRT(PGAP(I,M))
      PHIT2(I,M)=1.-PGAP2(I,M)
   10 CONTINUE
C
C...OBTAIN THE FREQUENCY OF OCCURENCE (FREQD) OF ELEMENTS IN EACH OF THE
C...NINE INCLINATION INTERVALS FOR EACH LAYER.
C
      DO 15 J=1,3
      ADD=0.0
      DO 20 N=1,9
      FREQD(N,J)= AYLFA(2*N,J)
      ADD=ADD + FREQD(N,J)
   20 CONTINUE
      DO 25 K=1,9
      FREQD(K,J)=FREQD(K,J)/ADD
   25 CONTINUE
   15 CONTINUE
      RETURN
      END
```

```
      SUBROUTINE SRVCMOD
C
C
C...SUBROUTINE SRVCMOD IS A MODIFIED VERSION OF A PORTION OF THE SRVC
C   MODEL WHICH CALCUALTES THE GEOMETRIC PARAMETERS OF A CANOPY.
C
C
      COMMON/GEO/ PHIT1(3,9),FLAI(3,1),SLAI(3,1),AXLFA(19,3),AYLFA(19,3)
      DIMENSION NANGLE(3,3),FLA(3,3,19),THETA(10)
      DIMENSION PHIT(3,3,10),MTR(3),OPM(10),XK(9),XLFA(19)
      DIMENSION YLFA(19), DM(17), F(19), DP(9)
      REAL INCLF
C
C
C....GENERAL SIMULATION CONSTRAINTS                                     SRVC
C
      CEPIO2= 1.57079632
      CE2PI=  6.28318530
      CE1PI=  3.14159265
      CEDTR=.017453293
      CERTD= 57.2957795
      CEMTR= .00029088821
      NBANDS=9
      NMAT=1
      NLAY=3
      BANDW=90/NBANDS                                                   SRVC
C
C....PARAMETER INITIALIZATION AND CONVERSION                            SRVC
C
      NSOUR=NBANDS+1                                                    SRVC
      BANDW=BANDW*CEDTR                                                 SRVC
C
C....COEFFICIENTS FOR DIFFUSE RADIATION VECTORS                         SRVC
C
      ALPHA2=0.                                                         SRVC
      SINA2=0.                                                          SRVC
      DO 2 I=1,NBANDS                                                   SRVC
      SINA1=SINA2                                                       SRVC
      ALPHA2=ALPHA2+BANDW                                               SRVC
      SINA2=SIN(ALPHA2)                                                 SRVC
      XK(I)=SINA2*SINA2-SINA1*SINA1                                     SRVC
    2 CONTINUE
C
C....SOURCE DIRECTION INCLINATION ANGLES                                SRVC
C
      TOTAL=0.                                                          SRVC
      THETA(1)=(BANDW/2.)-BANDW                                         SRVC
      DO 3 I=1,NBANDS                                                   SRVC
      THETA(I+1)=THETA(I)+BANDW                                         SRVC
    3 CONTINUE
C
C....CANOPY GEOMETRY.  EACH CANOPY LAYER IS COMPOSED OF ONE OPTICAL     SRVC
C....MATERIAL WHICH MAY BE SPECIFIED AND UNIQUE GEOMETRICAL PROPERTIES. SRVC
C....CANOPY GEOMETRIC PARAMETERS CONSIST OF (1)LEAF ANGLE FREQUENCY     SRVC
C....DISTRIBUTION FUNCTION DENOTED BY XLFA AND YLFA (2)LEAF AREA INDEX  SRVC
C....DENOTED BY FLAI AND (3)CANOPY DENSITY DENOTED BY SLAI.  XLFA (DEG) SRVC
C....AND YLFA MUST BE SPECIFIED AT AN ODD NUMBER (NANG) OF EVENLY SPACED SRVC
C....POINTS.  FLAI IS NON-NEGATIVE AND SLAI RANGES BETWEEN 0 AND 1.     SRVC
C
      DELF=10.*CEDTR                                                    SRVC
      DO 350 IL=1,NLAY                                                  SRVC
```

```
      NANG=19
C
C...ASSIGN THE NUMBER OF MATERIALS IN ANY GIVEN LAYER
C
      IMAT=1
      MTP(IL) = IMAT                                                    SRVC
      IMAT1=IMAT
      DO 351 J=1,IMAT1
      IMAT = J
      DO 41 MM=1,NANG
      XLFA(MM)=AXLFA(MM,IL)
      YLFA(MM)=AYLFA(MM,IL)
   41 CONTINUE
C
C....INTEGRATE AND NORMALIZE THE LEAF ANGLE FREQUENCY DISTRIBUTION      SRVC
C....FUNCTION USING SIMPSONS RULE--THIS IS TEMPORARILY DENOTED BY F.    SRVC
C....M-1 EQUALLY SPACED INTERVALS OF F ARE THEN DETERMINED AND DENOTED  SRVC
C....BY FLA (M POINTS).  THE TABLE FLA IS USED FOR RANDOMLY SELECTING   SRVC
C....LEAF INCLINATION ANGLES.                                           SRVC
C
      DO 305 I=1,NANG                                                   SRVC
305   XLFA(I)=XLFA(I)*CFDTR                                             SRVC
      M=((NANG-1)/2)+1                                                  SRVC
      NANGLE(IL,IMAT)=M                                                 SRVC
      CALL TBLP(M,XLFA,YLFA,DM,F)                                       SRVC
      DO 310 IANG=1,M                                                   SRVC
  310 FLA(IL,IMAT,IANG)=DM(IANG)                                        SRVC
C
C....NORMALIZE THE INPUT LEAF FREQUENCY DISTRIBUTION FUNCTION TO OBTAIN SRVC
C....A DENSITY FUNCTION F WHICH IS SPECIFIED AT M POINTS.               SRVC
C
      FTOT=0.                                                           SRVC
      DO 311 I=1,NANG                                                   SRVC
  311 FTOT=FTOT+YLFA(I)                                                 SRVC
      DO 312 I=1,9                                                      SRVC
  312 F(I)=(YLFA(2*I)+YLFA(2*I+1))/FTOT                                 SRVC
      DO 315 I=1,NANG                                                   SRVC
315   XLFA(I)=XLFA(I)*CFRTD                                             SRVC
      M=M+1                                                             SRVC
C
C....CALCULATE THE MEAN PROJECTION (OP) IN THE DIRECTION OF THE SOURCE  SRVC
C...(THETA) OF ONE UNIT LEAF AREA WITH INCLINATION INCLF.  THE LEAVES   SRVC
C....AT THIS ANGLE ARE ASSUMED TO BE AZIMUTHALLY ISOTROPIC.             SRVC
C
      DO 330 IANGLE=1,NSOUR                                             SRVC
      INCLF=-5.*CFDTR                                                   SRVC
      DO 320 I=1,9                                                      SRVC
      INCLF=INCLF+DELF                                                  SRVC
  320 CALL COP(INCLF,THETA(IANGLE),OP(I),CFPIO2)
C
C....CALCULATE THE MEAN PROJECTION (OPM) IN THE DIRECTION OF THE SOURCE SRVC
C....(THETA) OF ONE UNIT LEAF AREA AVERAGED OVER THE CANOPY LEAF ANGLE  SRVC
C....DENSITY FUNCTION F.                                                SRVC
C
      CALL COPM(F,OP,OPM(IANGLE))                                       SRVC
C
C....CALCULATE THE PROBABILITY OF A HIT (PHIT) FOR A LIGHT RAY WITH     SRVC
C....SOURCE DIRECTION THETA.                                            SRVC
C
      CALL PDENS(IL,IMAT,IANGLE,OPM(IANGLE),THETA,NANGLE,FLA,SLAI,FLAI,
     * PHIT)
  330 CONTINUE
  351 CONTINUE
  350 CONTINUE
       J=NMAT
      DO 228 I=1,3
      DO 228 M=1,9
      PHIT1(I,M)=PHIT(I,1,M+1)
  228 CONTINUE
      RETURN
      END
```

```
      SUBROUTINE COP(ALPHA,BETA,OP,CEPIO2)
C                                                                       COP
C
C....THIS PROGRAM CALCULATES THE MEAN PROJECTION OF A UNIT LEAF AREA IN  COP
C....THE DIRECTION OF THE SOURCE.  THE LEAF IS INCLINED AT AN ANGLE      COP
C....ALPHA AND IS ASSUMED TO BE AZIMUTHALLY ISOTROPIC.
C                                                                       COP
C
C
      OP=COS(ALPHA)*SIN(BETA)                                           COP
      IF(ALPHA.LE.BETA) RETURN                                          COP
C
C....THETAO IS THE LEAF AZIMUTH ANGLE AT WHICH OP BECOMES NEGATIVE AND  COP
C....IS IN THE FIRST QUADRANT.  THE FUNCTION OP IS SYMMETRIC AND HENCE  COP
C....IS AVERAGED OVER LEAF AZIMUTH ANGLES OF 0 TO PI RADIANS.           COP
C
      THETAO=ACOS(TAN(BETA)/TAN(ALPHA))                                 COP
      TANTO=TAN(THETAO)                                                 COP
      OP=OP*(1.+(TANTO-THETAO)/CEPIO2)                                  COP
      RETURN                                                            COP
      END                                                               COP
```

```
      SUBROUTINE COPM(G,OP,OPM)                                         COPM
C
C
C....THIS PROGRAM CALCULATES THE MEAN PROJECTION OF A UNIT LEAF AREA IN  COPM
C....THE DIRECTION OF THE SOURCE (OPM) FOR THE SIMULATED CANOPY.  THE    COPM
C....LEAVES OF THE CANOPY ARE ASSUMED TO BE AZIMUTHALLY ISOTROPIC.  THE  COPM
C....OP FUNCTION USED IN THE CALCULATION HAS BEEN PREVIOUSLY DETERMINED  COPM
C....FOR A GIVEN SOURCE DIRECTION FOR LEAF INCLINATION ANGLES OF         COPM
C....5, 15, ..., 85 DEGREES.  G IS THE LEAF INCLINATION ANGLE DENSITY    COPM
C....FUNCTION.                                                           COPM
C                                                                       COPM
C
      DIMENSION OP(9),G(9)                                              COPM
      OPM=0.                                                            COPM
      DO 1 I=1,9                                                        COPM
    1 OPM=OPM+OP(I)*G(I)                                                COPM
      RETURN                                                            COPM
      END                                                               COPM
```

```
      SUBROUTINE PDENS(IL,MTYPE,IANGLE,OPM,THETA,NANGLE,FLA,SLAI,FLAI,
     * PHIT)
C
C
C----THIS PROGRAM COMPUTES THE PROBABILITY THAT LIGHT AT INCIDENT ANGLE  PDENS
C    THETA(IANGLE) INTERACTS WITH MATERIAL TYPE MTYPE WITHIN CANOPY      PDENS
C    LAYER IL.                                                          PDENS
C                                                                       PDENS
C
C    INPUT                                                              PDENS
C      IL                                                               PDENS
C      MTYPE                                                            PDENS
C      IANGLE                                                           PDENS
C      OPM                                                              PDENS
C      SLAI                                                             PDENS
C      FLAI                                                             PDENS
C      THETA                                                            PDENS
C    OUTPUT                                                             PDENS
C      PHIT                                                             PDENS
C                                                                       PDENS
C
      DIMENSION DUM(257),THETA(10)
      DIMENSION NANGLE(3,3),FLA(3,3,10),SLAI(3,3),FLAI(3,3),PHIT(3,3,10) PDENS
      ARG=1.-(SLAI(IL,MTYPE)*OPM/SIN(THETA(IANGLE)))                    PDENS
      IF (ARG.LE.0.) GO TO 1                                            PDENS
      PO=ARG**(FLAI(IL,MTYPE)/SLAI(IL,MTYPE))                           PDENS
      GO TO 2                                                           PDENS
1     PO = 0.                                                           PDENS
2     CONTINUE                                                          PDENS
      PHIT(IL,MTYPE,IANGLE)=1.-PO                                       PDENS
      RETURN
      END                                                               PDENS
```

```
      SUBROUTINE TBLR(M, X, Y, XX, Z)                                   TBLR
C                                                                       TBLR
C
C....THIS PROGRAM FINDS THE INTEGRAL Z(X) OF THE FUNCTION Y(X) FROM X(1) TBLR
C....TO X(2M-1) USING SIMPSONS RULE.  THE INTEGRAL Z(X) IS NORMALIZED TO TBLR
C....1.0 AT X(2M-1).  THE TABLE OF Z VERSUS X IS THEN INVERTED TO DETER- TBLR
C....MINE X AS A FUNCTION OF Z AT M REGULARLY SPACED POINTS ALONG Z.     TBLR
C                                                                       TBLR
C
C      INPUT VARIABLES                                                  TBLR
C        M  = DESIRED NUMBER OF REGULARLY SPACED POINTS ALONG Z         TBLR
C        X  = SPECIFIED AT 2M-1 POINTS                                  TBLR
C        Y  = SPECIFIED AT 2M-1 POINTS                                  TBLR
C      OUTPUT VARIABLES                                                 TBLR
C        XX = THE TABLE OF X VALUES FOR M REGULARLY SPACED POINTS       TBLR
C             (M-1 INTERVALS) ALONG Z.                                  TBLR
C        Z  = THE NORMALIZED INTEGRAL OF Y AT X(1), X(3), ..., X(2M-1).  TBLR
C                                                                       TBLR
C
      DIMENSION X(19),Y(19),Z(10),XI(10),XX(10)                         TBLR
C
C....SIMPSONS RULE INTEGRATION                                          TBLR
C
10    Z(1) = 0.0                                                        TBLR
      DX = X(2) - X(1)                                                  TBLR
20    DO 50 J = 2,M                                                     TBLR
      J0 = 2*J - 3                                                      TBLR
30    J1 = 2*J - 2                                                      TBLR
      J2 = 2*J - 1                                                      TBLR
40    Z(J) = Z(J - 1) + DX*(Y(J0) +4.*Y(J1) + Y(J2))/3.0                TBLR
50    XI(J) = X(J2)                                                     TBLR
      XI(1)=X(1)                                                        TBLR
C
C....NORMALIZE INTEGRAL Z(X)                                            TBLR
C
60    DO 70 J = 1,M                                                     TBLR
70    Z(J) = Z(J)/Z(M)                                                  TBLR
C
C....FIND X AT M REGULARLY SPACED POINTS ALONG Z.                       TBLR
C
      XX(1) = X(1)                                                      TBLR
      EM = M - 1                                                        TBLR
      F = 1.0/EM                                                        TBLR
      JS=2                                                              TBLR
80    DO 120 K = 2,M                                                    TBLR
      ZT = K - 1                                                        TBLR
      ZT = ZT*F                                                         TBLR
90    DO 110 J =JS,M                                                    TBLR
      IF(Z(J) - ZT) 110, 100, 100                                       TBLR
100   G = (ZT - Z(J - 1))     /(Z(J) - Z(J - 1))                        TBLR
      XX(K) = XI(J - 1) + G*(XI(J) - XI(J - 1))                         TBLR
      GO TO 115                                                         TBLR
110   CONTINUE                                                          TBLR
115   JS=J                                                              TBLR
120   CONTINUE                                                          TBLR
      RETURN                                                            TBLR
      END                                                               TBLR
```

```
      SUBROUTINE SECTOR
C
C
C...SUBROUTINE SECTOR CALCULATES THE NORMALIZING FACTORS WHICH ACCOUNT FOR THE A
C   AREA OF EACH SOURCE SECTOR.
C
C
      COMMON /A/ WV,RH,RL,D(3)
      COMMON /B/ PGAP(3,9), PHIT(3,9),PGAP2(3,9), PHIT2(3,9),STEF
      COMMON/C/COSTA(9,9,18),EMISSV(4),ABSORP(3), ESKY, EGRD, SECTAR(9)
      COMMON/D/CONT(3,5,9),C(3,5,9), SUMT(3,9), KELV, CT, NUSIM, ITIME
      COMMON/E/AT,THETA(9),PHI(18),XLF(9), YLF(9), ZLF(9), XS(9,18)
      COMMON/F/YS(9,18),ZS(9), CEDTR, R, FREQD(9,3) , WA(15),EPS
      COMMON/G/NSIG,N, ITMAX
      BANDW= 10.*CEDTR
       ALPHA2= 0.
      SINA2=0.
      DO 2 I=1,9
      SINA1=SINA2
      ALPHA2= ALPHA2 + BANDW
      SINA2= SIN (ALPHA2)
C
C... NOTE WE MUST DIVIDE BY SIN(THETA) SINCE WE ARE INTERESTED IN THE FLUX
C     BEFORE IT HITS A HORIZONTAL PANAL.
C
      SECTAR(I)= (SINA2**2-SINA1**2)/(18.*SIN(THETA(I)))
    2 CONTINUE
      RETURN
      END
```

AD-A071 793 COLORADO STATE UNIV FORT COLLINS COLL OF FORESTRY AN--ETC F/G 2/6
TERRAIN FEATURE CANOPY MODELING.(U)
APR 79 D S KIMES, J A SMITH, K J RANSON DACW39-77-C-0073
UNCLASSIFIED ARO-13444.2-GS NL

3 OF 3
AD
A071793

END
DATE
FILMED
8-79
DDC

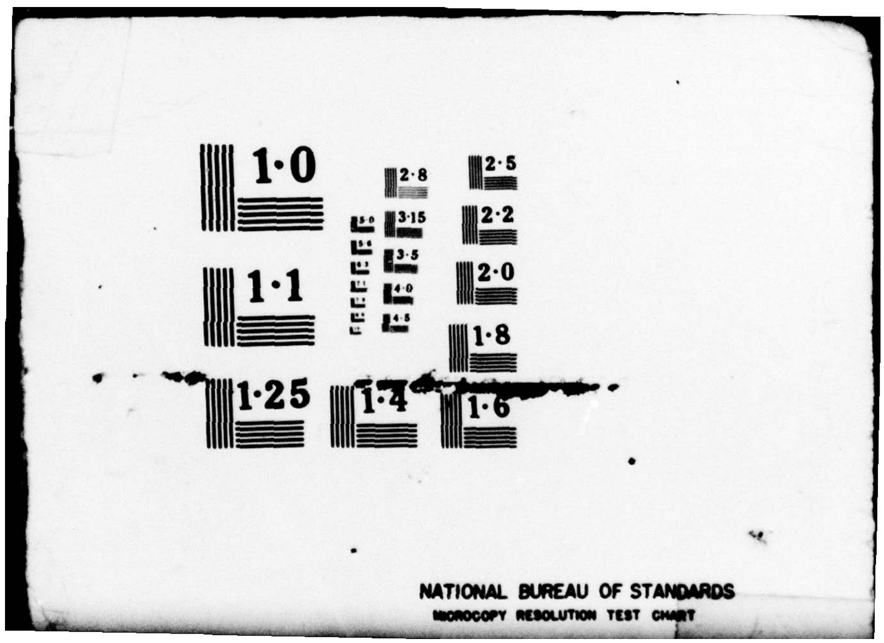
1·0
1·1
1·25
1·4
1·6
1·8
2·0
2·2
2·5
2·8
3·15
3·5
4·0
4·5
5·0
NATIONAL BUREAU OF STANDARDS
MICROCOPY RESOLUTION TEST CHART

```
      SUBROUTINE SENSOR
C
C
C...SUBROUTINE SENSOR CALCULATES THE THERMAL EXITANCE AND ERT FOR THE 9 VIEW
C    ANGLES ABOVE THE CANOPY AND THE 3 HORIZONTAL VIEW ANGLES WITHIN THE CANOPY.
C
C
      COMMON/SENS/  ELAYT(9),ELAYH(3),ERTT(9),ERTH(3)
      COMMON /A/ WV,RH,RL,D(3)
      COMMON /B/ PGAP(3,9), PHIT(3,9),PGAP2(3,9), PHIT2(3,9),STEF
      COMMON/C/COSTA(9,9,18),EMISSV(4),ABSORB(3), ESKY, EGRD, SECTAR(9)
      COMMON/D/CONT(3,5,9),C(3,5,9), SUMT(3,9), KELV, GT, NUSIM, ITIME
      COMMON/E/AT,THETA(9),PHI(18),XLF(9), YLF(9), ZLF(9), XS(9,18)
      COMMON/F/YS(9,18),ZS(9), CEDTR, B, FREQD(9), WA(15),EPS
      COMMON/G/NSIG,N, ITMAX
      COMMON /H/ INDEX1
      COMMON /I/ X(3)
      COMMON /J/ THERM,THMLEY,CONVEC,TRANS
C
C...CALCULATE THE THERMAL EXITANCE ABOVE THE CANOPY AT THE 9 DIFFERENT
C    VIEW ANGLES
C
      DO 2 M=1,9
      ELAYT(M)=
C
C..........CONTRIBUTION FROM LAYER 1
C
     $PHIT(1,M)*(EMISSV(1)*STEF*(X(1)+B)**4)
C
C..........CONTRIBUTION FROM LAYER 2
C
     $+(PGAP(1,M)-PGAP(1,M)*PGAP(2,M))*(EMISSV(2)*STEF*(X(2)+B)**4)
C
C..........CONTRIBUTION FROM LAYER 3
C
     $+(PGAP(1,M)*PGAP(2,M)-PGAP(1,M)*PGAP(2,M)*PGAP(3,M))*(EMISSV(3)
     $*STEF*(X(3)+B)**4)
C
C..........CONTRIBUTION FROM GROUND
C
     $+(PGAP(1,M)*PGAP(2,M)*PGAP(3,M))*(EMISSV(4)*STEF*(GT+B)**4)
    2 CONTINUE
C
C...CALCULATE THE THERMAL EXITANCE FROM EACH LAYER AT A HORIZONTAL VIEW
C    ANGLE.
C
      DO 3 I=1,3
      ELAYH(I)=EMISSV(I)*STEF*(X(I)+B)**4
    3 CONTINUE
C
C...CALCULATE THE EFFECTIVE RADIANT TEMPERATURE (ERT) OF A SENSOR AT THE
C    9 VIEW ANGLES ABOVE THE CANOPY.
C
      DO 4 I=1,9
      ERTT(I)=((ELAYT(I)/STEF)**0.25)-B
    4 CONTINUE
C
C...CALCULATE THE (ERT) OF A SENSOR LOOKING HORIZONTALLY INTO THE 3
C    LAYERS.
C
      DO 5 I=1,3
      ERTH(I)=((ELAYH(I)/STEF)**0.25)-B
    5 CONTINUE
      RETURN
      END
```

```
      SUBROUTINE SETO1(A,I)
C
C
C...SUBROUTINE SERO1 SETS ALL EMEMENTS OF A 1-DIMENSIONAL ARRAY TO 0.0
C
C
      DIMENSION A(I)
      DO 10 J=1,I
      A(J)=0.0
   10 CONTINUE
       RETURN
      END
```

```
      SUBROUTINE SETO2(A,I,J)
C
C
C...SUBROUTINE SETO2 SETS ALL ELEMENTS OF A 2-DIMENSIONAL ARRAY TO 0.0
C
C
       DIMENSION A(I,J)
      DO 10 K=1,I
      DO 10 L=1,J
      A(K,L)= 0.0
   10 CONTINUE
      RETURN
      END
```

```
      SUBROUTINE SETO3 (A,I,J,K)
C
C
C...SUBROUTINE SETO3 SETS ALL ELEMENTS  OF A  3-DIMENSIONAL ARRAY TO 0.0
C
C
       DIMENSION A(I,J,K)
      DO 10 L=1,I
      DO 10 M=1,J
      DO 10 N=1,K
      A(L,M,N)= 0.0
   10 CONTINUE
      RETURN
      END
```